



Hydrogeomechanics for rock engineering: coupling subsurface hydrogeomechanical assessment and hydrogeotechnical mapping on fractured rock masses

JOAO MIGUEL DE FREITAS MEIRINHOS

Outubro de 2015



Instituto Superior de Engenharia do Porto

DEPARTAMENTO DE ENGENHARIA GEOTÉCNICA



Hydrogeomechanics for rock engineering: coupling subsurface hydrogeomechanical assesment and hydrogeotechnical mapping on fractured rock masses

João Miguel de Freitas Meirinhos



2015

(This page intentionally left blank)



Instituto Superior de Engenharia do Porto

DEPARTAMENTO DE ENGENHARIA GEOTÉCNICA

Hydrogeomechanics for rock engineering: coupling subsurface hydrogeomechanical assesement and hydrogeotechnical mapping on fractured rock masses

João Miguel de Freitas Meirinhos

1090509

*Dissertação apresentada ao Instituto Superior de Engenharia do Porto para cumprimento dos requisitos necessários à obtenção do grau de **Mestre em Engenharia Geotécnica e Geoambiente**, realizada sob a orientação do Doutor Helder I. Chaminé, Professor Coordenador com Agregação e a co-orientação da Doutora Maria José Afonso, Professora Adjunta do Departamento de Engenharia Geotécnica do ISEP.*

(This page intentionally left blank)

Acknowledgements

I would like to deeply thank all the beautiful people that contributed decisively for the conclusion of my Master Dissertation. Without them, this almost two-year work would have been much harder.

I will start by saying that this work was “not only my work” but, it was somehow a *collective* work; in the sense that, it connected me with a lot of amazing people, being them: my friends that, when I lost my batteries, they helped me *pick it up back again*; the *creative, knowledge full and always available* Professors, friends and every postgraduate student colleagues who passed by the Laboratory of Cartography and Applied Geology (LABCARGA|ISEP); and, an important part of the core (or *cuore*, for heart in Italian) process where, my *energies are focused*, my dear Parents, Pedro and Célia and my Brother, Pedro. This was made possible as “we” work since, “we” are all together in this work, as well as, in this moment, breathing the same air, under the same sky and part of this amazing world. Together, “we” can create or “we” can tear, “we” can laugh or “we” can cry, “we” can rise or “we” can fall. Just remember, in my own thoughts: ***“If people exist, the sun has a way to shine. Even if it is behind the clouds, it remains divine.”***

Six years have passed, when I first stepped into the School of Engineering of Porto (ISEP). My alternative-young and rather naïve style, felt afraid of all the rules, all the mathematics and physics that I was about to encounter. Nevertheless, from the very first beginning, I was encouraged by one of the most significant mentors I have ever met along this path, the *passionate thriving, geological enthusiastic, pragmatic mentoring, geoengineering reasoning, further developing and supportive*, my scientific advisor Professor Helder I. Chaminé (DEG|ISEP). With a word of advice, always ready to share, motivate and pushing to think outside the box; Professor Chaminé made my path through ISEP thrilling, exciting and, culminating in the present study, challenging me to mix hard-rock geomechanics and hydrogeology. For this reason I have to express a special acknowledge, for all the energy dedicated to my work and mentoring! As you all start to understand, the “we” part of this work had started!

Along the way, several *human beings* had also augmented this “we” feeling, day-by-day. To all my friends whose destiny would join us in the Geotechnical Engineering Department at ISEP, I express my gratitude for all *kindness, friendship, unique personalities* and for *everything*. Although, in the early days of ISEP, I was in a state of shock, my first contact with the “system” was not the best and I have made some mistakes along the way but, one of the most impressive abilities of the *human being* is its capacity of adaptability. So, I did. I have adapted to this new environment, it became less and less strange and, in the current days and for all my future, I know and I am thankful for meeting each and every one of you. Tico, Ribeirão, João Sousa, Jorge, Diogo, Maria João, Roberto, Luciana, Daniel Oliveira, Daniel Monteiro, Diogo Silva, Hugo, Noé, Zé Miguel, Helen Meerkhan and every one that I did not specifically describe, a big thank you for your friendship. All of you have made this “we”-work a lot bigger and easier.

After two years of studying, when starting this work, Professor Chaminé, once again, allowed me the chance of being a part of another “professional family”, the Laboratory of Cartography and Applied Geology (Labcarga) of ISEP. In this small but, nevertheless, very special laboratory of ISEP, I found some of the most *helpful, dedicated* and *wonderful* people to whom I reserve a big thank you for all of your time. To Professor Maria José Afonso (DEG|ISEP), my scientific co-adviser, who continuously showed relentlessly *calm, interested* and *helpful* along the development of the thesis. To MSc. Liliana Freitas (LABCARGA|ISEP) who, besides carrying her PhD-work ahead with *dedication*, always had the time for *listening, taking a break* and *helping* me with all GSI mapping issues. To Professor José Teixeira (LABCARGA|ISEP) for the geographical information technologies insight *knowledge* that he *shared* easily, for the *informative* talks we had and for helping with the software mapping. Special thanks to Caldas da Cavaca Spa and Aguiar da Beira Municipality for the authorisation to access some hydrological data, as well as to Professor José Martins Carvalho (TARH Lda) for shared hydrogeological borehole data.

To all my friends in Maia, Porto, Portugal, I have found so *supportive* in dark rainy times. I wish I can redistribute all the love you incessantly give me, back to all of you. Rena, David, Carina, Santas, Amadeu, Teresinha, Sopas, Nuno, Daqui, Soares, Joana, Dani, André, Nelson, Eddy, Tomé; *you’ve marked my youth* and watched me grow from a boy to a kind-of-man... I hope!

My friends and *brothers from another lands*, Humberto DeMagistris, Elias Chemaly, Yara Seif, Marc Mallorquí, Borja Ruiz, Iñigo and Lorenzo Aragón, Héctor Tirapu, Laura Binaburo, Ahmed Badran, Giorgi Jangirashvili, Sara Balleroni, Anna and Annia, I am so glad that our paths have crossed and we have met on my Erasmus experience; so little time to do so much. Nevertheless, *I thank you deeply for your insights and our enchanting moments* and I hope we will meet again soon one day.

The best part... For last! To Célia, my Mom, the *foundation* and *balance* of my existence, thank you for your *guidance, wisdom* and *peaceful lessons*; To Pedro, my Dad, the bedrock columns that *withhold the foundation secure*, my greatest *influence* that keeps *showing* me the *example*; and, last but never the least, my brother Pedro, the *ignition spark* that *fuels* and *warms my heart*, the *brilliant mastermind* and *helpful advisor*; thank you for the *uplifting and blissful words* that always *support* my works and projects, a big thank you!

Once again, to every one of you that had crossed my existence the past few years; that I have and have not named, on the previous text: a big, big thank you. ***I shall carry you with me, on each and every up-to-come days, to wherever life leads me next.***

Obrigado !

Keywords

Rock masses, GIS mapping, hydrogeomechanics, rock mechanics, Caldas da Cavaca hydromineral system.

Abstract

The present work aims to achieve and further develop a hydrogeomechanical approach in Caldas da Cavaca hydromineral system rock mass (Aguiar da Beira, NW Portugal), and contribute to a better understanding of the hydrogeological conceptual site model. A collection of several data, namely geology, hydrogeology, rock and soil geotechnics, borehole hydraulics and hydrogeomechanics, was retrieved from three rock slopes (Lagoa, Amores and Cancela). To accomplish a comprehensive analysis and rock engineering conceptualisation of the site, a multi-technical approach were used, such as, field and laboratory techniques, hydrogeotechnical mapping, hydrogeomechanical zoning and hydrogeomechanical scheme classifications and indexes. In addition, a hydrogeomechanical data analysis and assessment, such as Hydro-Potential (HP)-Value technique, JW Joint Water Reduction index, Hydraulic Classification (HC) System were applied on rock slopes. The hydrogeomechanical zone HGMZ 1 of Lagoa slope achieved higher hydraulic conductivities with poorer rock mass quality results, followed by the hydrogeomechanical zone HGMZ 2 of Lagoa slope, with poor to fair rock mass quality and lower hydraulic parameters. In addition, Amores slope had a fair to good rock mass quality and the lowest hydraulic conductivity. The hydrogeomechanical zone HGMZ 3 of Lagoa slope, and the hydrogeomechanical zones HGMZ 1 and HGMZ 2 of Cancela slope had a fair to poor rock mass quality but were completely dry. Geographical Information Systems (GIS) mapping technologies was used in overall hydrogeological and hydrogeomechanical data integration in order to improve the hydrogeological conceptual site model.

(This page intentionally left blank)

Palavras-chave

Maciços rochosos, Cartografia SIG, Hidrogeomecânica, Mecânica das rochas, Sistema hidromineral das Caldas da Cavaca.

Resumo Alargado

A presente investigação apresenta como objectivo melhorar o conhecimento e a compreensão do comportamento hidrogeomecânico do maciço rochoso fracturado da área das Caldas da Cavaca (Aguiar da Beira, Portugal Central). Para tal, foram avaliadas as características hidrogeológicas, hidrogeotécnicas e hidrogeomecânicas de três taludes rochosos, bem como de duas sondagens hidrogeológicas através de uma metodologia composta por quatro fases fundamentais. Foi retomado todo o conhecimento prévio sobre a cartografia, a hidroclimatologia, a geologia, a morfotectónica, a hidrologia e as investigações hidrogeotécnicas “in situ” da área. Por fim, foram aplicadas classificações hidrogeomecânicas em meios rochosos fracturados, índices geotécnicos e esquemas classificativos geomecânicos aos taludes rochosos estudados e foi estudada, complementarmente, toda a informação de furos de captação de água subterrânea. Desta forma, foi possível obter os parâmetros necessários para definir o zonamento hidrogeomecânico e, conseqüentemente, redefinir a proposta de um modelo hidrogeológico conceptual com o enfoque da parametrização hidrogeomecânica do maciço rochoso. Numa primeira fase, foram delimitados os taludes de estudo na zona das Caldas da Cavaca, seleccionando-se o talude da Lagoa, o talude dos Amores e o talude da Cancela. O estudo dos taludes foi iniciado com a recolha de dados em, principalmente, três vertentes distintas: i) dados cartográficos, relativos à topografia local, fotogeologia, geologia estrutural, geomorfologia, hidrologia e climatologia; ii) dados de campo e laboratoriais, adquiridos através da execução da técnica de amostragem linear, inventário hidrogeológico, ensaios de resistência à compressão uniaxial, com objectivo de reunir dados sobre as condições geológico-geotécnicas, hidrogeotécnicas e geomecânicas das descontinuidades e rede da fracturação, bem como a compilação de todos os dados hidráulicos dos furos de captação de água e aspectos hidrodinâmicos; iii) dados bibliográficos, artigos, mapas antigos, referências locais e regionais.

O segundo estágio teve como objectivo a compilação e síntese de dados, através da descrição geológica dos taludes estudados (litologia, grau de alteração, grau de fracturação, características das descontinuidades e hidrogeologia), agrupando, sintetizando e definindo zonas hidrogeomecânicas com base na presença de água (características de drenagem, hidrogeologia e hidrogeotecnia). Neste estágio, foram definidas as seguintes zonas hidrogeomecânicas (HGMZ): i) o talude da Lagoa, constituído por dois taludes descontínuos, apresentando o primeiro uma extensão de 268 m, o qual foi subdividido em quatro HGMZ apresentando, a zona HGMZ 1 o maior fluxo de água, seguindo-se as zonas HGMZ 2 e HGMZ 3, as quais não apresentam qualquer fluxo de água; a zona HGMZ 4 compreende todas as secções do talude nas quais não foi possível a aquisição de dados das descontinuidades, pelo facto de o maciço se

encontrar extremamente alterado (W_5) ou de estar coberto de vegetação, tornando-o inacessível; o segundo talude, com uma extensão menor, 39 m, pertence inteiramente à zona HGMZ 3 por não apresentar nenhum fluxo de água; ii) o talude dos Amores, com uma extensão de 126 m, no qual foram definidas duas HGMZ, apresentando a zona HGMZ 1 um baixo fluxo de água e a zona HGMZ 2 características idênticas à zona HGMZ 4 do talude da Lagoa; iii) o talude da Cancela divide-se, igualmente, em dois taludes, o primeiro com uma extensão de 39 m e o segundo com uma extensão de 12 m; ambos os taludes foram incluídos na mesma HGMZ, uma vez que não apresentaram qualquer fluxo de água.

Numa terceira fase, e após reunidas as características de cada zona hidrogeomecânica, foram aplicadas várias classificações para determinar a qualidade do maciço rochoso, bem como o seu comportamento hidráulico. No cômputo de todas as zonas, a zona HGMZ 1 do talude da Lagoa obteve valores mais elevados de condutividade hidráulica, assim como os valores mais baixos de qualidade do maciço. Seguiu-se a zona HGMZ 2 do talude da Lagoa com valores baixos a razoáveis de qualidade do maciço e valores baixos de condutividade hidráulica. Considerando todas as zonas com fluxo de água, o talude dos Amores obteve os valores mais baixos de condutividade hidráulica, em conjunto com uma qualidade do maciço razoável a boa. A zona HGMZ 3 do talude da Lagoa, bem como as zonas HGMZ 1 e HGMZ 2 do talude da Cancela obtiveram valores razoáveis a bons de qualidade do maciço, mas não apresentaram qualquer fluxo de água.

Na última fase, com os dados previamente obtidos e com recurso à utilização das tecnologias dos sistemas de informação geográfica (SIG), foram elaborados vários mapas descrevendo a qualidade do maciço rochoso (RMR, SMR), índices geotécnicos (RQD, GSI) e índices/classificações hidrogeomecânicas (HP-Value, HC-System), mas agrupando, igualmente, as características de qualidade do maciço com a presença de água. Desta forma obteve-se uma cartografia do índice hidrogeomecânico HP-Value e da qualidade do maciço rochoso que reflectem o comportamento geohidráulico do maciço rochoso. Por fim, inseriram-se e cruzaram-se, em ambiente SIG, todos os dados obtidos, melhorando, desta forma a definição de algumas características hidráulicas do modelo hidrogeológico conceptual da área das Caldas da Cavaca.

INDEX

CHAPTER 1. GENERAL INTRODUCTION	1
1.1. Background.....	3
1.2. Earths system and engineering outlook: global tectonic and hydrologic systems.....	5
1.2.1. Global tectonic system and rock cycle	6
1.2.2. Global hydrologic system and groundwater circulation	10
1.3. Aims	15
1.4. Organisation of the dissertation	15
CHAPTER 2. HYDROGEOMECHANICAL ISSUES FROM A ROCK ENGINEERING POINT-OF-VIEW	19
2.1. Description of the rock masses: an engineering geoscience perspective.....	21
2.1.1. Rock discontinuities: genesis, types and characteristics	21
2.1.2. The importance of joints and its characteristics	24
2.1.3. Rock sampling techniques and engineering geoscience mapping	26
2.2. Groundwater flow in rock masses	29
2.2.1. Porosity, storage coefficient, permeability, transmissivity and specific capacity.....	30
2.2.2. Darcy's Law.....	31
2.2.2.1. Laminar and turbulent flow.....	32
2.2.3. Groundwater in fractured crystalline rocks.....	32
2.2.3.1. Intrinsic permeability.....	33
2.3. Bedrock parameters.....	33
2.3.1. Weathering degree	34
2.3.2. Fracturing degree.....	35
2.3.3. Block size	36
2.3.3.1. Measurement of the block volume, V_b	36
2.3.3.2. Volumetric joint count, J_v	37

2.3.3.3.	Rock Quality Designation (RQD) Index.....	38
2.3.4.	<i>In-situ</i> stress.....	40
2.4.	Geomechanical indexes and rock classification schemes.....	41
2.4.1.	Rock mass classification schemes: a brief historical overview	41
2.4.2.	General remarks	46
2.4.3.	Geomechanical calculators and analysis systems: MGC-RocDesign CALC.....	47
2.4.4.	Rock Mass Rating (RMR) by Z.T. Bieniawski	50
2.4.5.	Rock Mass Quality Q-system by Barton et al. (1974, 1977, 1980) and updated by NGI (2013) ..	59
2.4.6.	RMR-Q-system correlation: updated support chart.....	67
2.4.7.	Geological Strength Index (GSI)	70
2.4.8.	Hydrogeomechanical classification.....	73
2.4.8.1.	The Hydro-Potential (HP) Value.....	73
2.4.8.2.	The rock-mass Hydraulic Conductivity (HC) classification system	79
 CHAPTER 3. COUPLING HYDROGEOMECHANICAL CLASSIFICATIONS AND HYDROGEO TECHNICAL MAPPING: IMPORTANCE ON HARD ROCK HYDROGEOLOGY PRACTICE		82
3.1.	General remarks	84
3.2.	Regional and local framework	85
3.3.	Materials and methods	87
3.4.	Data and results.....	88
3.4.1.	Geomechanical rock mass description	89
3.4.2.	Hydrogeomechanical zoning.....	94
3.4.2.1.	Lagoa slope zoning	94
3.4.2.2.	Amores slope zoning	95
3.4.2.3.	Cancela slope zoning	95
3.4.3.	Rock mass classification or indexes.....	97
3.4.3.1.	Rock Mass Rating (RMR)	97

3.4.3.2.	Slope Mass Rating (SMR)	100
3.4.3.3.	Geological Strength Index (GSI)	100
3.4.4.	Hydrogeomechanical classifications or indexes	101
3.4.4.1.	Hydro-potential (HP) value.....	101
3.4.4.2.	Hydraulic-Conductivity (HC) System	104
3.5.	Discussion.....	105
3.5.1.	Overview	105
3.5.2.	Rock mass schemes and hydrogeomechanical classifications or indexes: an outline.....	106
3.5.3.	Rock mass hydraulic behaviour	108
3.5.3.1.	Lagoa slope hydrogeomechanical assessment	110
3.5.3.2.	Amores slope hydrogeomechanical assessment	111
3.5.3.3.	Boreholes: hydraulic and hydrogeomechanical studies.....	112
3.5.4.	HP-value chart (Gates, 2003) vs HP-value results	114
3.5.5.	Hydrogeomechanical zoning map.....	115
3.5.6.	Hydrogeological conceptual site model: subsurface hydrogeomechanical role.....	118
3.5.7.	Final remarks and outlook.....	122
CHAPTER 4. CONCLUSIONS.		125
4.1.	Concluding remarks	127
CHAPTER 5. REFERENCES		129

Figure index

Figure 1 – The tectonic system of Earth: its major layers (lithosphere, asthenosphere, mesosphere) and boundaries (convergent, divergent or transform), (Hamblin and Christiannsen, 2003).....	7
Figure 2 – The tectonic plate mosaic. Plates move away from the crests of the oceanic ridges colliding with others to form convergent boundaries. Plates also slide past one another, deforming and breaking the adjacent rock material within it, releasing energy under the form of earthquakes (Hamblin and Christiannsen, 2003).....	8
Figure 3 - The rock cycle in a geoscience engineering perspective (Chaminé et al., 2013b). This diagram shows the distinction between rock formation and its strength involving it with the concept of the anthropic intervention. Anthropic activity causes the change of the rock material considering all the rock made, modified or moved by humans (Underwood, 2001).	9
Figure 4 – The hydrologic cycle and all of its components (illustration by Dr. John Evans, USGS). As the sun heats the ocean water it evaporates into the atmosphere. Through the uneven heating of Earth’s surface, it causes the atmosphere to convection. This causes the evaporated water to circulate among the atmosphere and condenses, as rain or snow, on continents or oceans. Most of the water that falls on continents returns to the oceans by surface runoff or groundwater seepage. Variations on the flow of this system can be caused by the retention of water in lakes and glaciers (http://water.usgs.gov/edu/watercyclesummary.html).	11
Figure 5 - Types of voids or pore spaces which allow water circulation in rocks (Hamblin and Christiannsen, 2003).....	13
Figure 6 - The different components of underground circulation and the different types of aquifers (Hamblin and Christiannsen, 2003).....	14
Figure 7 – Conceptual flowchart representing the methodologies used in the current research: “hydrogeomechanics for rock engineering: coupling hydrogeomechanics classifications and hydrogeotechnical mapping on fractured rock masses”	17
Figure 8 – The description/classification/behaviour versus assessment/design/modelling of heterogeneous and fractured rock masses (Chaminé et al., 2015).	22
Figure 9 - The main scientific and technical fields of applications of scanline sampling technique surveys related to engineering geosciences, rock engineering and geotechnical engineering (Chaminé et al., 2015).	26
Figure 10 – Examples of rock scanline techniques (after Watkins et al., 2015): a) Fractures attributes, including orientation, length, aperture, spacing and fracture fill are measured for each fracture that intersects a linear scanline (tape measure). b) Three evenly spaced fracture sets at different orientations (N-S, NE-SW, NW-SE) recorded on a linear scanline (dashed line). True spacing for each set is 11 cm, and true intensity is 8 per metre; only the true spacing and intensity of fractures perpendicular to the scan line (N-S set) are recorded as the other two sets are oblique to the scan line, giving 15 cm spacing and only 6 fractures per metre. c) Large scale discontinuities mapped using areal sampling from an aerial photograph. d) Fracture traces mapped onto bedding planes from a field photograph. e) Fracture attributes, including	

orientation, length, aperture, spacing and fracture fill are measured for each fracture within a sampling area (black box) using rectangular window sampling. f) Circular scan line data collection; fracture intersections with the sampling circle (black dots) and fracture terminations within the circle (black squares) are counted to estimate fracture intensity, density and mean trace length. 27

Figure 11 – Illustration of scanline sampling technique applied on a fractured rock mass for determination of discontinuity characteristics. Rock scanline surveys framework to rock design (slope, tunnel, quarry and cavern): a reliable tool to reduce the intrinsic geologic variability and uncertainty (adapted from Chaminé et al., 2015). 28

Figure 12 - Weathering types according to each geological material (Gonzalez de Vallejo and Ferrer, 2011). 34

Figure 13 - RQD measuring and determination procedure (Gonzalez de Vallejo and Ferrer, 2011). 39

Figure 14 – Terzaghi’s rock-load concept applied to tunnels (Terzaghi, 1946). 43

Figure 15 - An overview of rock-mass classifications (empirical classifications: RLM, ST, NATM; rating methods classifications and derivative schemes: RSR, RMR, Q-system, MRMR, Q-TBM, SRC), geotechnical indexes or indicators (RQD, GSI, R_{Mi}, HP-value, RME), rock analysis systems (BGD, TIA) and the most important milestones regarding key publications for mining, tunnelling and/or underground excavation design (details in: Bieniawski, 1973, 1976, 1989; Barton et al., 1974, 1980; Hudson, 1992; Barton, 2000, 2006; Palmström, 1996a,b; Palmström and Stille, 2010; ITA-Austria, 2012; NGI, 2013; Hoek et al., 2013; Celada et al., 2014a,b; and references therein). (after Pinheiro et al., 2014). 45

Figure 16 – Some selected examples of commercial programmes or informatics applications related to professional or academic use (examples: ClasRock32 – Classification of Rock Masses by Geo & Soft International, <http://www.geoandsoft.com/> [RMR, Q-system], RMR|Calc by EduMine Online Tool, <http://www.edumine.com> [RMR], Combining RMR-Q-R_{Mi} by Palmström (1995), <http://www.rockmass.net> [RMR-Q-system-R_{Mi}], ClassMass by Deliormanli and Onargan (2003) [RMR, Q-system], RocData/RocSupport/RocLab by RocScience, <http://www.rocscience.com/> [GSI, etc.]) and other advanced expert systems like TiAS Database System from Marinos et al. (2013). (After Pinheiro et al., 2014). 48

Figure 17 - MGC–RocDesign|CALC: a geomechanical calculator tool for rock engineering characterisation and design; a) interdisciplinary framework; b) schematic concept. (After Pinheiro et al., 2014). 50

Figure 18 - Chart for determination of the theoretical RQD_t within the average spacing of discontinuities for a general threshold value *t* (adapted from Priest and Hudson 1976, Priest 1993)..... 53

Figure 19 - Q-system classification and rock support chart for retrieving the reinforcement category (adapted from Barton et al., 1974, 1980). After: NGI (2013)..... 66

Figure 20 - The support selection chart, with the addition of alternate correlations between RMR and Q (after Barton and Bieniawski, 2008). 68

Figure 21 - A) Static modulus of deformation *E_m* versus RMR and Q-system; B) Stand-up time data versus RMR from case histories, where red dots represents tunnel, and green signifies mine results (case histories and RMR data compiled by Bieniawski, 1989; Q-system relationship by Barton, 2002). 69

Figure 22 – GSI-2000 chart (adapted from the version Hoek and Marinos, 2000): estimate of GSI based on in-situ geostructure of the rock mass and geotechnical discontinuities conditions (adapted from Hoek and Marinos, 2000; and updated from Cai et al., 2004 in terms of its quantification by block volume and joint condition factor is also shown on the right side).	72
Figure 23 – GSI-2013 chart (adapted from the version Hoek et al., 2013): modified Geological Strength Index chart and the quantification GSI geomechanical classification proposal by Hoek et al. (2013).....	72
Figure 24 - Comparison of HP-values to yields and specific capacities of local bedrock wells (adapted from Gates, 2003).	78
Figure 25 - Regional framework of the Caldas da Cavaca hydromineral system, Aguiar da Beira municipality: A location of study area; B satellite image (compiled from Landsat 7 ETM+ data, 2000/01; all IR colour, bands 7-4-5 = RGB; adapted from Global Land Cover Facility); C shaded relief, regional geology (adapted from Oliveira et al., 1992) and hydrogeology (adapted from Carvalho, 2006; Carvalho et al., 2007) and main hydromineral springs (adapted from Carvalho, 2006). After: Teixeira et al. (2015).	86
Figure 26 – Location of the three studied slopes according to the scanline sampling technique (Caldas da Cavaca site, Aguiar da Beira).	88
Figure 27 – HP-value chart (Gates, 2003) comparison versus achieved HP-values for studied area.	114
Figure 28 – Relationship of HP-values to discharge from wells located in fractured bedrock and seepage from fractured rocks (Gates, 2003) versus study area results.	115
Figure 29 – Hydrogeomechanical map: coupling GIS mapping with RQD index.	116
Figure 30 – Hydrogeomechanical map: coupling GIS mapping with GSI index.	117
Figure 31 – Hydrogeomechanical map: coupling GIS mapping with a HP-value vs. Rock-mass quality approach.....	118
Figure 32 – General (A) and detailed (B) hydrogeological conceptual model from Caldas da Cavaca hydromineral system (after Teixeira et al., 2015).	119
Figure 33 – Hydrogeological conceptual site model: a subsurface hydrogeomechanical input.	121

Table index

Table 1 - Different discontinuities types: its formation, characteristics and relation to groundwater occurrence (compiled from: Scesi and Gattinoni, 2009; Singhal and Gupta, 2010; Gustafson, 2012).....	23
Table 2 - Summary of the main geological and geotechnical parameters of discontinuities: basic description and methods/techniques (compiled from: ISRM, 1978, 1981; GSE, 1995; CFCFF, 1996).	25
Table 3 - Values of the coefficient K (Huntley et al., 1992).	31
Table 4 – Weathering degrees applicable to rock masses (adapted from ISRM, 1981; GSE, 1995).	35
Table 5 – Palmström’s classification for Block Volume, V_b (Palmström and Stille, 2010).	37
Table 6 – Palmström’s classification for Volumetric Joint Count, J_v (Palmström and Stille, 2010).	38
Table 7 - Description of RQD based on the calculated index (Deere et al., 1967).	39
Table 8 - An overview of the main rock mass classifications or indexes and hydrogeomechanical systems used in rock engineering practice (compiled and adapted from Kirkaldie, 1988; Bieniawski, 1989; Bell, 1992; Hoek, 2007; Barton, 2008; Scesi and Gattinoni, 2009; Singh and Goel, 2011).	47
Table 9 - Strength of intact rock material (adapted from Bieniawski, 1989).	52
Table 10 - Rock Quality Designation (RQD) index (adapted from Bieniawski, 1989).	52
Table 11 - Spacing of discontinuities (adapted from Bieniawski, 1989).	53
Table 12 - Condition of discontinuities (adapted from Bieniawski 1989).	54
Table 13 - RMR System: guidelines for classification of discontinuity conditions (adapted from Bieniawski, 1989).	54
Table 14 - Groundwater conditions (adapted from Bieniawski, 1989).	55
Table 15 - Assessment of joint orientation effect on tunnels (adapted from Bieniawski, 1989).	55
Table 16 - RMR adjustment for joint orientation (adapted from Bieniawski, 1989).	55
Table 17 – Design parameters and engineering properties of rock mass (adapted from Bieniawski, 1989)..	56
Table 18 - Guidelines for excavation and support of 10 m span rock tunnels in accordance with the RMR system (after Bieniawski, 1989). Hoek et al. (1998) reported that these guidelines have been published for a 10 m span horseshoe shaped tunnel, constructed using drill and blast methods, in a rock mass subjected to a vertical stress <25 MPa (equivalent to a depth below surface of <900 m). It should be noted also has not had a major revision since 1973. In many mining and civil engineering applications, steel fibre reinforced shotcrete may be considered in place of wire mesh and shotcrete.	57
Table 19 - Direct relations between rock mass classification and properties of rock mass (adapted from Aydan et al., 2014, In: Abbas and Konietzky, 2015).	58
Table 20 - Rock Quality Designation (adapted from Barton et al., 1974, 1980).	60
Table 21 – Number of discontinuities sets (J_n) (adapted from Barton et al., 1974, 1980).	60
Table 22 - Discontinuities wall roughness (J_r) (adapted from Barton et al., 1974, 1980).	61
Table 23 – Discontinuities alteration factor (J_a) (adapted from Barton et al., 1974, 1980).	61
Table 24 – Estimation of Angle of Internal Friction from the parameters J_r and J_a (Barton and Bieniawski, 2008).	62
Table 25 - Joint water reduction factor J_w (adapted from Barton et al., 1974, 1980).	63

Table 26 - Stress Reduction Factor (adapted from Barton et al., 1974, 1980).	64
Table 27 - Values of Excavation Support Ratio (Barton, 2008).	65
Table 28 – ESR values when considering the excavation for tunnels by Tunnel Boring Machines (TBM) (Barton, 2000). When calculating car traffic tunnels or high velocity train tunnels the used value shall be 0.5 (Hoek, 2007).	65
Table 29 - Correlation proposal for the RMR - Q-system from different authors (Bieniawski, 1989; Barton, 2006).	67
Table 30 - GSI rock mass qualitative classification (adapted from Hoek, 2007)	70
Table 31 – RQD classification (after Deere, 1963; adapted from Gates, 1997, 2003).	74
Table 32 – Description and ratings for joint set number (after Barton et al., 1974; adapted from Gates, 1997, 2003).	75
Table 33 – Description and ratings for joint roughness number, <i>Jr</i> (after Barton et al., 1974; adapted from Gates, 1997, 2003).	76
Table 34 – Description and ratings for joint aperture factor, <i>Jaf</i> (modified from Harp and Noble, 1993; adapted from Gates, 1997, 2003).	76
Table 35 – Descriptions and ratings for average hydraulic joint conductivity number, <i>Jk</i> (modified from Freeze and Cherry, 1979; adapted from Gates, 1997, 2003).	77
Table 36 – Description and rating for joint water factor, <i>Jw</i> (modified from Barton et al, 1974; adapted from Gates, 1997, 2003).	77
Table 37 – Description and ratings for lithology permeability index (adapted from Hsu et al. 2008, 2011)...81	81
Table 38 - Basic geotechnical and geomechanical parameters for Lagoa slope, Caldas da Cavaca.	91
Table 39 - Basic geotechnical and geomechanical parameters for Amores slope, Caldas da Cavaca.	92
Table 40 - Basic geotechnical and geomechanical parameters for Cancela slope, Caldas da Cavaca.	93
Table 41 - Summary of the basic hydrogeomechanical parameters from the studied rock slopes, Caldas da Cavaca.	96
Table 42 - Synthesis of the geomechanical parameters for Lagoa slope rock mass rating (version 1989 – RMR ₈₉ ; Bieniawski, 1989).	98
Table 43 – Synthesis of the geomechanical parameters for Amores slope rock mass rating (version 1989 – RMR ₈₉ ; Bieniawski, 1989).	99
Table 44 - Synthesis of the geomechanical parameters for Cancela slope rock mass rating (version 1989 – RMR ₈₉ ; Bieniawski, 1989).	99
Table 45 - Synthesis of the Slope Mass Rating parameters for the three studied rock slopes.	100
Table 46 - Synthesis of the Geological Strength Index parameters for the three studied rock slopes.	101
Table 47 - Synthesis of the HP-value parameters for the Lagoa slope.	102
Table 48 - Synthesis of the HP-value parameters for the Amores slope.	103
Table 49 - Synthesis of the HP-value parameters for the Cancela slope.	103
Table 50 – Synthesis of the Geological Strength Index parameters for the three studied rock slopes.	105

Table 51 – Synthesis of rock mass indexes and/or classification schemes and hydrogeomechanical classifications for Lagoa slope.	107
Table 52 – Synthesis of rock mass indexes and/or classification schemes and hydrogeomechanical classifications for Amores slope.	108
Table 53 – Synthesis of rock mass indexes and/or classification schemes and hydrogeomechanical classifications Cancela slope.....	108
Table 54 – Hydrogeomechanical parameters for Lagoa slope.	110
Table 55 – Hydrogeomechanical parameters for Amores slope.	112
Table 56 – Hydrogeomechanical parameters for RA1C and RAM2 boreholes.....	113



Chapter 1.
General Introduction



Synopsis

Oddly enough, when you look into a rock there are more things for it to tell than what we know about and can explain. This enigmatic perspective for an ordinary person shall range from its origin, properties and geodynamical journey throughout the time, up to its geotechnical description, geomechanical behaviour and engineering applications at the present-day. The rock ground comprehension gathered over the years, allows them to be the supporting foundations of a building, a dam, a bridge, a reservoir, an underground exploration or a tunnel. The current rock engineering works were possible due to the accurate study, development and evolution of theories, concepts, models and site characterisation that define what is needed to know about the ground surface.

1.1. Background

From the earlier of geoscience investigations up until the present time, hydrogeology gained a greater importance due to the Earth's fluid composition on rock systems. More than 50% of the continents surface area is composed by hard-rock, being it igneous, metamorphic rocks and/or strongly cemented sedimentary rocks. On the current days, one of the most important reasons for developing hydrogeological conceptual models derives, for example, from the need of supplying safe drinkable water, particularly on developing countries and large urban areas, as well as for the assessment of hydromineral resources and for groundwater role on major engineering projects.

Every time it is referred about applied geosciences (e.g., applied geology, applied geomorphology, engineering geology, hydrogeology, mining geology, petroleum geology, economic geology, etc.) and geoengineering study fields (e.g., geological engineering, geotechnical engineering, mining engineering, rock engineering, ground engineering, foundations engineering, etc.), it is fundamental to understand their connection to the basic geology, rock formation, evolution and their properties. In this dissertation, we need to define the concept of hydrogeology, merging it with the applicability of rock mechanics (or geomechanics of discontinuous media), in order to fully understand what hydrogeomechanics is about.

Hydrogeology, as the term means, is the connection of Earth studies (geology) with the superficial/underground occurrence, nature and circulation of water (hydro). These studies emphasis the water chemistry, flow systems, and relation to the geologic environment (e.g., Davis and DeWist, 1966; Freeze and Cherry, 1979; Younger, 2007; Fitts, 2013; Fetter, 2014). When hydrogeology is being considered, the field concerning geologic environment and processes does not hypothesise only the rock itself but applies important considerations about fractures and partitioning damage zones.

On the other hand, geomechanics is related to the mechanical behaviour of soil and rock formations, based on the main disciplines: geology (e.g., structural geology, sedimentary geology, etc.), engineering geology, soil mechanics and rock mechanics. Often, the term geomechanics

focus on rock behaviour (Mello Mendes, 1967; Hoek, 2007; Palmström and Stille, 2010). During the geological orogenesis systems — a major tectonic process that affects the earth's crust along time, causing, for example, the formation of big mountain chains — the rock mass is subjected to stress, strain, deformation and movement of interlocking of crustal blocks. This approach represents a major importance since the key to comprehend the geological framework of a site comes from its tectonic evolution which in turn, defines the rock mass properties. Likewise, when engineering works are constructed on or in a rock mass, they induce several stress changes on it. This means that fractures, as well as intact rock, are subjected to strain. In addition, the rock deformation, rock matrix stiffness and geofluids lead to the rock mechanical behaviour. So, considering the effects on existing fractures, these can close, open or grow and new fractures may be induced (e.g., CFCFF, 1996; Hoek, 2007; Rocha, 2013).

Merging the two concepts described above, the hydrogeomechanics field or hydrogeology for rock engineering is achieved (Gustafson, 2012). The integration of hydrogeology and rock mechanics addresses an interdisciplinary knowledge for ground hydrogeomechanical conditions and behaviour of groundwater in fractured rocks. In this case, the aim is to combine the rock mass behaviour with the hydrogeological properties (e.g., Scesi and Gattinoni, 2009; Singhal and Gupta, 2010; Gustafson, 2012; Bense et al., 2013). The constant modification of these properties represents a directly proportional relationship to the groundwater flow by its connection to the hard rock permeability, being mainly governed by rock discontinuities and fault zones (Snow, 1969; Simpson, 1977; Wei et al., 1995; Evans et al., 1997; Ingebritsen and Manning, 1999; Wang, 2000; Ingebritsen et al., 2006; Faulkner et al., 2010). In addition, Caine et al. (1996) argued the fault core and damage zone are distinct structural and hydrogeologic units that reflect the material properties and deformation conditions within a fault zone. Whether a fault zone will act as a conduit, barrier, or combined conduit-barrier system, it is controlled by the relative percentage of fault core and damage zone structures and the inherent variability in grain scale and fracture permeability.

The development of petroleum and gas reservoirs, underground disposal for nuclear waste, construction of underground rock cavities for storing water, underground passages like tunnels and several hydrogeomechanical problems as, rock slope stability or seepage from dams, redirects us to the hydraulic characterisation and evaluation of the rock masses (e.g., Barton et al., 1985; Wei et al., 1995; Tóth, 1999; Barton and Quadros, 2002; Hoek, 2007; Hamm et al., 2007; Zhou et al., 2008; Scesi and Gattinoni, 2009; Chen et al., 2011; Hsu et al., 2011; Gustafson, 2012 and references therein). The determination of hydraulic conductivity on fractured rock masses is one of the most challenging issues. Jing (2003) stated an important topic: *“this difficulty comes from the fact that rock is a heterogeneous geological material that contains various natural*

fractures of different scales". This approach allows the development of accurate and reliable groundwater conceptual models supported by numerical modelling and back analysis framework (e.g., Carvalho, 2006; Kresik and Mikszewski, 2013; Chaminé et al., 2013a; Chaminé, 2015).

1.2. Earths system and engineering outlook: global tectonic and hydrologic systems

Although it is not something of quick comprehension, there is a global connection of every distinct and isolated natural phenomenon suggesting an organisation and interdependence of actions. This connection of singularities drives everything in motion, from natural activities up to the anthropogenic ones and it is defined as a global system. Within the Earth's composition, it is mandatory to speak about several natural systems working unanimously that, describe how natural events are linked and how they operate. In engineering, a system can be seen as a group of interacting devices working for a specific task (for example, the electrical or the heating system). The common points of natural and artificial systems is the capacity of transferring material or energy from one place to another and each system needs an energy source to make it able to operate. These types of material and energy moving systems are called dynamic. Geologically speaking, there are two main types of system: *"a closed system exchanges only heat (no matter); an open system exchanges both heat and matter with its surroundings."* (Hamblin and Christiannsen, 2003).

The first important fact to know about Earth's dynamic system is that it suffers from slow to quick changes along time. These changes are mostly physical and chemical reactions occurring on their sub-systems, such as, the cool down of a lava flow, the erosion of the sediments along a river or the formation of windblown sand dunes. The main energy source that drives this global dynamic system is the Sun, who acts on Earth's surface fluids, air and water, consequently giving motion to complex natural system, for instance, the tectonic and hydrologic systems (Grotzinger et al., 2010). In the hydrological system, water evaporates from oceans into the atmosphere, condenses into land and flows back to oceans again. The global tectonic system, even though seems stationary, is in constant motion but in a much slower pace causing continent splitting and drifting. Therefore, the origins of all of Earth's structural features are the result of moving lithospheric plates (e.g., Wegener, 1924; Holmes, 1929; William, 1975; Ribeiro, 2002; Foulger, 2010 and references therein).

The Planet Earth is composed by a junction of open and closed systems but, Earth itself is essentially considered a closed system (Hamblin and Christiannsen, 2003). This lays on the fact that since the heavy meteorite bombardment, there was no significant mass transfer inside or outside its atmosphere. A river, on the other hand, is an open system due to the loss of water and sediments to oceans and the recharge of water trough rain and underground aquifers.

Metaphorically speaking, this connectivity of all present systems on Earth is similar to an invisible web where, changing a small part of one pulls a thread of many others towards a state of equilibrium. The equilibrium is reached when the system loses energy, arriving to the lowest possible energy level. All materials attempt to achieve a balance of the physical and chemical forces acting upon them. These forces are caused by exposing the materials to different environments since their own formation. For example, a hot lava flow loses heat to the surrounding environment in order to reach its equilibrium state. If some action changes this equilibrium, the system will naturally move until it re-establishes the equilibrium under the new conditions. On rivers, the gravitational potential energy determines the river flow until it reaches a state of the lowest possible energy on its arrival to the sea (details in Hamblin and Christiannsen, 2003; Grotzinger et al., 2010).

1.2.1. Global tectonic system and rock cycle

“The birth of the oceans is a matter of conjecture, the subsequent history is obscure, and the present structure is just beginning to be understood. Fascinating speculation on these subjects has been plentiful, but not much of it predating the last decade holds water.” (Hess, 1922)

Apparently, random phenomena on dynamic geologic systems are ruled by natural laws. From a grain of sand on the beach to a river, a canyon or a mountain range, everything was formed by a *“specific way due to Earth constant changes and organised interactions of matter and energy”* (Hamblin and Christiannsen, 2003).

As previously said, the major Earth systems that defines itself as the liveable place of currently are the global tectonic system and the hydrological system. The theory to describe Earth’s dynamics was developed in the middle 1960s (e.g., Hess, 1962; Vine and Matthews, 1963; Vine and Matthews, 1963; Wilson, 1963, 1966; Vine and Wilson, 1965; Vine, 1966; Heirtzler et al., 1966; Le Pichon, 1968) and is well-known as plate tectonics (previously designated as: sea-floor spreading and continental drift). Nowadays, it is called global tectonics (details in Ribeiro, 2002). This theory explains the *“formation and deformation of Earth’s crust that results in large-scale features”* (Hamblin and Christiannsen, 2003). In addition to all these theories, for one to be reliable it is needed to show evidence of its working congruence with what it states. To prove it, there are many different data sources: structure, topography and magnetic patterns of the ocean floor, location of earthquakes and volcanic activity, paleontological records, structural and geographic fit of the continents and the history of mountain belts. The global tectonics theory relies on few principal concepts to explain Earth’s dynamics (William, 1975).

Firstly, as Figure 1 shows, planet Earth is divided in diverse layers, each one with different properties and composition. This diversity of layers and mechanical properties gives the tectonic system a dynamic continuous movement. New approaches and a vivid debate still exist (see, for example, the works of Ribeiro, 2002 and Foulger, 2010).

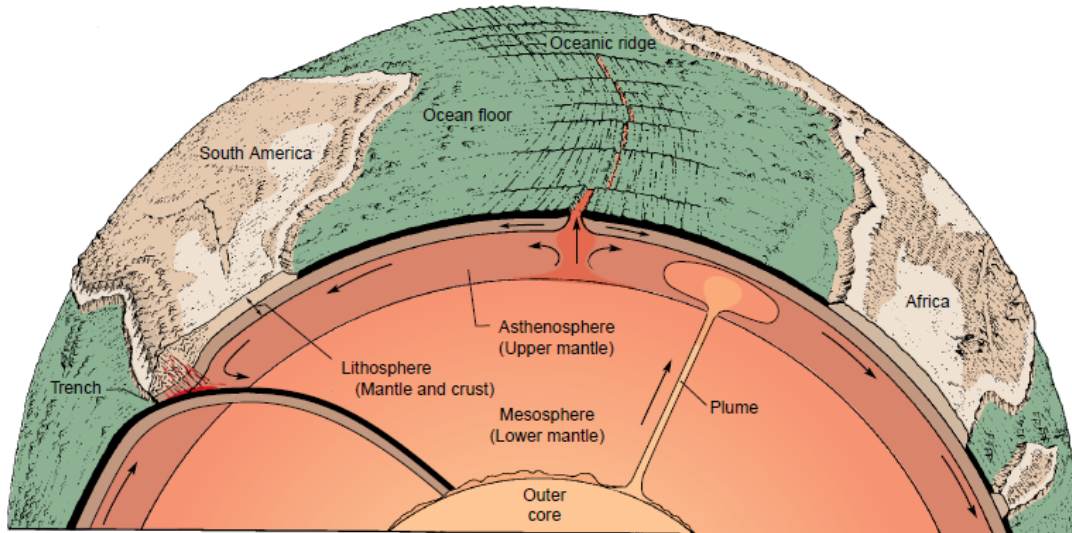


Figure 1 – The tectonic system of Earth: its major layers (lithosphere, asthenosphere, mesosphere) and boundaries (convergent, divergent or transform), (Hamblin and Christiannsen, 2003).

The layers presented in this system are (Hamblin and Christiannsen, 2003; Grotzinger et al., 2010): *lithosphere* – crust and uppermost solid part of the mantle; *asthenosphere* – upper mantle; *mesosphere* – lower mantle; and also the inner and outer core of the Earth. The lithosphere is composed by relatively cool and rigid plates that split and move as single mechanical units. Below it a more plastic layer than the lithosphere and the lower mantle appears, called asthenosphere. From the asthenosphere, molten rock rises to fill the voids created by the split of the lithosphere plates, forming divergent plate boundaries or oceanic ridges. The plates are consumed in subduction zones by the absorption of a converging plate into the hotter mantle below. The previous zones are marked by deep sea trenches that border island arcs and some continents. The energy source that drives all these huge dynamic moves, comes from the Earth's internal heat generation process called convection (Ribeiro, 2002). Convection can be explained by the rise of hot mantle material to the lithosphere's base, making it move laterally, cooling and eventually descending to be reheated and the cycle continues again.

Therefore, the active geodynamic processes are generally located in the boundaries of tectonic plates. Plate boundaries can coincide with the geographical continent limits but not always since some are located in the middle of the ocean (Figure 2). About plate boundaries, it is possible to define three major types: convergent, divergent and transforming. In the convergent type, plates move towards one another creating intense compression zones that rumple the lithosphere and build mountain chains. This phenomenon is complemented by the formation of trenches, volcanoes and the occurrence of earthquakes on the plate margins. As compression is created by the plunge of a lithosphere plate into the mantle, the rock material becomes heated and dehydrated where some of it melts, becomes less dense and rises while some of it erupts (see details in Hamblin and Christiannsen, 2003; Grotzinger et al., 2010).

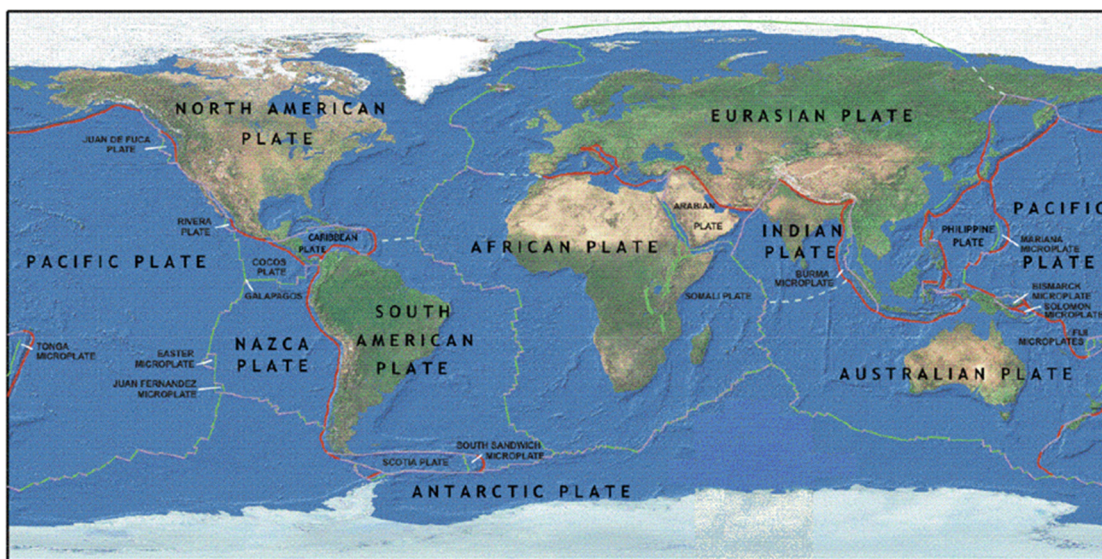


Figure 2 – The tectonic plate mosaic. Plates move away from the crests of the oceanic ridges colliding with others to form convergent boundaries. Plates also slide past one another, deforming and breaking the adjacent rock material within it, releasing energy under the form of earthquakes (Hamblin and Christiannsen, 2003).

The formation of the Andes Mountains in South America is explained by a convergent plate boundary. Crust in continents and island is less dense than the oceanic crust; thus, it floats and resists subduction into the dense mantle. Consequently, the sedimentary rock layers fold, rises and deform by the collision of the two plates. The divergent type is explained by, two plates moving apart while hot molten material from the deeper mantle is rising to fill the void. This molten rock erupts on the seafloor as lava and solidifies to form new lithosphere. Commonly, these divergent formations can be found on mid-oceanic ridges with the particularity of standing higher than the colder adjacent oceanic crust due to its hot and less dense material. When there is a divergent boundary on a continent, eventually, the formation of new ocean basin occurs. For

instance, the result of this process happens on the rift of the Red Sea, where there is a splitting of the Arabian and Sinai Peninsulas from Africa, with the formation of new seafloor in the bottom of the Red Sea. The transforming plate boundary type is defined by plates sliding horizontally past one another. Occurrence of earthquakes is common on this type of boundaries but the formation of volcanoes is unusual. These boundaries are usually found on the seafloor but the best known example of this type of mechanism is the great San Andreas Fault system in California. The building of stress between the sliding plates deforms the rock until it breaks, suddenly releasing energy and causing earthquakes along the fault (details in Hamblin and Christiannsen, 2003; Grotzinger et al., 2010).

Concerning the rock material, Chaminé et al. (2013b) stated: “rocks are formed in an continuous geodynamic cycle (involving numerous internal and external processes) throughout the geological time, that result for engineering purposes in hard rocks (unweathered, strong and durable), soft rocks (weak and easily deformable) and soils (unconsolidated sedimentary deposits overlying bedrock)” (Figure 3).

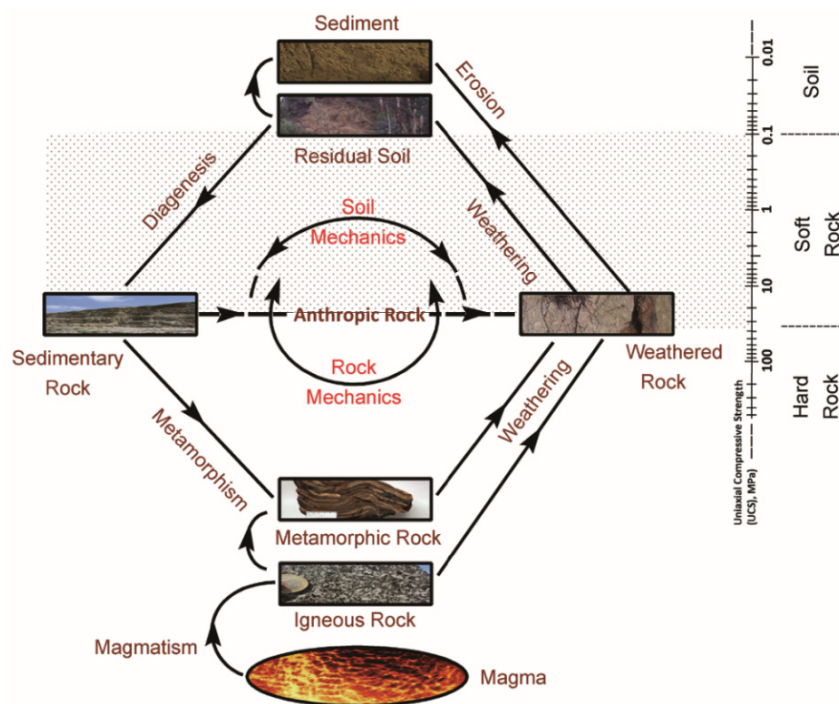


Figure 3 - The rock cycle in a geoscience engineering perspective (Chaminé et al., 2013b). This diagram shows the distinction between rock formation and its strength involving it with the concept of the anthropic intervention. Anthropoc activity causes the change of the rock material considering all the rock made, modified or moved by humans (Underwood, 2001).

Nevertheless, it does not cover the earthy materials forming the ground in which plants can grow (“soil” in a pedological sense). Rocks may be surveyed in several backgrounds: i) at the surface

and subsurface (outcrops, cliffs, quarries, etc.), ii) underground (tunnels, mines, boreholes). Since the dawn of civilization, rock has been used as a construction material. Diverse constructions and structures have been built on, in or of rock, including houses, bridges, dams, tunnels and caverns. Particularly, crushed rock aggregates are fundamental to the man-made environment and represent a large proportion of the raw material produced by the quarrying industries and used in construction (details in Chaminé et al., 2013b).

1.2.2. Global hydrologic system and groundwater circulation

“(...) water in the hydrologic system is constantly moving as vapour, rain, snow, surface runoff, groundwater, and glaciers, or even in ocean waves and currents.” (Hamblin and Christiannsen, 2003)

The hydrologic system involves all the water circulation on Earth. This system unites all possible paths of water into a single, enormous system of motion (Fitts, 2013). The existence of this system is due to the Earth’s position related to the Sun. It is so particular that water is able to exist on Earth in three different states: solid, liquid or gas. If the distance was any different it would be impossible to have all this diversity; if Earth was further away, the oceans would freeze, if it was closer, the oceans would evaporate. Thus, the energy source that powers all this system in motion is the heat from the Sun. As it is heated, water evaporates from oceans, condenses into the clouds and then, through the action of rain, returns to the oceans. The return of water to oceans can also occur by surface runoff in the river system, one of the main sub-systems of the hydrologic system. Another important sub-system is the groundwater system that carries the water that seeps through the ground and moves slowly within the voids in soils and fractures in rocks. Part of the water on the surface runoff does not reach the oceans due to plants evapotranspiration. In Polar Regions or in places with high altitude such as, high mountains, water can be retained for a longer time in glacial ice that melts as the weather gets warmer or moves to a warmer place, and then it joins the ocean by surface runoff. Consequently, the water movement along the surface of the Earth erodes and transport rock material resulting in a continuous change of the landscape (Hamblin and Christiannsen, 2003; Grotzinger et al., 2010).

All the energy that composes the hydrologic system is divided by its sub-systems, being those, rivers, oceans, groundwater, glaciers and wind, to originate the so-called water cycle (Figure 4).

Another major system embodies the interaction between the atmosphere and the oceans. The vast amount of liquid water stored in oceans, together with the gases in the atmosphere create the climate system. As it was said before, the energy source that gives motion to this system,

giving it dynamic properties, is the Sun. The irregular heat transmissions to the Earth's surface provide the conditions to exist convection — as the warm air rises, cool air is drawn in to replace it —, winds to blow, evaporation of water into the atmosphere and drives ocean currents. Evapotranspiration from land occurs as the heat is transferred to the Earth's surface.

The river system returns most water directly to oceans through surface drainage. Due to the very rapid water flow in rivers, the volume of water present on it, at a given time, is not big but the total volume that passes through a river system is much higher. As a result, one of the most predominant structures of landscapes is formed by running water.

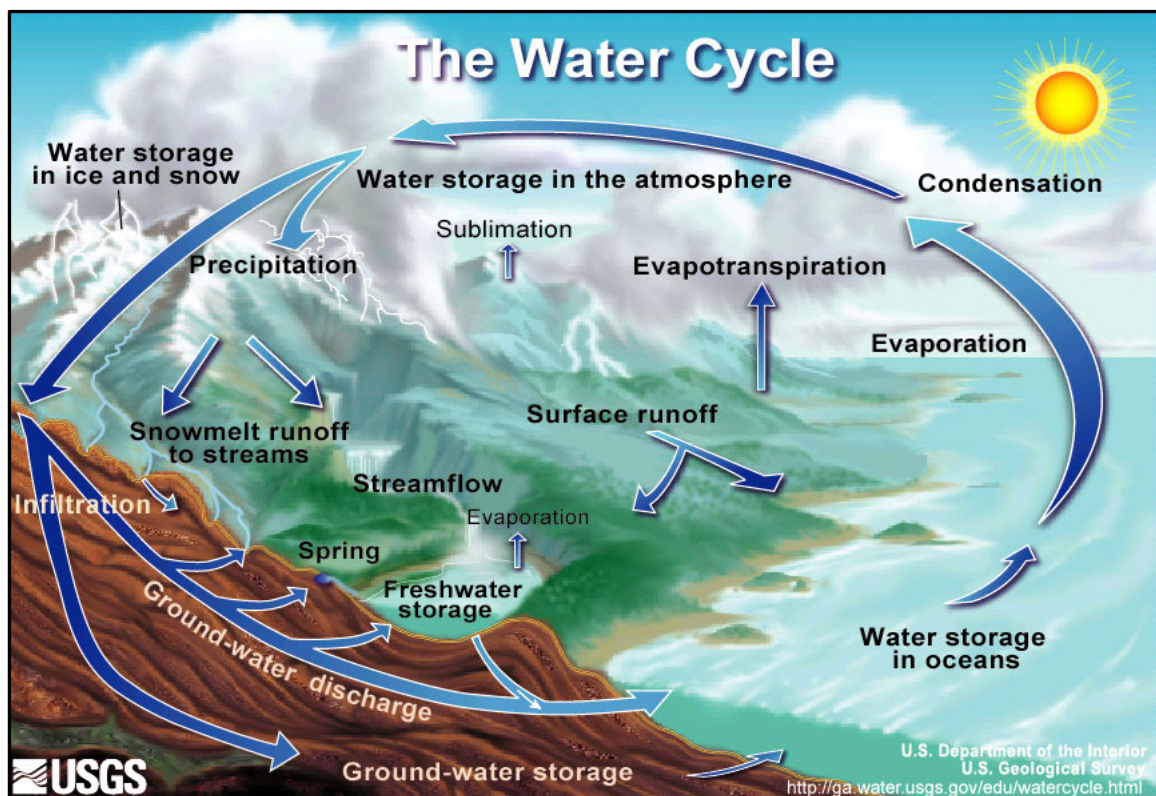


Figure 4 – The hydrologic cycle and all of its components (illustration by Dr. John Evans, USGS). As the sun heats the ocean water it evaporates into the atmosphere. Through the uneven heating of Earth's surface, it causes the atmosphere to convection. This causes the evaporated water to circulate among the atmosphere and condenses, as rain or snow, on continents or oceans. Most of the water that falls on continents returns to the oceans by surface runoff or groundwater seepage. Variations on the flow of this system can be caused by the retention of water in lakes and glaciers (<http://water.usgs.gov/edu/watercyclesummary.html>).

In cold climates, another process takes place. Precipitation falls as snow and most of which remains frozen before returning to the ocean as surface runoff. Glacier sub-system can induce several changes in the normal hydrologic system by retaining water from the water cycle for a longer time. Only until the glaciers melt, water flows back to the sea, seeps into the ground or evaporate to the atmosphere. Almost the whole continent of Antarctica is covered by a

continental glacier that covers an area of 13 million km², which represents an area larger than the United States and Mexico combined. The shores of continents, island or inland lakes are also subjected to a shoreline sub-system. This system acts by the work of waves, tides and currents upon the shores that erode and transport vast quantities of sediments. The convection effect in the atmosphere gives birth to the eolian system. The wind, another fluid that composes the atmosphere is also considered to be a part of the hydrologic system. Thus, it acts on the most arid regions of the planet leaving no completely dry place on Earth, even in the most arid regions where some rain falls and climate patterns change over the years (Hamblin and Christiannsen, 2003).

The last system completing the hydrologic system which is going to be the subject of development of this thesis is the groundwater system applied on fractured rock masses. Groundwater is not rare or unusual. Surprisingly, it represents about 20% of the water that is not on the oceans and it appears everywhere beneath the surface of Earth, occurring not only in humid but in desert or high altitude/cold regions. In many areas, the amount of water that infiltrates the ground, equals or exceeds the surface runoff (Lloyd, 1999; Younger, 2007; Fitts, 2013). Groundwater is also not stationary or motionless. Gravity is the driving force for the flow of this system. When compared with surface runoff, the water movement is very slow and it is controlled by the characteristics of the material through which the water moves namely the permeability and porosity of the rock mass. The groundwater system being a part of a natural open hydrologic system is itself an open system. Water enters in that system when surface water infiltrates the ground (recharge), moves through the voids and leaves the system by discharge in streams, springs or lakes (Fitts, 2013; Fetter, 2014). Along the flow path, groundwater, like river water, can pick up materials and transport them and may also dissolve soluble rocks and create caverns or underground caves (*Karst media*).

It is possible to consider four main types of pore spaces or voids in rocks where air and/or water flow: spaces between mineral grains (void ratio), fractures, solution cavities and vesicles. In sand and gravel, pore spaces may reach 12% to 45% of the total volume, which means they have high permeability as an aquifer. In rocks, porosity is ruled by fractures and, in some denser intact rocks, it is the only significant pore space. When the dissolution of rocks occurs, there is an enlargement of the joints along the way, developing passageways that may turn into caves (limestone). In the volcanic rocks, vesicles are formed near the top of a lava flow and form zones of very high porosity (Hamblin and Christiannsen, 2003) (Figure 5).

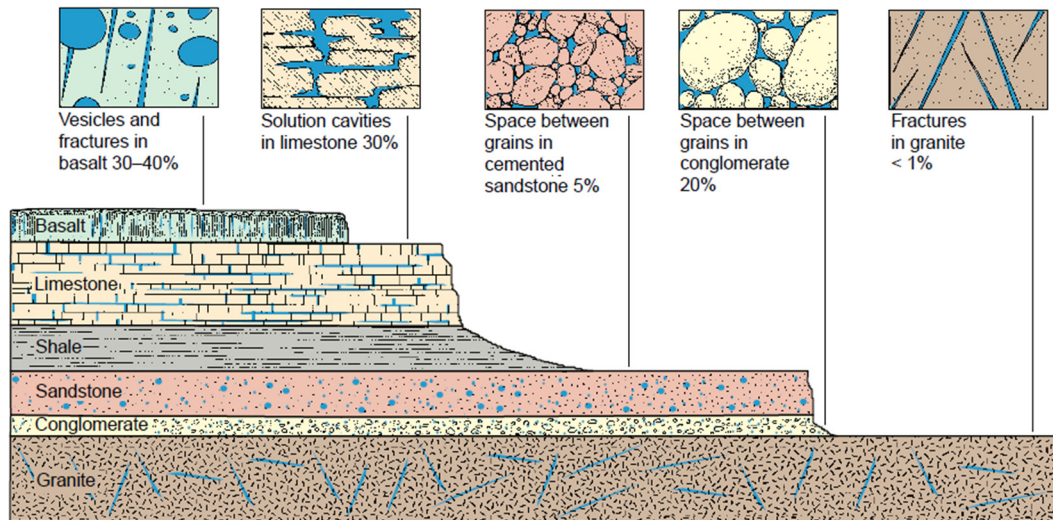


Figure 5 - Types of voids or pore spaces which allow water circulation in rocks (Hamblin and Christiannsen, 2003).

Water is stored in the geological formations by infiltration into the ground by gravity. When there is a natural zone or geological structure saturated with water that conducts water thus has hydraulic conductivity, it is called an aquifer (Fetter, 2014). Aquitard represents a geological formation with low permeability to make them a source of water but allows a slow vertical leakage to the surrounding layers, as shown on Figure 6. Rock materials like silt or clay can be found as aquitards, also described as, semi-confining layers. Aquiclude have the lowest values of hydraulic conductivity and usually appear like confining formations such as, crystalline rocks without fractures or impermeable clay layers. In aquifers, as water seeps into the ground, it passes through two distinct zones, and what distinguish them are the fluids filling the voids. The pore spaces on the region near the surface are mainly composed by water and air forming the zone of aeration while, the region beneath is saturated with water, the saturated zone. The top limit of the saturated zone is the water table or piezometric level. Water table is a definition typically used in unconfined aquifers. For engineering geoscience purposes, it does not give any idea of the working capacity of a hydraulic system. However, the piezometric level can be used to define the level where the water of an aquifer reaches when it is freed to atmospheric pressure. This level is often different from the water table on confined aquifers. The water present on an unconfined aquifer circulates freely, filling and recharging an aquifer through the aeration zone (Figure 6, well A). The amount of water contained in the aquifer is indicated by the height of the water table. However, as we go deeper, the voids tend to close due to the existence of high

tensions on the rock mass, making the presence of water impossible. Thus, the limit or base of the groundwater system is defined.

Another type of aquifer displayed, in Figure 6, is the perched aquifer. This kind of aquifers are one particularly type of unconfined aquifers but generally found above the regular water table. They are found in the zone of aeration where the bottom layer is an impermeable layer composed, for example, by clayed formations. Also, they can be used as a water source with limited usage due to its minor hydraulic capacities, which are controlled by the characteristics of the impermeable layer.

Confined aquifers are permeable rock units with an impermeable layer between them, allowing the circulation of water. They can also be called, artesian aquifer due to the build-up of high pressure water in the confined impermeable layer, causing the piezometric level of the aquifer to be higher than the water table (Figure 6, well B). In igneous and metamorphic rocks, groundwater occurs under confined conditions and usually appears in joints and fractures (see Carvalho, 2006; Fitts, 2013; Fetter, 2014).

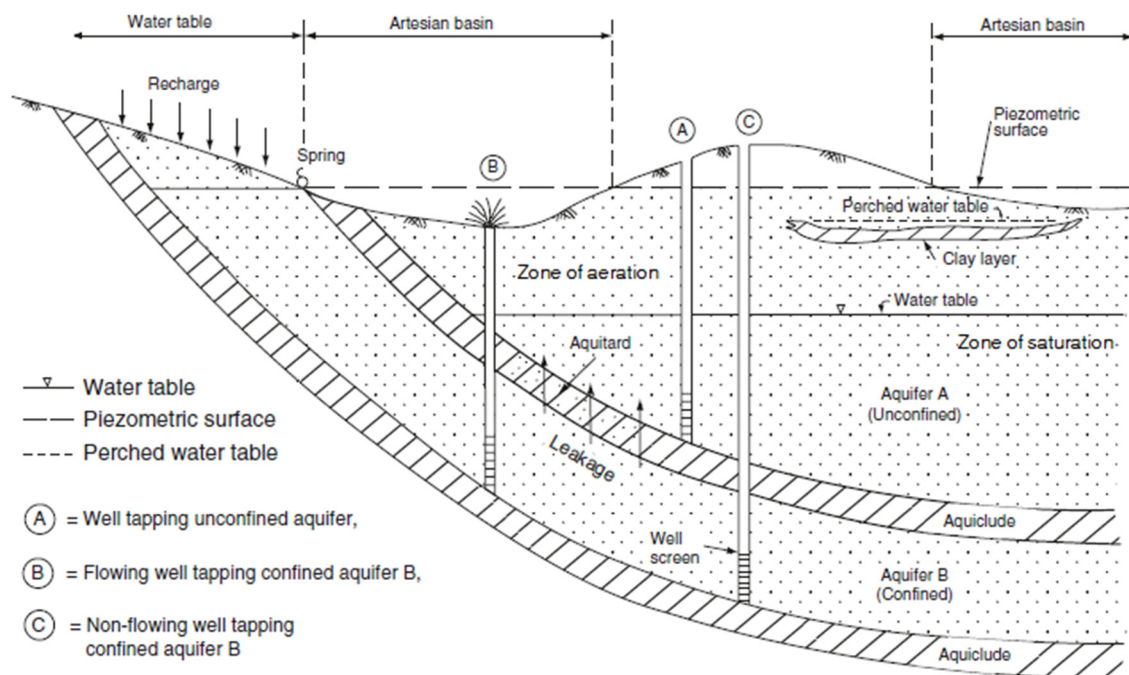


Figure 6 - The different components of underground circulation and the different types of aquifers (Hamblin and Christiannsen, 2003).

1.3. Aims

The main aim of this dissertation goes from the geological and geomechanical study of rock masses, to the application of hydrogeomechanical classifications with thorough hydrogeomechanical zoning map assessment, attaining a full range characterization together with the correspondent hydraulic behaviour. A comprehensive procedural method is proposed to assess rock masses, in terms of hydrogeomechanics. To achieve this goal, hydrogeomechanical classifications and indexes were applied on fractured rock masses (namely HP – Hydro Potential Value from Gates, 1997, 2003, HC – Hydraulic Conductivity System after Hsu et al., 2008, 2011; Jw – Joint Water reduction factor of Q-system after Barton et al., 1974, 1980) and confronted with hydrological and hydraulic well data of the study site (Caldas da Cavaca hydromineral system, in Aguiar da Beira, NW Portugal). The role of hydrogeomechanics on improving hydrogeomechanical conceptual modelling for rock mass sites with hydromineral resources is also analysed.

1.4. Organisation of the dissertation

“When Yves Lacroix asked K. Terzaghi how much time he ought to spend on writing his report, he got the following advice: “Spend on it as much time as necessary to inform the reader with as few words as practicable about all the significant findings and about the essential features of the construction operations which have been performed” (In: Karl Terzaghi – the engineer as artist, by Richard E. Goodman published by ASCE Press, 1999).

The present dissertation is divided into two major parts. The first part includes two chapters that explore a theoretical background approach on the hydrogeomechanics subject. The second part comprises two chapters and constitutes a practical approach to the theme. Moreover the achieved results on a pilot site (Caldas da Cavaca hydromineral system, Aguiar da Beira, NW Portugal) play the main role for the methodological issues raised from the hydrogeomechanical research.

The chapter one of the first part is focused on general geology and hydrogeology knowledge, being outlined by the imperceptible but constant motion, under the general framework of the rock cycle and the global tectonic system, covering briefly the topics about Earth formation and geodynamic changes regarding solid and molten rock material. Still, in an introductory tone, it is presented a brief summary of one of the most beautiful, extraordinary and major natural system, the so-called hydrologic cycle or water cycle, as well as the general aspects of the water circulation system, above and underneath the ground.

The first part of the second chapter attempts to cover all the scientific concepts, in order to understand the central role played by the hydrogeomechanical study in rock engineering.

Concepts, such as the intact rock scale issues and their composition; relationship between rock mass fractures and their hydrogeological features; which joint characteristics have to be considered when assessing a field observation with data collection on a worksheet; how groundwater is driven through rock masses and the parameters that affect it.

The chapter two of the second part presents a brief outline about the evolution of the rock mass classification systems and shows the actual state-of-the-art related to the hydrogeomechanical schemes and indexes. Some of these rock classifications and indexes were proposed on mid-60s and early 70s of 20th century, and were updated throughout the years. Although they are still used in the major type of rock engineering works.

The chapter three addresses all the elements of the study site. It starts with a general description of the study site, followed by its regional and local framework. The sections of this chapter present an overview of the materials and methods used, followed by a display of the data and results. This chapter ends with a discussion about the data results analysis, comprehensively considering what was achieved and what the meaning of these results is. To support this discussion, several maps were created with different types of outputs in order to support the general in situ investigation, the role of hydrogeomechanics and the conceptual model of the site. The final chapter outline the main conclusions of the research with an outlook of the future possibilities within this field of study.

Figure 7 illustrates the conceptual flowchart representing the methodologies used in this dissertation.

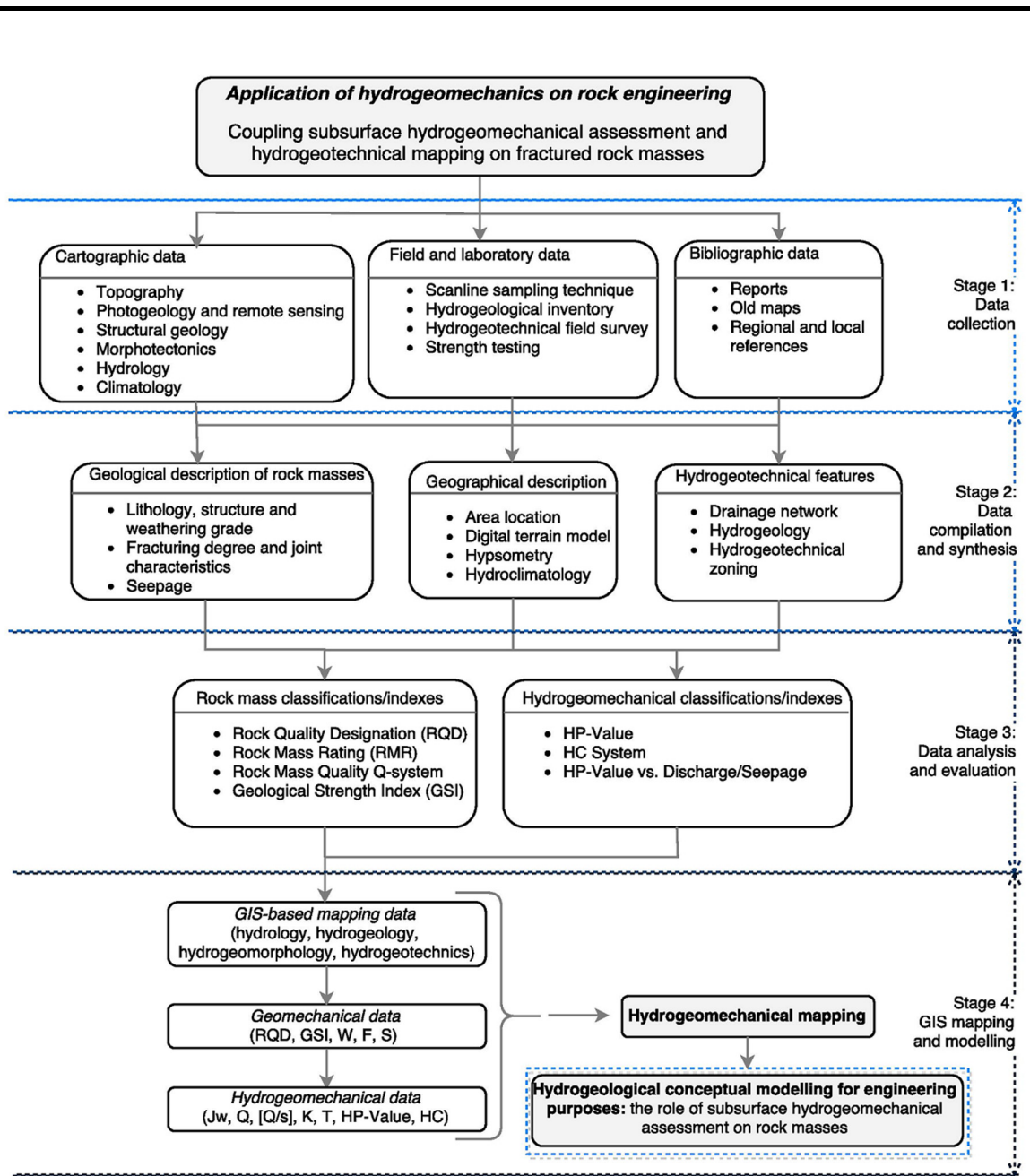


Figure 7 – Conceptual flowchart representing the methodologies used in the current research: “hydrogeomechanics for rock engineering: coupling hydrogeomechanics classifications and hydrogeotechnical mapping on fractured rock masses”.



Chapter 2.

Hydrogeomechanical issues from a rock engineering point-of-view: an outline

Synopsis

To study how water flows in rock masses, it is required to understand its different components and applicable laws. In order to do so, a comprehensive description, analysis and assessment between various types of rocks and different flowing characteristics with, diverse existent methods were assembled on the rock mass, to fulfil the specific requirements of hard rock hydrogeology and rock engineering. This chapter is an overlaying of theoretical concepts necessary to understand how the water flow is formed and circulates with, an emphasis on fractured rock masses and its complex nature, as well as, the hydrogeomechanical behaviour of rock media.

2.1. Description of the rock masses: an engineering geoscience perspective

Concerning rock masses it is essential to define two important concepts in rock engineering: intact rock and rock mass. Intact rock is an “element constituted by granules or crystals, bound by permanent cohesive forces, with no discontinuities”, whereas rock mass is a “physical body constituted by blocks of intact rock separated by discontinuities” (Hoek, 2007; Scesi and Gattinoni, 2009; Palmström and Stille 2010). These concepts, along with a few more inputs, regulate the flowing methods and geomechanical schemes designed to study fractured rock masses and its formations, being discontinuities the higher subject of significance to study. In short, rock mass is referred to an assemblage of rock material separated by rock discontinuities, mostly by joints, bedding planes, dyke intrusions and faults (Abbas and Konietzky, 2015).

Permeability, transmissivity and groundwater flow are important characteristics of fractured hard rocks, particularly for their quantitative aspects, on attaining main flow paths representation along joints, fractures, shear zones, faults and other discontinuities types (details in Scesi and Gattinoni, 2009; Singhal and Gupta, 2010; Gustafson, 2012).

2.1.1. Rock discontinuities: genesis, types and characteristics

“The discontinuities network divides the rock in portions and the water flow is strongly influenced by the geometric and mechanical characteristics of those vacuums.” (Scesi and Gattinoni, 2009)

Discontinuities are the most important feature on rock mass, since they convert the rock mass on a discontinuous and anisotropic material, allowing the water to flow along planes of fracture and weathering (CFCFF, 1996). They are used to define any plane of separation or weakness in a rock mass. Strength, deformability and permeability characteristics of a rock-mass are strongly influenced by its discontinuities. Scanline surveys are a reliable technique in which a line is drawn over an outcropped rock surface and all the discontinuities intersecting the line are described after the geotechnical parameters proposed by ISRM (1981). The discontinuity geometry for a rock-mass is characterised by the number of discontinuity sets, mean density and the

distributions for location, orientation, size and spacing/fracture intercept (Chaminé et al., 2015), Figure 8.

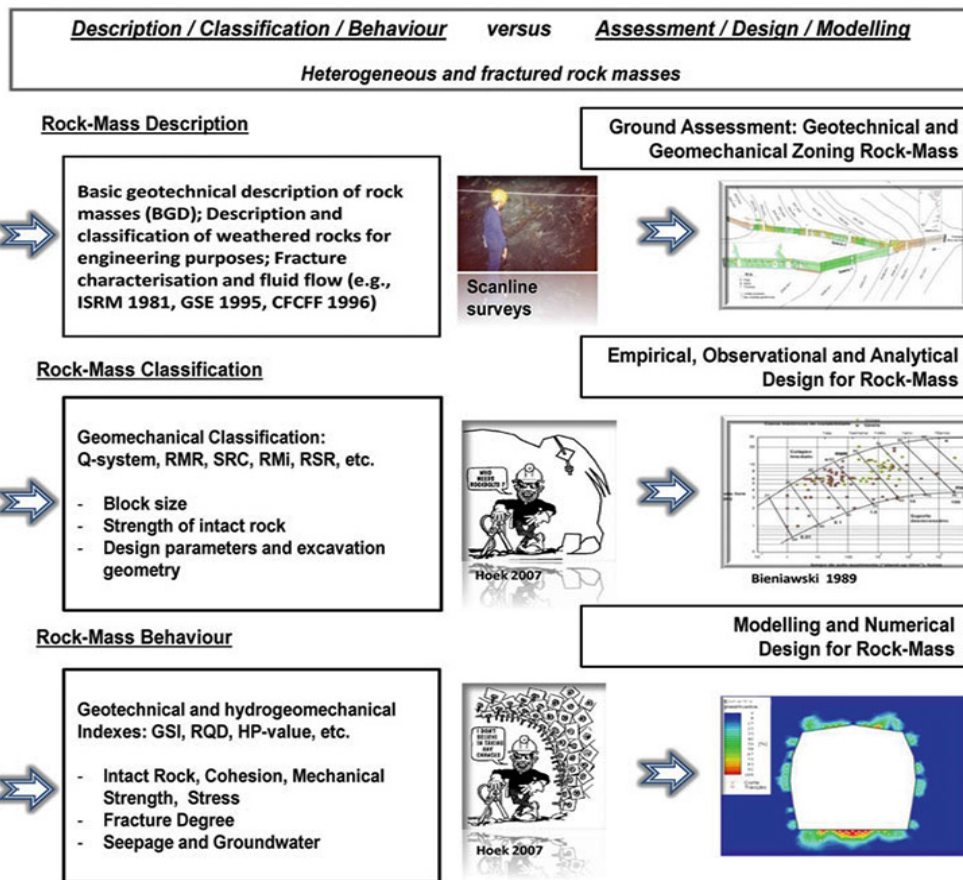


Figure 8 – The description/classification/behaviour versus assessment/design/modelling of heterogeneous and fractured rock masses (Chaminé et al., 2015).

When this approach is applied, under an engineering perspective, its studies can be used in various fields, such as, engineering geology, geological engineering, geotechnical engineering, civil engineering or mining engineering. For example, the stability level of a foundation or excavation on a rock mass depends on the orientation, weathering degree, fracturing grade, seepage and strength of the rock discontinuities. Water circulation in rocks occurs through a system of voids that is quite different from the ones on soils regarding dimensions, shape and density. In most rock masses, water circulation occurs through the many primary discontinuities (stratification, schistosity) and/or secondary discontinuities (joints, fractures, faults, karstic cavities). Table 1 shows the main types of discontinuities, as well as its features and relationship to groundwater occurrence.

Table 1 - Different discontinuities types: its formation, characteristics and relation to groundwater occurrence (compiled from: Scesi and Gattinoni, 2009; Singhal and Gupta, 2010; Gustafson, 2012).

Discontinuities types						
Type	Bedding planes	Karstic cavities	Faults and shear zones	Joints	Foliation planes	
					Gneissic banding	Schistosity
Characteristics	Sedimentary rocks marked by well-defined divisional planes separating it from layers above and below	Cavities formed by dissolution of the rock	Represented by a break along the rock mass where there has been displacement of the sides, relative to each other, formed throughout geological time	Fracture or failure surfaces where there has been little or no displacement of the joint walls	Tectonic origin and occur in rocks that were under medium to high conditions of temperature and pressure. They are formed perpendicularly to the maximum compressive stress and the smaller the grain of the rock, the more likely these systematic discontinuities are to develop	
Observation scale	Over a wide area, with spacing between beds ranging from a few centimeters to several meters	From a few meters to km	Minor faults ranging from decimeter to a meter and major faults from several metres to hundreds of metres	From a few meters to km	From a few meters to Km	
Rock formations	Sedimentary rocks	Limestones and dolomites	Rocks under conditions of high pressures or temperatures	Magmatic and metamorphic formations	Gneisses	Schists and shales Slates
Features for groundwater occurrence	Intergranular pore spaces	Fractures and solution cavities	Weathered horizon, fault spacing and lineaments, fault gouges	Aperture, roughness, filling, continuity, persistence, joint stress condition, number of sets		Similar joint study

2.1.2. The importance of joints and its characteristics

Along the late 60s and the beginning of the 70s of the XX century, there was the need to connect geology with engineering. By that time, the International Society for Rock Mechanics (ISRM) apprehended that necessity by creating a relation between the rock mass structure and lithology description with the nature of the discontinuities (e.g., ISRM, 2007). The ability of quantifying these parameters gave continuity to the understanding of stability analysis on rock masses, as well as, any type of study involving the physical and mechanical behaviour of it. In the present study, the relation of the discontinuities characteristics and all of its knowledge are applied on a hydrogeomechanical perspective.

The discontinuities orientation addresses a major issue on the water flow path. Discontinuities with different orientations form a grid of intersecting surfaces that allow water flowing through more paths. Merging this concept with discontinuities with a closer spacing and a higher persistence increases the possibility of their intersection due to a larger discontinuities frequency. The roughness found along a discontinuity creates more or less friction force on water along its percolation that permits, with wider apertures, higher yield values on the final hydraulic conductivity. If the filling of a discontinuity is a consolidated clay, then water flow is almost impossible, however, if it is unconsolidated sand, there exist more possibilities of water occurrence along the discontinuity. Water seepage along a discontinuity represents a major indicator of water presence, since it verifies the possibility of water flowing on it. Discontinuity walls that show lower values of shear strength augment the possibility of water percolation due to weaker forces binding the rock mass (details in Scesi and Gattinoni, 2009; Singhal and Gupta, 2010; Gustafson, 2012).

In Table 2 it is possible to observe the main discontinuities characteristics to acquire in a field survey and data collection, with their respective basic description, methodologies and/or techniques, and subsequent classification (ISRM, 1981; GSE, 1995; CFCFF, 1996) with a representative scheme, showing a simple example layout.

Table 2 - Summary of the main geological and geotechnical parameters of discontinuities: basic description and methods/techniques (compiled from: ISRM, 1978, 1981; GSE, 1995; CFCFF, 1996).

Parameter	Description	Determination method	Description and classification	Representative scheme																														
Lithology/Structure Weathering grade	Depends on the type of material appearing in most quantity on the study area. The state of weathering resulting physical and chemical processes may be	Visual observation and macroscopic petrographic description; could be complemented with microscopic analysis.	Geology: lithology and structure Weathering grade codes for engineering purposes by ISRM (1978, 1981) and GSE (1995)																															
Orientation	The orientation of a discontinuity in space. It is described by the dip direction (azimuth - angle with respect to north) and dip of the line of steepest declination in the plane of the discontinuity (angle with horizontal plane).	Geologist compass: magnetic compass with clinometer.	Orientation: dip and dip-direction (planes) or plunge and plunge-direction (lines)																															
Fracturing degree: Spacing/ Fracturing intercept	The spacing between discontinuities conditions the block size of intact rock. Thus, it represents a major characteristics when defining the mechanical behaviour of the rock mass. It is defined as the distance measured perpendicularly between two discontinuity planes belonging to the same set.	Measured line with a length big enough for coverage of a representative part of the frequency of discontinuities.	<table border="1"> <thead> <tr> <th colspan="2">Description of spacing</th> <th>Description term</th> </tr> </thead> <tbody> <tr> <td>Spacing (cm)</td> <td>Symbol</td> <td></td> </tr> <tr> <td>> 200</td> <td>F1</td> <td>Very wide spacing</td> </tr> <tr> <td>60 - 200</td> <td>F2</td> <td>Wide spacing</td> </tr> <tr> <td>20 - 60</td> <td>F3</td> <td>Moderate spacing</td> </tr> <tr> <td>6 - 20</td> <td>F4</td> <td>Close spacing</td> </tr> <tr> <td>< 6</td> <td>F5</td> <td>Very close spacing</td> </tr> </tbody> </table>	Description of spacing		Description term	Spacing (cm)	Symbol		> 200	F1	Very wide spacing	60 - 200	F2	Wide spacing	20 - 60	F3	Moderate spacing	6 - 20	F4	Close spacing	< 6	F5	Very close spacing										
Description of spacing		Description term																																
Spacing (cm)	Symbol																																	
> 200	F1	Very wide spacing																																
60 - 200	F2	Wide spacing																																
20 - 60	F3	Moderate spacing																																
6 - 20	F4	Close spacing																																
< 6	F5	Very close spacing																																
Roughness	The roughness of a discontinuity is associated with the irregularities of the discontinuity walls. By evaluating the roughness of a discontinuity it's possible to have an indication of its shear strength.	Visual observation appealing to touch sensitivity with a comparison to a standard surface.	<table border="1"> <thead> <tr> <th colspan="2">Description of roughness</th> <th>Profile form</th> </tr> </thead> <tbody> <tr> <td>Class</td> <td>Description</td> <td></td> </tr> <tr> <td>I</td> <td>Smooth</td> <td>Stepped</td> </tr> <tr> <td>II</td> <td>Slightly-irregular</td> <td></td> </tr> <tr> <td>III</td> <td>Rough</td> <td></td> </tr> <tr> <td>IV</td> <td>Smooth</td> <td>Undulating</td> </tr> <tr> <td>V</td> <td>Slightly-irregular</td> <td></td> </tr> <tr> <td>VI</td> <td>Rough</td> <td></td> </tr> <tr> <td>VII</td> <td>Smooth</td> <td>Planar</td> </tr> <tr> <td>VIII</td> <td>Slightly-irregular</td> <td></td> </tr> </tbody> </table>	Description of roughness		Profile form	Class	Description		I	Smooth	Stepped	II	Slightly-irregular		III	Rough		IV	Smooth	Undulating	V	Slightly-irregular		VI	Rough		VII	Smooth	Planar	VIII	Slightly-irregular		
Description of roughness		Profile form																																
Class	Description																																	
I	Smooth	Stepped																																
II	Slightly-irregular																																	
III	Rough																																	
IV	Smooth	Undulating																																
V	Slightly-irregular																																	
VI	Rough																																	
VII	Smooth	Planar																																
VIII	Slightly-irregular																																	
Persistence/ Continuity	The persistence of a discontinuity represents the size of it within a plane. It can be of difficult quantification due to the limited observation space on the outcrop or exposed rock site.	Measured with a measuring tape.	<table border="1"> <thead> <tr> <th colspan="2">Description of persistence</th> </tr> </thead> <tbody> <tr> <td>Persistence Length (m)</td> <td></td> </tr> <tr> <td>Very low</td> <td>< 1</td> </tr> <tr> <td>Low</td> <td>1 - 3</td> </tr> <tr> <td>Medium</td> <td>3 - 10</td> </tr> <tr> <td>High</td> <td>10 - 20</td> </tr> <tr> <td>Very high</td> <td>> 20</td> </tr> </tbody> </table>	Description of persistence		Persistence Length (m)		Very low	< 1	Low	1 - 3	Medium	3 - 10	High	10 - 20	Very high	> 20																	
Description of persistence																																		
Persistence Length (m)																																		
Very low	< 1																																	
Low	1 - 3																																	
Medium	3 - 10																																	
High	10 - 20																																	
Very high	> 20																																	
Aperture	Its the perpendicular distance separating discontinuity walls when there is no filling. This parameter has the tendency to decrease with depth and may even close.	Measured with a measuring tape.	<table border="1"> <thead> <tr> <th colspan="2">Classification of discontinuity aperture</th> </tr> </thead> <tbody> <tr> <td>Aperture</td> <td>Description</td> </tr> <tr> <td>< 0.1 mm</td> <td>Very tight</td> </tr> <tr> <td>0.1 - 0.25 mm</td> <td>Tight</td> </tr> <tr> <td>0.25 - 0.5 mm</td> <td>Partly open</td> </tr> <tr> <td>0.5 - 2.5 mm</td> <td>Open</td> </tr> <tr> <td>2.5 - 10 mm</td> <td>Widely open</td> </tr> <tr> <td>1 - 10 cm</td> <td>Very widely open</td> </tr> <tr> <td>10 - 100 cm</td> <td>Extremely widely open</td> </tr> <tr> <td>> 1 m</td> <td>Cavernous</td> </tr> </tbody> </table>	Classification of discontinuity aperture		Aperture	Description	< 0.1 mm	Very tight	0.1 - 0.25 mm	Tight	0.25 - 0.5 mm	Partly open	0.5 - 2.5 mm	Open	2.5 - 10 mm	Widely open	1 - 10 cm	Very widely open	10 - 100 cm	Extremely widely open	> 1 m	Cavernous											
Classification of discontinuity aperture																																		
Aperture	Description																																	
< 0.1 mm	Very tight																																	
0.1 - 0.25 mm	Tight																																	
0.25 - 0.5 mm	Partly open																																	
0.5 - 2.5 mm	Open																																	
2.5 - 10 mm	Widely open																																	
1 - 10 cm	Very widely open																																	
10 - 100 cm	Extremely widely open																																	
> 1 m	Cavernous																																	
Filling	The space between the discontinuity walls can be filled with rock material, different from that of the wall rock. Since there are many varieties of fill with different mechanical responses, such as, clay or smashed rock, the filling material should be recognised and well described. Properties such as nature, shear strength and permeability of filling material are of maximum interest.	Visual observation with a measuring tape. The width should be measured while the material itself should be classified depending on its nature.	The classification is made due to the material typologic, e.g., soft clay, smashed rock, etc.																															
Wall strength	Corresponds to the uniaxial compression strength of the wall. It influences the shear strength and deformability of the rock mass. The degree of weathering of the discontinuity walls is lesser than the intact rock due to alteration processes on the walls.	Visual observation appealing to touch sensitivity.	<table border="1"> <thead> <tr> <th colspan="2">Uniaxial compressive strength of the rock</th> <th>Description terms</th> </tr> </thead> <tbody> <tr> <td>Interval (MPa)</td> <td>Symbol</td> <td></td> </tr> <tr> <td>> 200</td> <td>S₁</td> <td>Very high</td> </tr> <tr> <td>60 - 200</td> <td>S₂</td> <td>High</td> </tr> <tr> <td>20 - 60</td> <td>S₃</td> <td>Moderate</td> </tr> <tr> <td>6 - 20</td> <td>S₄</td> <td>Low</td> </tr> <tr> <td>< 6</td> <td>S₅</td> <td>Very low</td> </tr> </tbody> </table>	Uniaxial compressive strength of the rock		Description terms	Interval (MPa)	Symbol		> 200	S ₁	Very high	60 - 200	S ₂	High	20 - 60	S ₃	Moderate	6 - 20	S ₄	Low	< 6	S ₅	Very low										
Uniaxial compressive strength of the rock		Description terms																																
Interval (MPa)	Symbol																																	
> 200	S ₁	Very high																																
60 - 200	S ₂	High																																
20 - 60	S ₃	Moderate																																
6 - 20	S ₄	Low																																
< 6	S ₅	Very low																																
Seepage	Water present in the discontinuity due to the its percolation through the rock mass. This water flow, depending on yield, usually indicates weathering on the rock mass or some instability problems.	Visual observation appealing to touch sensitivity.	Dry Slightly humid, Humid, Dropping, Flowing																															

2.1.3. Rock sampling techniques and engineering geoscience mapping

A clear geology and structural geology framework play a key-role to support the investigation of all rock engineering projects (e.g., Hudson and Cosgrove, 1997; Hoek, 2007; de Freitas, 2009; Chaminé et al., 2013b, 2015; Shipley et al., 2013). The heterogeneity of the geological properties of rock masses is very significant in geoengineering issues (Hudson and Cosgrove, 1997). In addition, the evaluation based on engineering geosciences, geohydraulic and geotechnical features of rock masses involve combining parameters to derive quantitative geomechanical classifications for geoengineering design (e.g., Bieniawski, 1973, 1989, 1993; Barton et al., 1974, 1980; Gates, 1997, 2003; Smith, 2004; Barton and Bieniawski, 2008; Hoek et al., 2013; Celada et al., 2014a,b).

Discontinuity surveys are based on collecting rock data from fieldwork and are an essential component of rock-mass quality estimation in rock engineering. Scanline surveys will provide an amount of reliable information concerning structural geology, petrophysical and geotechnical features of rock masses, either in boreholes or exposed rock surfaces (Chaminé et al., 2015; Watkins et al., 2015), Figure 9. However, some procedures must be fulfilled to avoid systematic or random errors (Terzaghi, 1965; ISRM, 1981; Priest, 1993; CFCFF, 1996; Hudson and Cosgrove, 1997; Chaminé et al., 2015). Collecting data for the basic geotechnical description of rock masses is of considerable importance for the prediction of scale effects in rock mechanical behaviour (Cunha and Muralha, 1990).

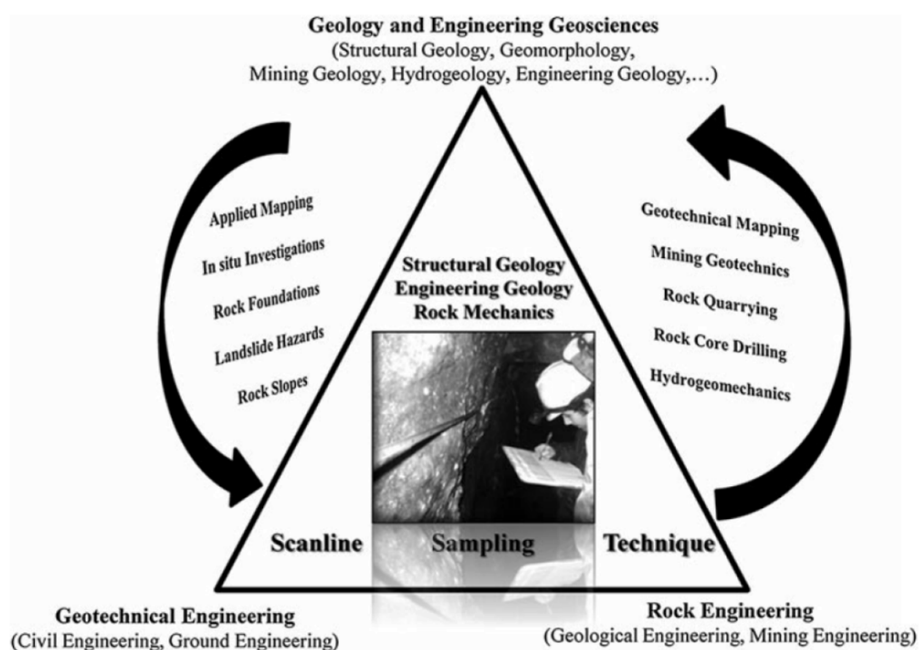


Figure 9 - The main scientific and technical fields of applications of scanline sampling technique surveys related to engineering geosciences, rock engineering and geotechnical engineering (Chaminé et al., 2015).

Linear and circular sampling or sampling within windows along a scanline are accurate approaches to the systematic record of rock discontinuities (joints, fractures, faults, veins, etc.) in the field (Figure 10). The linear scanline technique tends to be favoured as it is a fast method for recording a wide range of fracture attributes. This technique involves laying a tape on an outcrop and measuring attribute (including orientation, length, aperture, intensity, fracture fill and spacing) of each fracture that intersects the tape (Priest, 1993; Chaminé et al., 2015; Mahé et al., 2015; Watkins et al., 2015).

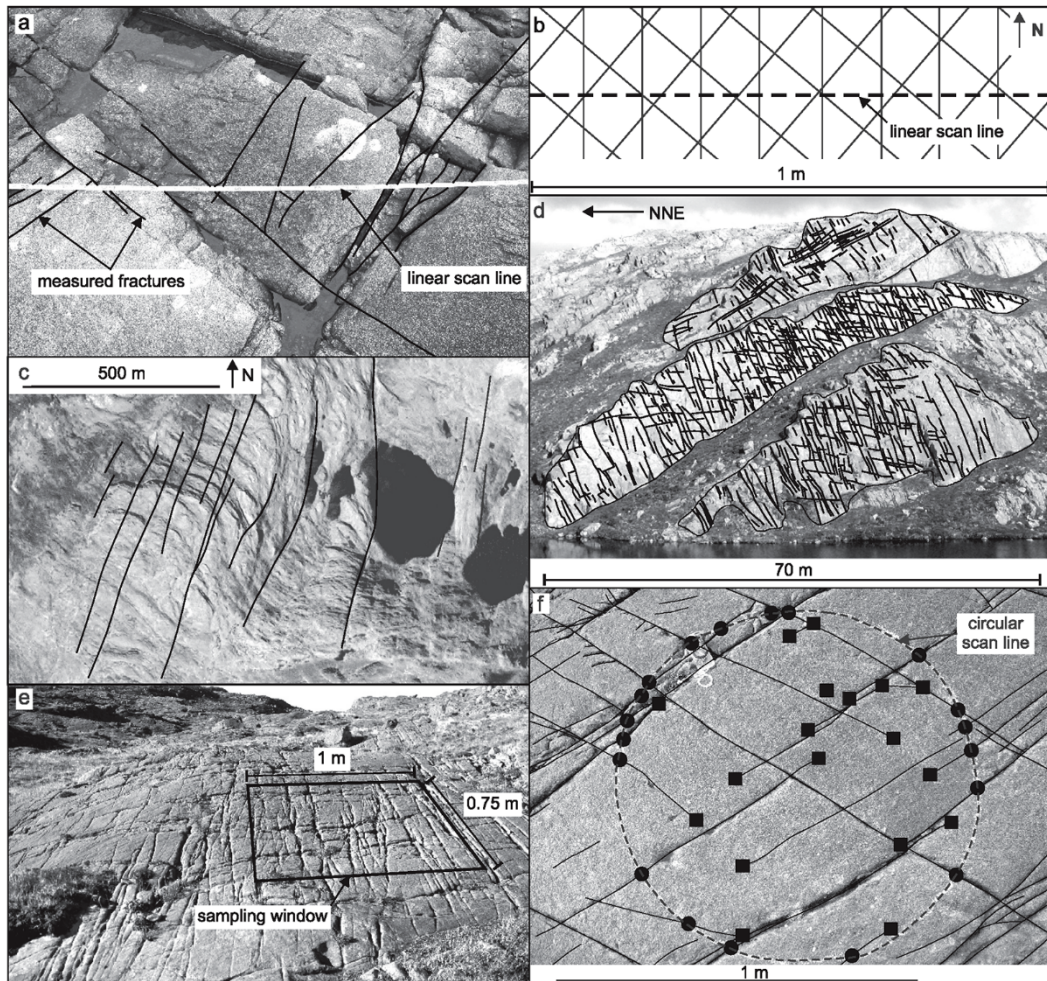


Figure 10 – Examples of rock scanline techniques (after Watkins et al., 2015): a) Fractures attributes, including orientation, length, aperture, spacing and fracture fill are measured for each fracture that intersects a linear scanline (tape measure). b) Three evenly spaced fracture sets at different orientations (N-S, NE-SW, NW-SE) recorded on a linear scanline (dashed line). True spacing for each set is 11 cm, and true intensity is 8 per metre; only the true spacing and intensity of fractures perpendicular to the scan line (N-S set) are recorded as the other two sets are oblique to the scan line, giving 15 cm spacing and only 6 fractures per metre. c) Large scale discontinuities mapped using areal sampling from an aerial photograph. d) Fracture traces mapped onto bedding planes from a field photograph. e) Fracture attributes, including orientation, length, aperture, spacing and fracture fill are measured for each fracture within a sampling area (black box) using rectangular window sampling. f) Circular scan line data collection; fracture intersections with the sampling circle (black dots) and fracture terminations within the circle (black squares) are counted to estimate fracture intensity, density and mean trace length.

Discontinuity features play a major role in controlling the mechanical behaviour of a rock-mass (Priest and Hudson, 1976, 1981; Hudson and Priest, 1983; Priest, 1993; Dinis da Gama, 1995; Chaminé et al., 2015; Mahé et al., 2015; Watkins et al., 2015). ISRM (1981) stated that a scanline survey is a practical technique for collecting and describing rock fracturing on a rock-mass exposure (Figure 11).

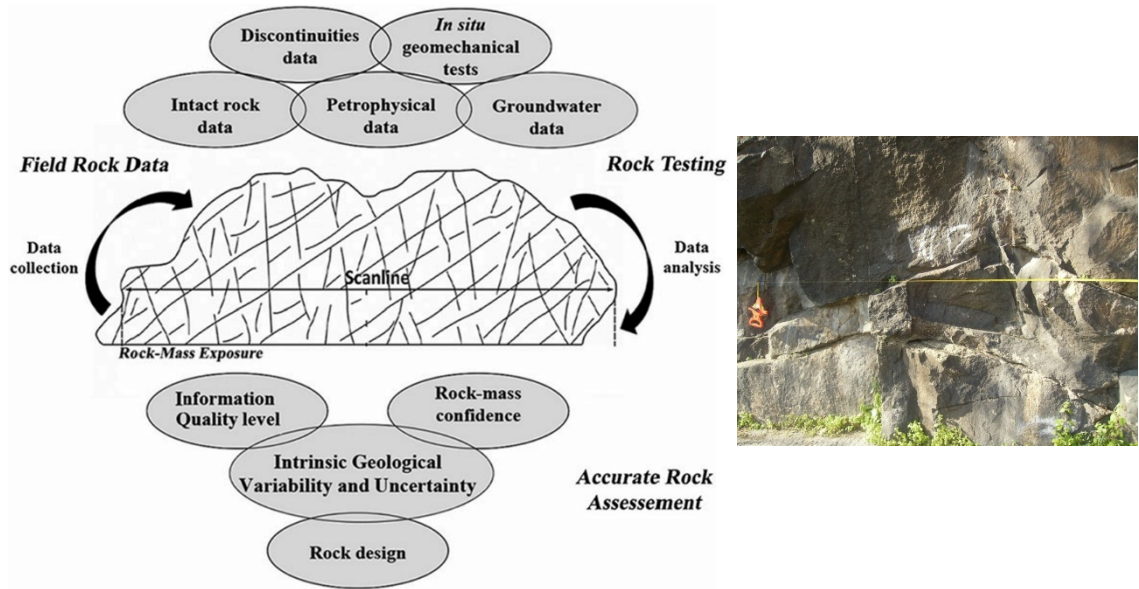


Figure 11 – Illustration of scanline sampling technique applied on a fractured rock mass for determination of discontinuity characteristics. Rock scanline surveys framework to rock design (slope, tunnel, quarry and cavern): a reliable tool to reduce the intrinsic geologic variability and uncertainty (adapted from Chaminé et al., 2015).

The rock sampling technique and the rock mass zone mapping are measures of extreme importance when studying a site for an engineering work, such as a dam, a building or any other type of work involving rock masses. They combine some of the characteristics described above, to group zones with similar characteristics along the rock mass to study; at first glance, the rock mass can be distinguished within its general differences. With the division of the rock mass in zones, geo-professionals can assign specifically measures for each zone. These geotechnical units and their spatial distribution are generally established from the lithological heterogeneities, origin and geological characteristics of the materials, specified from existing information and geological maps, photointerpretation, field observations and measurements (Gonzalez de Vallejo and Ferrer, 2011). To start the definition of different zones, it is necessary to obtain all the different characteristics of discontinuities. To obtain the characteristics the scanline sampling technique is applied.

Therefore, in each planar discontinuity (being it a bedding plane, a foliation plane or a simple fracture or joint) intersected by the measured scanline, it is made a data collection of some

geotechnical specifications, such as (ISRM, 1978, 1981): height and location of the scanline; orientation; number of discontinuity sets and mean density; orientation of the surface outcrop or exposed rock mass; observed lithology and weathering grade; distributions for location, orientation, size and spacing/fracture intercept.

It is also collected and described several discontinuity characteristics of the rock mass, such as (Chaminé and Gaspar, 1995; Dinis da Gama, 1995; Brady and Brown, 2004; Chaminé et al., 2013b, 2015):

- Discontinuity distance to the beginning of the measured line (D);
- Semi-length of the exposed part of the discontinuity, measured only above the scanline (L);
- Termination type of the discontinuity, whether it is on the rock (R), in another discontinuity (D) or unknown (O);
- Orientation of the discontinuity measured on the point of intersection between the scanline and the discontinuity itself;
- Discontinuity curvature, measured between C1 – planar surface, and C5 – very curved surface;
- Discontinuity roughness, measured between R1 – flat surface, and R5 – very rough surface;
- Other properties (seepage, aperture, filling, etc.).

After collecting the data with the added topographical map data of the referred zone, an engineering geoscience zoning map or geotechnical zoning map is established (see Figure 11). Geotechnical zoning combines zones where rock mass share the same characteristics, defining units geotechnically homogeneous. The, to be defined, degree of homogeneity of a unit depends on the scale, the purpose of the map and the data available, since one unit can be divided into sub-units.

2.2. Groundwater flow in rock masses

The fundamental causes for groundwater's active role in nature are its ability to interact with the environment and the systematised spatial distribution of its flow. Interaction and flow occur simultaneously at all scales of space and time, although at correspondingly varying rates and intensities (Tóth, 1999).

In the first chapter it has been referred the different types of permeability related to the water circulation on rock masses. In hydrogeology, it is necessary to quantify the water storage and

transmission capacity of an aquifer to be able to evaluate hydrogeological formations and their characteristics/limitations. Thus, there are a few basic parameters that describe how geological formations can contain and transmit water.

2.2.1. Porosity, storage coefficient, permeability, transmissivity and specific capacity

The definition of porosity states that this parameter is the ratio between the pore volume and the total rock volume. It is a dimensionless parameter and depends only on the rock or soil composition (Wang, 2000; Gonzalez de Vallejo and Ferrer, 2011) Depending on the rock nature, the voids can be intergranular spaces in sedimentary formations or fractures/fissures in fractured rocks. There are two approaches to porosity depending on the pores connectivity. The first method defines the total porosity, n , and relates to the total pore volume – even if the pores are connected or not. The second approach represents the effective porosity, n_e , as a ratio between the pores that are connected, where water can circulate freely, and the total volume of a representative sample of the medium.

Storage coefficient (S) represents the aquifer's capacity to retain water. Normally is defined as the volume of water which a prism with unit base and height, representing an aquifer, releases when the piezometric surface falls 1m. It is a physical dimensionless parameter of the aquifer that characterises the volume of water released per volume unit.

Permeability, evaluates the formation's water transfer capacity depending on its texture but not relating it to the structure or geometric form. Effective permeability or hydraulic conductivity, k , is a type of permeability linked to the textural characteristics of the physical medium and the fluid it transmits, while intrinsic permeability (K) only depends on the internal characteristics of the permeable medium. It is possible to relate these intrinsic permeability and effective permeability with parameters relating the fluid characteristics, resulting in, respectively, kinematic viscosity and dynamic fluid viscosity. The effective permeability, k , can be measured as cm/s or m/day while, the intrinsic permeability K , is usually measured as a $[L]^2$ unit, like, m^2 .

Transmissivity (T) is the rate at which water can pass through the full thickness of aquifer per unit width under a unit hydraulic gradient. The transmissivity in a uniform aquifer is the hydraulic conductivity (K) multiplied by the saturated aquifer thickness (b), (Misstear et al., 2006), as shown on the following formula [1]:

$$T = K \times b, (m^2/day); \quad [1]$$

A number of simplifications have been proposed to evaluate the transmissivity, considering specific capacity, defined as the ratio of total discharge to total drawdown (Q/s). Three different

approaches are presented here, including that by Logan (1964; In: Misstear et al., 2006) [2], Huntley et al. (1992) [3] and Batu (1998) [4]:

$$\text{Logan (1964): } T = 1,22x \left[\frac{Q}{s} \right], (\text{m}^2/\text{day}); \quad [2]$$

$$\text{Huntley et al. (1992): } T = Kx \left[\frac{Q}{s} \right]^{1,18}, (\text{m}^2/\text{day}); \quad [3]$$

$$\text{Batu (1998): } T = 1,385x \left[\frac{Q}{s} \right], (\text{m}^2/\text{day}); \quad [4]$$

The coefficient K for Huntley et al. (1992) formula is given in the Table 3.

Table 3 - Values of the coefficient K (Huntley et al., 1992).

τ	Q/s						
	m^2/s	m^2/min	m^2/day	ft^2/s	ft^2/min	ft^2/day	gpm/ft
m^2/s	0,93	0,0074	1,40E-08	0,056	4,50E-04	8,40E-08	4,20E-05
m^2/min	55,8	0,445	8,30E-05	3,38	0,027	5,10E-06	0,0025
m^2/day	80300	640	0,12	4870	38,8	0,0073	3,61E+00
m^3/yr	2,90E+07	2,30E+03	43,9	1,78E+06	1,42E+04	2,66E+00	1,32E+03
ft^2/s	10	0,078	1,50E-05	0,61	0,0048	9,10E-07	4,50E-04
ft^2/min	600	4,78	9,00E-04	36,4	0,29	5,40E-05	2,70E-02
ft^2/day	8,64E+05	6890	1,29	52400	418	7,80E-02	3,89E+01
ft^2/yr	3,16E+08	2,52E+06	4,72E+02	1,91E+07	1,53E+05	2,86E+01	1,42E+04

2.2.2. Darcy's Law

Darcy's law is mainly applicable to porous media; consequently, it will not be described in full extent but with a surficial approach regarding the key points of its conceptualisation. Darcy's Law was formulated in 1856, stating that "the discharge Q , which passes through a permeable medium, is proportional to the cross sectional area normal to flow of the permeable medium, A , and the piezometric gradient between the entry and exit of the flow in the permeable medium, i (Gonzalez de Vallejo and Ferrer, 2011). The piezometric gradient or hydraulic gradient, i , is defined as a ratio between the difference of two hydraulic heights (usually in meters) and the flow path length between the two piezometers (also in meters).

By combining the above relations, Darcy's law can be written as [5]:

$$Q = KAi = KA \frac{dh}{dx} \quad [5]$$

A second approach to Darcy's law can be written as [6]:

$$q = V = \frac{Q}{A} = K \frac{dh}{dx} \quad [6]$$

Where, V (or q), is the specific discharge or Darcy velocity. This velocity implies that the flow occurs through the entire cross section of the aquifer; however, in nature the actual flow takes place only through the interstitial spaces (pores). Thus, in the previous equation 2, the parameter A is switched for the total porosity of the studied material, n . If the purpose is to study the average velocity (interstitial velocity) one should use the effective porosity (n_e), instead of the total porosity. Darcy's law governs the flow of groundwater in porous media except in some situations where either the hydraulic gradients are very steep or in rocks with large cavities, for example, karstic formations (Singhal and Gupta, 2010).

2.2.2.1. Laminar and turbulent flow

Darcy's law considers a laminar flow when there are large viscous forces acting, small velocities and momentum and no type of swirls develop. On the contrary, a turbulent flow is characterized by chaotic swirls similar to the ones in the atmosphere or flowing water streams. A measure of the flow indicating if a flow tends toward laminar or turbulent behaviour is the Reynolds number, Re . The Reynolds number is a dimensionless parameter used in fluid mechanics that relates the fluid properties with its velocity and the structural characteristics of the percolation medium, such as, the mean pore diameter or mean grain size. The turbulent flow is typical on media with large pores and high groundwater velocities, hence, the flow will obey to Darcy's law if it is laminar, not turbulent (Gonzalez de Vallejo and Ferrer, 2011).

2.2.3. Groundwater in fractured crystalline rocks

The least predictable scenario on groundwater circulation is found in igneous and metamorphic rocks due to their very low porosity and permeability limited by an irregular network of discontinuities. While much of the porosity is in the form of small, unconnected pores between crystals, the pores that conduct fluid flow are the interconnected ones, which in most crystalline rocks are found in fractures (Fitts, 2013). As it was shown before on Figure 5, the porosity of intrusive igneous rocks and metamorphic rocks is very low and in some cases below 1%. Crystalline rocks that are intact have lower permeability than large-scale fractured masses of the same rock.

Fractures usually occur in roughly parallel sets and the rock mass is usually presented with several distinct sets. These fracture sets are developed due to large-scale crustal stresses of tectonic origins. One common set found within a few meters of depth is parallel to the ground surface and is called sheeting. Sheeting is originated by unloading that occurs as erosion peels away overlying rock over millions of years (Singhal and Gupta 2010; Gonzalez de Vallejo and Ferrer, 2011).

The occurrence of groundwater in many extrusive igneous rocks happens due to its matrix porosity, in addition to fracture porosity. A type of matrix porosity usually found in igneous rocks was described before as vesicles or otherwise known as gas bubbles. Gas bubbles are formed upon the ascension and cooling of magma on the surface with a drop of pressure within it (Fitts, 2013).

2.2.3.1. Intrinsic permeability

While the hydraulic conductivity is a specific parameter of the water flow through a medium, the flow of other fluids can be of interest, particularly in the analysis of petroleum reservoirs and some contaminant migration problems. Intrinsic permeability k , unlike hydraulic conductivity K , is independent of fluid properties and only depends on the medium. The two parameters are proportional and related as follows [7] (Hubbert, 1940; in: Fitts, 2013):

$$k = \frac{K\mu}{\rho_w g} \quad [7]$$

Where μ and ρ_w are the dynamic viscosity and density of water, and g is gravitational acceleration. Analysing the dimensions of k reveals that it is, $[L^2]$. For fresh water at 20° C, $k(\text{cm}^2) = 0.001K (\text{m/s})$. It makes intuitive sense that k has units of area, since the primary factor determining a medium's resistance to flow is the typical cross-sectional area of its pores. Studies indicate that for uniform grain-size granular materials, k is proportional to the square of grain diameter (Hubbert, 1956; in: Fitts, 2013).

2.3. Bedrock parameters

Besides the characteristics found on intact rock, there are other important parameters to consider on rock mass. Parameters related to the rock mass, as a full rock body, with its evolutionary stress state along time, fracture composition matrix and weathering state are described in this section. The quality characteristics of a rock mass are a consequence, among others, of its weathering and fracturing degree and the geo-hydraulic circulation of underground water.

2.3.1. Weathering degree

The weathering process affects not only the intact rock but also its discontinuities and the general stability of the rock mass. The weathering can be mechanical or physical due to the break of contact between mineral grains. The effect of weathering may cause a further opening of the discontinuities already existent or the formation of new ones. Weathering processes affect different lithologies to different extents, increasing in intensity with longer exposure to atmospheric agents. The depth of weathering depends on the type of rock, the climate and the amount of exposure to weathering. Clay rocks, porous sandstones and weak limestones often alter to a greater depth than granites or metamorphic rocks. In humid tropical climates soils produced by the weathering of rock masses may reach thicknesses as much as 20 to 30 m (Gonzalez de Vallejo and Ferrer, 2011). When water is present, it contributes to the weathering degree causing chemical processes that transform the rock mass and its composition minerals. Figure 12 shows the different weathering types that are commonly found in different lithologies.

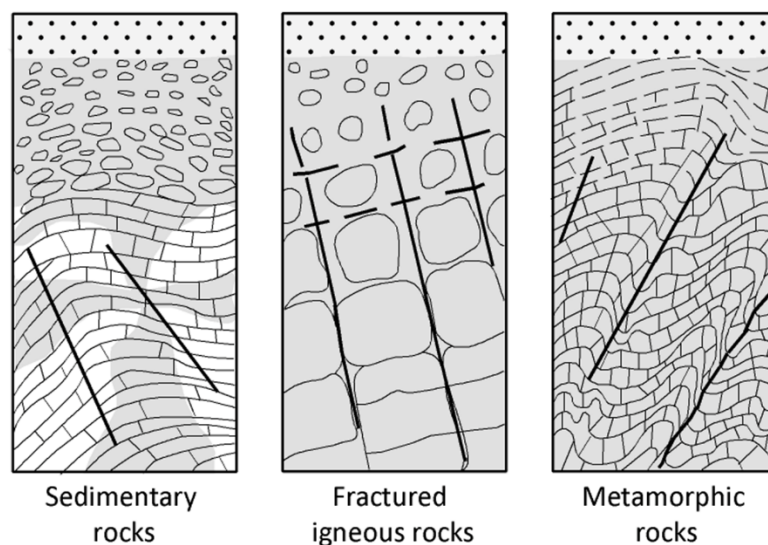


Figure 12 - Weathering types according to each geological material (Gonzalez de Vallejo and Ferrer, 2011).

According to ISRM (1981), it is possible to classify the weathering degree in rock masses in five different geotechnical descriptions with the possibility of simplifying it in three. The weather degree recognition can also be made by direct observation of exposed outcrops, though this evaluation is subjective to the observer's experience. Table 4 shows the description and evolution of the weathering degree in a rock mass.

Table 4 – Weathering degrees applicable to rock masses (adapted from ISRM, 1981; GSE, 1995).

Weathering degree	Symbols	Description
Fresh	W_1	Fresh - No visible sign of weathering of the rock material
Slightly weathered	W_{1-2}	Discoloured - Change in colour of the original rock material. The degree of change from the original colour should be indicated. If the colour change is confined to particular mineral constituents this should be mentioned.
	W_2	
Moderately weathered	W_3 W_3	Less than half of the rock material is weathered to the condition of a soil in which the original fabric is still intact.
Highly weathered	W_4	More than half of the rock material is weathered to the condition of a soil in which the original fabric is still intact. The rock material is friable.
	W_{4-5}	
Completely weathered	W_5	Decomposed - All of the mineral grains are decomposed and weathered to a condition of residual soil.

2.3.2. Fracturing degree

The fracturing degree is defined by the quantity and proximity of discontinuities present on a rock mass, being directly related to the permeability on a fractured medium (ISRM, 1981). Thus, when studying the water content of a rock, a good indicator of its higher occurrence is zones with higher fracturing degree (e.g., shear zones, fault zones). Spacing, fracture intercept and frequency, Rock Quality Designation (RQD) and unitary rock volume are characteristics that permit the conceptualisation of the permeability and the fracturing degree of a rock mass. According to ISRM (1981), depending on the area and the study objectives, it must be collected, at least, a range of 150 to 200 discontinuities to understand the mechanical behaviour and the rupture mechanisms of a given rock mass. The fracturing degree and the block size are settled by the number of discontinuities sets and the corresponding spacing. The discontinuities sets are defined by their space orientation, their properties and the related characteristics of the defining structural planes of each family. The fracturing degree classification can be seen on Table 2, the description of discontinuities parameters table, on the respective spacing/fracturing intercept parameter.

Using the scanline sampling technique to collect discontinuity data from the rock mass followed by the application of geological-structural diagrams (particularly, stereonet and rose diagrams), it is possible to analyse and define the number of discontinuity sets and the average orientation of each set (e.g., Priest, 1993; Watkins et al., 2014; Chaminé et al., 2015).

For the application of geomechanical classification systems, when studying the rock mass according to the number of discontinuities sets, the following nine cases are considered (ISRM, 1978):

- Case 1: Compact rock mass with the presence of random occasional discontinuities;
- Case 2: One discontinuity set;
- Case 3: One discontinuity set and presence of random occasional discontinuities;
- Case 4: Two discontinuities sets;
- Case 5: Two discontinuities sets plus random;
- Case 6: Three discontinuities sets;
- Case 7: Three discontinuities sets plus random;
- Case 8: Four or more discontinuities sets, random, heavily jointed, 'sugar cube', etc.;
- Case 9: Crushed rock, soil like.

2.3.3. Block size

Block size is usually called to the block bounded and defined by the fracture network (ISRM, 1981). The shape of the block is defined by the discontinuities sets and orientation, while the block dimension is determined by their spacing, continuity and also by the discontinuities sets. The block shape usually depends on the lithology of the local rock mass, as it tends to have a certain shape according to its mineral composition. There are several shapes of the matrix block unit, such as, prismatic, cubical or tabular. The dimension of the block determines the rock mass behaviour, its strength properties and its deformability. The block unit has a direct and major importance, in geoenvironmental works, since, when opening underground tunnels or blasting rock, this bedrock parameter defines where the rock has a major fracture plane.

In order to define the block size, it is required to obtain some parameters of the rock mass, but its definition can mostly be done by the volumetric fracture count parameter, J_v (Palmström, 1995; Palmström and Stille, 2010). Other important parameters, such as spacing/fracturing degree, RQD and block size index are significant when understanding the typical block size of a rock mass.

2.3.3.1. Measurement of the block volume, V_b

Where individual blocks can be observed in a surface, their volumes can be directly measured by selecting several representative blocks and measuring their average dimensions. For small blocks

or fragments having volumes of dm³ or less, the following measurement [8] is often the quickest method as it is easiest to estimate the block size when compared to the registry of the many joints involved. For example, where three joint sets occur, the block volume can be determined as (Palmström, 1995; Palmström and Stille, 2010):

$$V_b = \frac{S_1 * S_2 * S_3}{\sin \gamma_1 * \sin \gamma_2 * \sin \gamma_3} \quad [8]$$

where, S_1, S_2, S_3 , are the spacings for the three joint sets, and $\gamma_1, \gamma_2, \gamma_3$ are the angles between the joint sets. The block measures have to be registered one by one, either in rock surfaces, from scanlines, or from drill cores. From these measurements the apparent smallest and largest block can be reported, but often a representative or an equivalent block size is inconsistently recorded and used for input in rock engineering (details in: Palmström and Stille, 2010). The block volume can be classified as suggested by Palmström (1995) in Table 5.

Table 5 – Palmström’s classification for Block Volume, V_b (Palmström and Stille, 2010).

Designation	Size
Very small	10 – 200 cm ³
Small	0.2 – 10 dm ³
Moderate	10 – 200 dm ³
Large	0.2–10 m ³
Very large	> 10 m ³

2.3.3.2. Volumetric joint count, J_v

The volumetric joint count parameter (J_v) allows the definition of the block size, representing the total discontinuities intersecting one unit volume (1 m³) of the rock mass (ISRM, 1981). It was described by Palmström (1995) as the following equation [9] (details in: Palmström and Stille, 2010):

$$J_v = \sum_{i=1}^J \left(\frac{1}{S_i} \right) \quad [9]$$

where, S_i is the average joint spacing in meters for the i^{th} joint set and J is the total number of joints except the random joint set.

Random joints can be included by assuming a random spacing (S_r) for each of these. Experience indicates that this can be set to $S_r = 5$ m; thus, the volumetric joint count can be generally expressed as [10]:

$$J_v = \sum_{i=1}^J \left(\frac{1}{S_i} \right) + \frac{Nr}{S_r=5} \quad [10]$$

where, Nr is the number of random joints.

J_v can be easily calculated through the scanline sampling technique, since it is based on measurements of joint sets spacing. As the volumetric joint count takes into account, by definition in an unambiguous way, all the occurring joints in a rock mass, it is often appropriate to correlate J_v to other measurements, such as RQD. Table 6 classifies the volumetric joint count according to its degree (Palmström, 1995).

Table 6 – Palmström’s classification for Volumetric Joint Count, J_v (Palmström and Stille, 2010).

S. No.	Degree of jointing	J_v
2	Very low	< 1,0
3	Low	1 – 3
4	Moderately	3 – 10
5	High	10 – 30
6	Very high	30 – 60
7	Crushed	> 60

The J_v parameter is commonly used in studies of medium to slightly fractured rock masses and less used in very fractured rock masses.

2.3.3.3. Rock Quality Designation (RQD) Index

Another way to evaluate the quality of a rock mass is using the RQD Index classification (Deere, 1963, 1989; Deere and Miller, 1966; Deere et al., 1967; Deere and Deere, 1988; Sem, 1984, 1990). The RQD index is based upon the ratio between the sum of the lengths of core fragments longer than 10 cm and the total length of the core run. This way, the following equation [11] is obtainable (Deere et al., 1967):

$$RQD = \frac{\sum \text{lengths of core fragments} \geq 10 \text{cm}}{\text{total length of core run}} \times 100 \quad [11]$$

Only fresh or hard pieces of rock mass are considered for estimating RQD. Those showing significant weathering are eliminated with an RQD index considered of 0%. It is recommended that the operational run length should not exceed 1,5 m and the minimum core diameter, on which the index should be calculated, is 48 mm. Table 7 describes the rock quality based on its index value and Figure 13 shows the RQD measuring and procedure.

Table 7 - Description of RQD based on the calculated index (Deere et al., 1967).

RQD %	Quality
<25	Very poor
25-50	Poor
50-75	Fair
75-90	Good
90-100	Very good

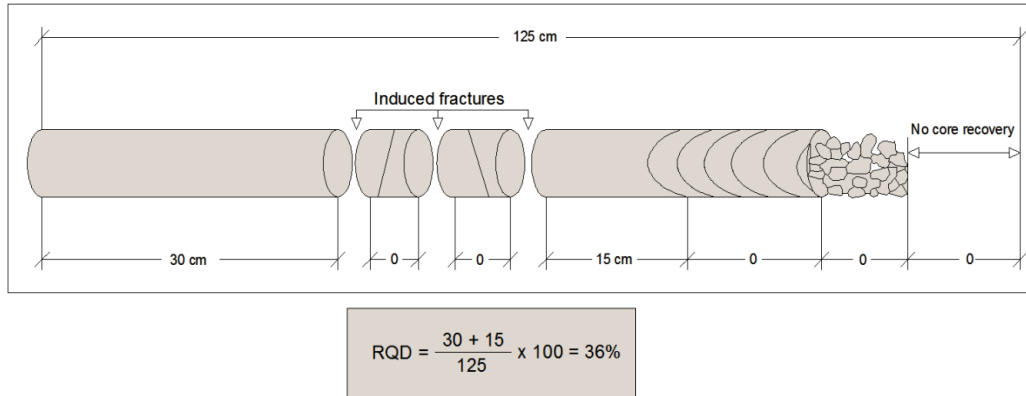


Figure 13 - RQD measuring and determination procedure (Gonzalez de Vallejo and Ferrer, 2011).

The length of the core piece is measured along its central axis, using fragments that have at least one complete diameter. It must be remembered that RQD is a function of the direction in which it is measured, which can result in different values for RQD being obtained from the same rock mass (Gonzalez de Vallejo and Ferrer, 2011).

When cores are not available, RQD may be estimated from the number of joints (discontinuities) per unit volume (J_v). The relationship [12] converts J_v into RQD for clay-free rock masses (Palmström, 1995; Palmström and Stille, 2010):

$$RQD = 115 - 3,3J_v \quad [12]$$

where, J_v represents the volumetric joint count – the total number of joints per cubic meter. Palmström (2005) proposed a new equation [13] (details in Palmström and Stille, 2010):

$$RQD = 115 - 2,5J_v \quad [13]$$

The new correlation probably gives a more appropriate average correlation than the existing one, which may be representative for the long or flat blocks, while the new one is better used for blocks of a cubical shape (Palmström, 2005; Palmström and Stille, 2010).

However, the RQD index only represents the degree of fracturing of the rock mass. It does not take into account the strength of the rock or the mechanical and other geometrical properties of the joints.

2.3.4. *In-situ* stress

The current topic was summarised from Gonzalez de Vallejo and Ferrer (2011). The state of stress of any system is the result of the forces acting on it, as they define the state and mechanical behaviour of it. Geological materials are subjected to natural stresses as a result of their geological history. Stress inside a rock mass is generated by external forces and by its own weight. Tectonic forces are the main cause of stresses stored in rocks which can be released in many different ways, from earthquakes and fault movements to rock bursts, fracturing and deformations in underground excavations. The resulting state of stress is usually complex since it is a heterogeneous, discontinuous and anisotropic medium. The outcome is a significant variation between adjacent areas. Engineering projects affect the *in situ* state of stress, adding new forces or modifying the distribution of existing forces, inducing other stress states. In geological engineering, the most important applications of the study of natural stresses are tunnels and underground excavations, where the stability depends on the magnitude and direction of stresses, being essential to know the *in situ* stress.

If the forces in a system vary, the state of stress associated with the planes under consideration also change. Two types of acting forces may be considered in rock masses: surface forces, which are exerted on the body by its surrounding materials and gravitational or body forces, where, $F = m * g$. The first type act on the contact surfaces between the adjacent parts of the rock system and are transmitted to any point within the body (e.g., tectonic forces applied on rocks). When a force is applied on a plane, it is called normal force if it is perpendicular to the plane and tangential or shear force if it is parallel to the plane. The first type may be compressive or tensile, but not the second. For shear forces, a sign convention has to be defined, whether the force vector and the related vector on the surface are anti-clockwise, the force is positive, and negative in the opposite relation.

Stress is a quantifiable parameter but cannot be directly measured, since the physical parameter measured is force. If the force acts uniformly over a surface, the stress indicates the intensity of the forces that act on the plane. At any point subjected to stress, three mutually orthogonal planes are found where shear stresses are zero. Such planes are called principal planes of stress and the normal stresses acting on them are the principal stresses. Of the three stresses, the greatest is σ_1 , the intermediate, σ_2 , and the smallest is σ_3 , thus: $\sigma_1 > \sigma_2 > \sigma_3$. Assuming that stresses at a point are due only to gravitational forces, the horizontal plane and all the vertical planes that pass through that point will be principal planes of stress. If $\sigma_1 = \sigma_2 = \sigma_3$, the state of stress is called isotropic or hydrostatic, the same as for fluids. All self-supporting walls of surface and underground excavations are principal planes of stress on which shear stresses do not act. In

contrast to what occurs with shear stress, there is no orientation in space for a surface on which the normal stress is zero; in other words, the sum of the principal stresses on a body under unchanging forces always has the same value regardless of the orientation of the principal stresses: $\sigma_1 + \sigma_2 + \sigma_3 = \text{constant}$.

2.4. Geomechanical indexes and rock classification schemes

2.4.1. Rock mass classification schemes: a brief historical overview

“The rock mass classification systems were designed to act as an engineering design aid, and were not intended to substitute field observations, analytical considerations, measurements, and engineering judgment” (Bieniawski, 1993)

Rock mass classification is the process of placing a rock mass into groups or classes on defined relationships (Bieniawski, 1989). In practice rock mass classification systems have provided a valuable systematic design aid on numerous engineering works particularly on underground excavations, tunnelling and mining projects (e.g., Kirkaldie, 1988; Bieniawski, 1989; Bell, 1992; Hoek, 2007; Singh and Goel, 2011). In addition, the rock mass description and classification is a mean to properly communicate the estimated rock mass characteristics and should not be taken as an alternative to detailed engineering design procedures (Abbas and Konietzky, 2015). It gives not only information about the composition, strength, deformation properties and characteristics of a rock mass required for estimating the support requirements, but also shows which information is relevant and required (Bieniawski, 1989; Abbas and Konietzky, 2015). In the feasibility and preliminary design stages of a project, comprehensive information related to the rock mass parameters, in situ stress and hydrogeologic characteristics is mostly unavailable. Thus rock mass classification proves to be helpful at this stage for assessing rock mass behaviour (Abbas and Konietzky, 2015). The rock mass classification systems were designed to act as an engineering design aid, and were not intended to substitute field observations, analytical considerations, measurements, and engineering judgment (Bieniawski, 1993).

According to Bieniawski (1993), the objectives of rock mass characterisation and classification are: i) to identify the most significant parameters influencing the behaviour of a rock mass; ii) to divide a particular rock mass formation into a number of rock mass classes of varying quality; iii) to provide a basis for understanding the characteristics of each rock mass class; iv) to derive quantitative data for engineering design; v) to recommend support guidelines for tunnels and mines; vi) to provide a common basis for communication between engineers and geologists; vii)

to relate the experience on rock conditions at one site to the conditions encountered and experience gained at other.

Currently, rock mass classification schemes are also used in conjunction with numerical simulations, especially in early stages of geotechnical projects, where data are often rare (Abbas and Konietzky, 2015). Based on rock mass classifications, strength (e.g. Barton and Choubey, 1977; Bieniawski 1993; Hoek, 1994, 2007) and deformation (e.g., Hoek and Diederichs, 2006) parameters according to specific constitutive laws or the rock mass (e.g., Mohr-Coulomb or Hoek-Brown material models; Hoek and Brown, 1980a,b, 2007; Hoek et al., 1992, 2002; Hoek and Marinos, 2007 and references therein) can be deduced and applied in numerical simulations to consider stability, failure pattern, factor-of-safety, deformations etc. (Abbas and Konietzky, 2015). A quantified classification assists proper and effective communication as a foundation for sound engineering judgment on a given project (Bieniawski 1989, 1990).

Rock mass classification schemes and geotechnical indexes for tunnel design have been developed for over 130 years. The earlier systems used to characterise the rock mass behaviour were mainly based on description and qualitative approaches. Rock mass classification schemes owe its origin to 1879 when Ritter (1879) devised an empirical approach to tunnel design for finding out support requirements (Hoek, 2007).

Terzaghi (1946) presented the rock-load mass classification system that has revealed successful in tunnelling with steel supports mainly in United States of America for over 30 years (Pinheiro et al., 2014). In the mid-1940s, Terzaghi made the first attempt on creating a classification for rock masses applied to engineering purposes. The objective of this system was to estimate the rock load to be carried by the steel arches installed to support a tunnel. As discussed earlier, it was not the first classification system but it was the first one in English language that integrated geology into the design of tunnel support (Abbas and Konietzky, 2015).

Terzaghi (1946) proposed the rock load factor (H_p) which is characterised by the height of the loosening zone over the tunnel roof that is likely to load the steel arches (Figure 14). These rock load factors were estimated from a 5.5m-wide steel-arch supported railroad tunnel in the Alps during the late 1920s, which eventually became a disadvantage because the rock load factor was limited to dimensions below 5.5m. Rock load factor was defined for each rock class and accordingly the appropriate support intensity was recommended. Recommendations and comments were given related to characteristic observations from different tunnels. Terzaghi devised the equation $p = H_p \cdot \gamma \cdot H$ to obtain support pressure (p) from the rock load factor (H_p), where γ is the unit weight of the rock mass, H is the tunnel depth or thickness of the overburden (Terzaghi, 1946). Later on, the classification suffered some updates from other researchers, such as Proctor and White (1946) that considered the variations of cementing effect on discontinuities

With the lack of an adequate and generally accepted method to describe an overall classification, in 1981, the International Society for Rock Mechanics (ISRM) decided to create a Commission on Classification of Rocks and Rock Masses, to reduce the gap between knowledge and practical interpretation (ISRM, 1981). The gathering and study of documents, in particular of numerous classification systems currently in use, gave birth to the “Basic Geotechnical Description of Rock Masses”, the so-called BGD (ISRM, 1981). In his own words: *“The intent of the BGD is to characterise in simplified form the various zones that constitute a given rock mass, using information obtained from the observation of outcrops, trenches, adits and boreholes”*. The BGD is frequently used on several geotechnical fieldwork, rock sampling techniques and technical reports (Bell, 1992).

Later, a rock mass evaluation based mainly on engineering geology, geohydraulic and geotechnical features appeared, combining several parameters to derive quantitative geomechanical classifications for rock engineering design. Nowadays, the international relevant multi-parametric classifications in rock engineering practice for underground environment are (Barton and Bieniawski, 2008): i) RMR – Rock Mass Rating (Bieniawski, 1973, 1976, 1979, 1988, 1989, 1990, 1993, 1997; Serafim and Pereira, 1983; Celada et al., 2014a,b and references therein); ii) Q-System: Rock Tunnelling Quality Index (Barton et al., 1974, 1977, 1980; Barton and Choubey, 1977; Barton, 2000, 2006; NGI, 2013 and references therein).

In the United States of America was developed the Rock Structure Rating (RSR) for tunnelling (e.g., Wickham et al., 1972, 1974; Skinner, 1988), that was intensively used in that country over 20 years.

Bieniawski (1973) proposed, in South Africa, the so-called Rock Mass Rating (RMR) system, and sustained its development (now, in United States of America) until 1989 (e.g., Bieniawski, 1976, 1979) and is commonly entitled RMR89 (details in Bieniawski, 1988, 1989, 1993, 1997). Through the available data its versions founded more than 350 applications in underground opening, tunnels, underground mines, and open-pit slope designs. Recently that classification was revisited and called RMR2014 by Celada et al. (2014a,b).

The Q-system, a rock mass classification based on approximately 200 case histories of tunnels and caverns, was originally proposed by Barton et al. (1974) at the Norwegian Geotechnical Institute (NGI), in Sweden. It is used mainly for design of support in underground excavations. Several updates were made, namely, Barton et al. (1977, 1980) and recently by NGI (2013). The outputs made by Barton and Choubey (1977), Barton (2000, 2006, 2007, 2012), Barton and Quadros (2002), Barton and Bieniawski (2008) has such importance to a good use of the Q-system or derivate systems.

2.4.2. General remarks

*“Experienced field engineers and geologists generally show a liking for a simple and fast, yet reliable classification that is based on visual inspection of geological conditions.”
(Singh and Goel, 2011)*

Rock mass classification schemes form the backbone of the support design approach that are widely employed in rock engineering (e.g., Kirkaldie, 1988; Bieniawski, 1989; Bell, 1992; Hoek, 2007; Barton, 2008; Singh and Goel, 2011 and references therein). In many projects, the classification approach is the only practical basis for the design of complex underground structures. Geomechanical evaluation of a rock mass can be carried out using data obtained from the description and measurement of the characteristics and properties of intact rock, discontinuities, geohydraulics and rock mass parameters. The application of geomechanical classifications based on these data allows the estimation of quality and approximate rock strength parameters, in terms of friction and cohesion (Singh and Goel, 2011).

The main advantage of geomechanical classifications is that they provide an easy and simple estimate of the mechanical parameters of the rock mass. However, their over-simplification must be taken into account by registering fuzzy variation of rock parameters after allowing uncertainty; thus, it is better to assign a range of ratings for each parameter (Mazzoccola et al., 1997). There can be a wide variation in the engineering classifications at a location. Hoek and Brown (1997) realised that a classification system must be non-linear to classify poor rock masses realistically. In other words, the reduction in strength parameters should be non-linear in classifications, unlike RMR in which strength parameters decrease linearly with decreasing RMR (i.e., that strength parameters decrease non-linearly with RMR for dry rock masses; Mehrotra, 1993). When designing a project, the average of rock mass ratings (RMR) and geological strength index (GSI) should be considered in the design of support systems. For rock mass quality (Q-system), a geometric mean of the minimum and the maximum values should also be considered in the design (Singh and Goel, 2011).

Hudson and Harrison (2000) stated an important issue: *“(...) The two main classification systems—those of RMR and Q-system utilize six main parameters which are not the same. The developers of these systems have decided on which parameters are most important for tunnel design, and designed their classifications accordingly. Both proponents of the systems have warned users not to attempt to extrapolate the classification methods without modification and not to make predictions outside the original subjects for which the classification schemes were intended.”* To manipulate or create a rock classification scheme several issues have to be considered (see details in Hudson, 1992).

Table 8 presents the main rock mass classification schemes or indexes, as well as hydrogeomechanical systems used in rock engineering practice.

Table 8 - An overview of the main rock mass classifications or indexes and hydrogeomechanical systems used in rock engineering practice (compiled and adapted from Kirkaldie, 1988; Bieniawski, 1989; Bell, 1992; Hoek, 2007; Barton, 2008; Scesi and Gattinoni, 2009; Singh and Goel, 2011).

Geomechanical Classification or Index	Parameters	Assesment	References
RQD <i>Rock Quality Designation</i>	<ul style="list-style-type: none"> ● Geological description from core recovery ● Rock material fracturing degree ● Intact rock pieces > 10 cm; borehole length 	<ul style="list-style-type: none"> ● Geology, rock type and geological structure ● Fracture degree quantification and core recovery 	Deere (1963, 1989); Deere and Miller (1966), Deere et al. (1967); Deere and Deere (1988)
RMR <i>Rock Mass Rating</i>	<ul style="list-style-type: none"> ● Strength of intact rock material: UCS - Uniaxial Compressive Strength PLT - Point Load Test ● Rock quality designation index, RQD ● Spacing of Discontinuities ● Geological and geotechnical condition of discontinuities ● Groundwater flow ● Discontinuities strike and dip effect on tunnelling 	<ul style="list-style-type: none"> ● Geomechanical rock mass quality ● Cohesion and angle of internal friction ● Deformation modulus ● Average stand-up time ● Estimation of excavation and support measures 	Bieniawski (1973, 1976, 1979, 1989, 1993); Serafim and Pereira (1983); Celada et al. (2014a,b)
Q-system <i>Rock Tunnelling Quality Index</i>	<ul style="list-style-type: none"> ● Rock quality designation index, RQD ● Joint set number ● Joint roughness ● Joint wall alteration ● Joint water flow, Jw ● Excavation surrounding stress factor 	<ul style="list-style-type: none"> ● Geomechanical rock mass quality ● Deformation modulus ● Support and reinforcement category retrieval ● Maximum span for a self-supporting rock mass 	Barton et al. (1974, 1977, 1980); Barton (2000); Barton and Quadros (2002), NGI (2013)
GSI <i>Geological Strength Index</i>	<ul style="list-style-type: none"> ● Geo-structure description according to rock block size and geological-geotechnical structural conditions of the surface structures ● Intact rock strength 	<ul style="list-style-type: none"> ● Geological-geomechanical rock mass quality ● Deformation modulus ● Cohesion and angle of internal friction 	Hoek and Brown (1997); Hoek et al. (1998); Marinos and Hoek (2000); Marinos et al. (2005); Hoek et al. (2013)
HP-value <i>Hydro-Potential Value</i>	<ul style="list-style-type: none"> ● Rock quality designation index, RQD ● Joint set number ● Joint roughness ● Discontinuity aperture and shape ● Water flow condition on discontinuities 	<ul style="list-style-type: none"> ● Rock mass hydrogeomechanical quality ● Rock mass water yield and specific capacity ● Seepage prediction problems 	Gates (1995, 1997, 2003)
HC System <i>Hydraulic Conductivity system</i>	<ul style="list-style-type: none"> ● Rock quality designation index, RQD ● Depth Index, DI ● Gauge content designation index, GCI ● Lithology permeability index, LPI 	<ul style="list-style-type: none"> ● Rock mass hydrogeomechanical quality ● Rock mass hydraulic conductivity of fractured rocks 	Hsu et al. (2008, 2011); Chen and Zhou (2011)

2.4.3. Geomechanical calculators and analysis systems: MGC-RocDesign | CALC

There are some commercial programmes or informatics applications related to professional or academic use, such as (details in Figure 16): Tunnex – Expert System for Rock Tunnelling (Palassi and Franklin, 1998); RMi – Combining RMR-Q-RMi Calculator (Palmström, 1995); REX – Rock Excavation Decision Support Expert System (Tapia et al., 1998); ClassMass (Deliormanli and Onargan, 2003); PDA field book for rock mass characterization and classification (Vardakos, 2004; Vardakos and Gutierrez, 2005); AMADEUS – Information Technology-based tunnelling system (Gutierrez et al., 2006); Tunnelling Analyst: a 3D GIS extension for rock mass classification and fault zone analysis in tunnelling (Choi et al., 2009); TIA – Tunnel Information and Analysis System

The “MGC–RocDesign|CALC – Mining Geomechanics Classification System Calculator for Rock Engineering Design” (Pineiro et al., 2014) provides an interactive tool for the use and application of the major rock-mass classifications and geotechnical indexes (e.g., RMR, Q-system, RSR, SRC, GSI, RQD, HP-value, etc.). The MGC–RocDesign|CALC tool was developed and designed in Microsoft Excel™ spreadsheet software in Visual Basic for Applications shell on a PC platform which runs under MS. Windows operative system (versions 7, 8, 8.1). This framework provides a friendly and environmental data loading more appealing to the end-user in the planning and design stages. The geomechanical calculator was merged with a rock-mass database – GeoTech|CalcTools – which is based on the so-called BGD – “Basic Geotechnical Description of Rock Masses” proposed by ISRM (1981). This database integrates two original geotechnical spreadsheets named ScanGeoData|BGD and SchmidtData|UCS (Fonseca et al., 2010; Chaminé et al., 2013, and references therein). In addition, all the information was integrated successfully on a Geographic Information System (GIS) based mapping (Pineiro et al., 2014).

The MGC–RocDesign|CALC is an interactive system and was designed to be friendly to use and a powerful tool. All the commands are located inside a menu of options. Each menu contains a list of commands that one can select with the mouse or the keyboard cursor keys. The arrangement of the option menus and dialog boxes was displayed with functional criteria. In addition, it follows the logical order of the operations and constraining the access to further procedures until all the required loading data. Some explanation functions are provided in the main menu. The main knowledge structure is as follow: i) open database file (GeoTech|CalcTools); ii) input data; iii) output data (Figure 17).

The MGC–RocDesign|CALC tool was developed in order to obtain a useful assessment for rock engineering design by taking into account complex geological background and the multiple goals supporting decision (Pineiro et al., 2014):

- i) engineering geosciences desk studies throughout the rock-mass database (GeoTech|CalcTools) analysis, which is an effective geotechnical tool to collect, analyse and evaluate the in situ data and laboratory testing data;
- ii) evaluation of several geological and geotechnical index for the study of the rock-mass behaviour;
- iii) geomechanical assessment with multi-criteria rating methods of rock-mass classification for underground excavation or tunnelling purposes;
- iv) GIS-based geoengineering mapping assessment to produce geological and engineering geoscience maps and geotechnical zoning maps, which incorporate design parameters to elaborate geomechanical mapping.

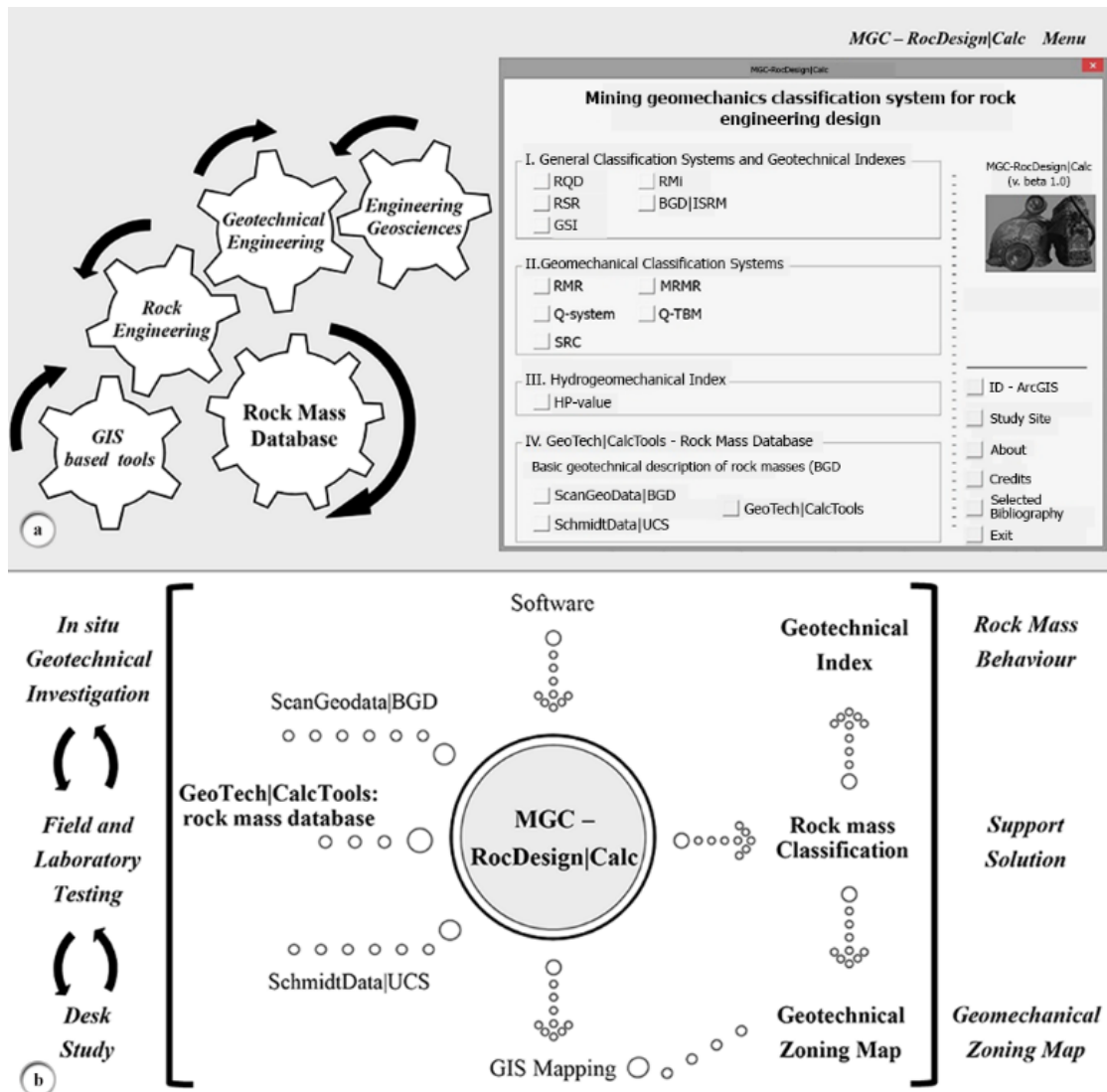


Figure 17 - MGC–RocDesign|CALC: a geomechanical calculator tool for rock engineering characterisation and design; a) interdisciplinary framework; b) schematic concept. (After Pinheiro et al., 2014).

2.4.4. Rock Mass Rating (RMR) by Z.T. Bieniawski

When considering the geomechanical classifications, the so-called Rock Mass Rating (RMR), was firstly presented by Z. T. Bieniawski in 1973. Since its creation in 1973, there have been several updates to the original proposal (mainly the versions RMR76, RMR79, RMR89, RMR2014; see details in Bieniawski, 1989 and Celada et al., 2014a,b). Therefore, it is important to state which version is used when RMR values are rated. The main development of the classification was made during the 70's (Bieniawski, 1973, 1976, 1979). In 1989, the geomechanical classification, RMR, was improved based on 350 study cases, adjusting it for diverse engineering applications (Bieniawski, 1989, 1993, 1997) and recently was proposed a new update by Celada et al. (2014a,b). This classification is internationally well-known due to its versatility in the rock

engineering field, ranging from the project of underground excavations, caves, mining tunnels and slope stability. This classification should also be used as a complement to the structural design and not as an answer to the diverse problems that may outcome an engineering project. The topical bibliography related to RMR is the following: Bieniawski (1973, 1976, 1979, 1988, 1989, 1990, 1993, 1997), Serafim and Pereira (1983), Barton and Bieniawski (2008), Celada et al. (2014a,b).

To apply RMR geomechanical classification system, a given rock mass site should be divided into a number of geotechnical zoning units in such a way that each type of rock mass is represented by its geostructural and geotechnical characteristics. That zoning must be prepared using rock field surveys, like scanlines, windows or grids sampling techniques (e.g., Peacock et al., 2003; Smith, 2004; Peacock, 2006; Chaminé et al., 2015; Watkins et al., 2015) and based on geotechnical description of the rock masses (BGD methodology; ISRM, 1981; Bell, 1992). That classification does not include in-situ stress conditions. The rock mass rating takes the following geomechanical parameters into account which can vary from 0 to 100 (Bieniawski, 1989):

- P1:** Strength of intact rock material (Uniaxial Compressive Strength – UCS and/or Point Load Strength Test – PLT);
- P2:** Rock Quality Designation (RQD) index;
- P3:** Spacing of discontinuities;
- P4:** Geological-geotechnical conditions of discontinuities;
- P5:** Groundwater conditions;
- P6:** Value correction due to discontinuities orientation relation to the excavation direction.

A brief description of the previous parameters is presented.

P1: Strength of intact rock material

The strength evaluation of the rock material should be obtained, preferably from core-recovery of the intact rock, in site conditions, through the Point Load Test (PLT) or using the Schmidt hammer to achieve the Uniaxial Compressive Strength (UCS). Table 9 shows the rating for the first parameter (intact rock strength). All strength data obtained from both techniques must be accordingly the ISRM/ASTM (details in ISRM, 2007, 2015) procedures and statistical representative (e.g., Schmidt, 1951; Miller, 1966; Broch and Franklin, 1972; Bieniawski, 1975; Franklin, 1985; ISRM, 1985; Cargill and Shakoor, 1990; Katza et al., 2000; Kahraman, 2001; Hack and Huisman, 2002; Kahraman et al., 2002, Aydin and Basu, 2005; Aydin, 2015, and references therein).

Table 9 - Strength of intact rock material (adapted from Bieniawski, 1989).

Description	Uniaxial Compression Strength (σ_c), UCS (MPa)	Point Load Strength Test, (IS50), PLT (MPa)	Rating
Extremely Strong*	> 250	8	15
Very Strong	100 - 250	4 - 8	12
Strong	50 - 100	2 - 4	7
Medium Strong*	25 - 50	1 - 2	4
Weak	5 - 25		2
Very Weak	1 - 5	Use of UCS is preferred	1
Extremely Weak	< 1		0

At compressive strength of less than 1.0 MPa, many rock materials would be regarded as soil.

**Terms redefined according to ISSO 14689*

P2: Rock Quality Designation (RQD) index

To define the Rock Quality Designation (RQD) index, it is used the classification introduced by Deere (1963) and updated by Deere et al. (1967), Deere and Miller (1966) and Deere and Deere (1988). It is determined by the evaluation of the core-recovery probes, rating it using Table 10.

Table 10 - Rock Quality Designation (RQD) index (adapted from Bieniawski, 1989).

Qualitative description	RQD (%)	Rating
Excellent	90 - 100	20
Good	75 - 90	17
Fair	50 - 75	13
Poor	25 - 50	8
Very Poor	< 25	3

The chart of Figure 18 shows how to obtain the theoretical RQD (RQD_t) rating for a general threshold value t , from the average spacing of a discontinuity set (details in Priest and Hudson, 1976; Priest, 1993).

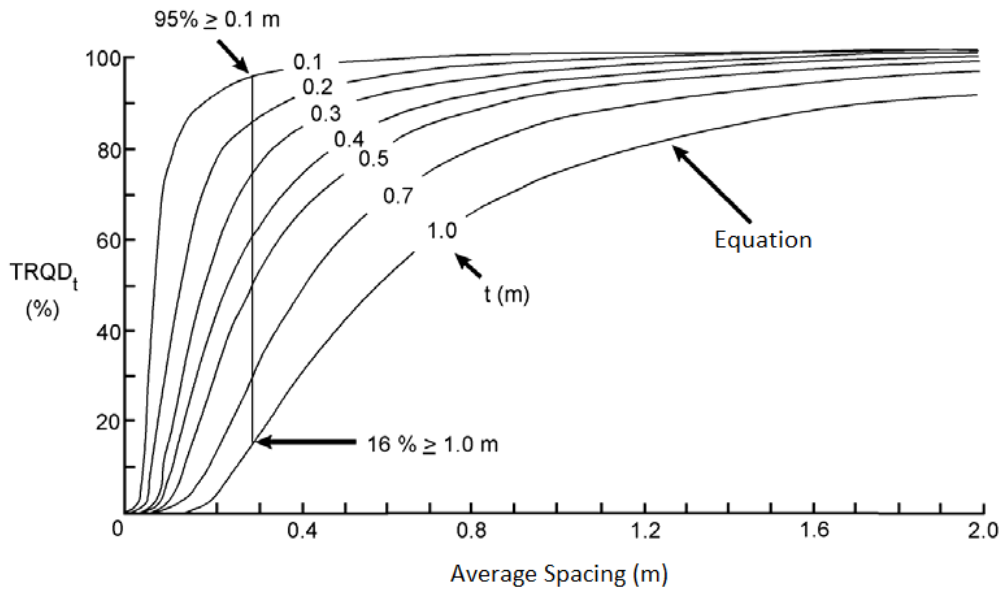


Figure 18 - Chart for determination of the theoretical RQD_t within the average spacing of discontinuities for a general threshold value t (adapted from Priest and Hudson 1976, Priest 1993).

P3: Spacing between discontinuities

The distance between two adjacent discontinuities should be measured in the discontinuity network based on accurate geostructural sampling surveys and geotechnical description of the rock masses (ISRM, 1981; Chaminé et al., 2005). The rating used in the RMR classification must correspond to the spacing (or “fracture intercept” concept introduced by ISRM, 1981) of the prevailing discontinuity set found on the rock mass and if possible an accurate global study of the block size. Table 11 shows the ratings purposes on this parameter.

Table 11 - Spacing of discontinuities (adapted from Bieniawski, 1989).

Description	Spacing (m)	Rating
Very Wide	> 2	20
Wide	0.6 - 2	15
Moderate	0.2 - 0.6	10
Close	0.06 - 0.2	8
Very Close	< 0.06	5

If more than one discontinuity set is present and the spacing of discontinuities of each set varies, consider the unfavorably oriented set with lowest rating. ISSO 14689 uses the term “extremely close” for joint spacing less than 0.02 m.

P4: Geological-geotechnical conditions of discontinuities

This parameter includes several discontinuity parameters, such as, continuity, roughness, aperture, filling and the weathering degree of the discontinuity walls. For the field surveying and the description of the rock mass it is recommended following the ISRM (1978, 1981) and CFCFF (1996), Table 12.

Table 12 - Condition of discontinuities (adapted from Bieniawski 1989).

Description	Joint Separation (mm)	Rating
Very rough and unweathered, wall rock tight and discontinuous, no separation	0	30
Rough and slightly weathered, wall rock surface separation <1 mm	< 1	25
Slightly rough and moderately to highly weathered, wall rock surface separation <1 mm	< 1	20
Slickensided wall rock surface, or 1 - 5 mm thick gouge, or 1 - 5 mm wide continuous discontinuity	1 - 5	10
5 mm thick soft gouge, 5 mm wide continuous discontinuity	>5	0

To support the description of the previous parameter, Bieniawski (1989) proposed some guidelines (Table 13).

Table 13 - RMR System: guidelines for classification of discontinuity conditions (adapted from Bieniawski, 1989).

Parameter	Rating				
Discontinuity length (persistence/continuity)	<1 m	1 - 3 m	3 - 10 m	10 - 20 m	>20 m
	6	4	2	1	0
Separation (aperture)	None	<0.1 mm	0.1 - 1.0 mm	1 - 5 mm	>20 m
	6	5	4	1	0
Roughness of discontinuity surface	Very rough	Rough	Slightly rough	Smooth	Slickensided
	6	5	3	1	0
Infillings (gouge)	Hard filling		Soft filling		
	None	<5 mm	>5 mm	<5 mm	>5 mm
	6	4	2	2	0
Weathering discontinuity surface	Unweathered	Slightly weathered	Moderately weathered	Highly weathered	Decomposed
	6	5	3	1	0

P5: Groundwater conditions

In underground excavations (or mining tunnels) it should be determined the water flow (in liters per minute, L/min, by each 10 m of the study tunnel/gallery length). Otherwise, it can be generally assessed as dry, damp, wet, etc. (CFCFF, 1996). Table 14 shows the ratings for this parameter.

Table 14 - Groundwater conditions (adapted from Bieniawski, 1989).

Inflow per 10 m tunnel length (L/min)	None	<10	10 - 25	25 - 125	>125
Ratio of joint water pressure to major principal stress	0	0 - 0.1	0.1 - 0.2	0.2 - 0.5	>0.5
General description	Completely Dry	Damp	Wet	Dripping	Flowing
Rating	15	10	7	4	0

P6: Correction value of the discontinuities orientation relating to the excavation direction

The influence of the discontinuities orientation is considered regarding the excavation direction and the slope angle of the excavation regarding the excavation alignment. As there can be different discontinuities sets along the rock mass, the dominant set will be the main target of this classification. However, it is important to do an overall structural geology analysis of the global set for the final correction inputs of this parameter. To decide if the strike and dip of discontinuities are favourable or not, Tables 15 and 16 should be considered.

Table 15 - Assessment of joint orientation effect on tunnels (adapted from Bieniawski, 1989).

Strike perpendicular to tunnel axis				Strike parallel to tunnel axis		Irrespective of strike
Drive with dip		Drive against dip				
Dip 45° - 90°	Dip 20° - 45°	Dip 45° - 90°	Dip 20° - 45°	Dip 20° - 45°	Dip 45° - 90°	Dip 0° - 20°
Very favourable	Favourable	Fair	Unfavourable	Fair	Very unfavourable	Fair

Table 16 - RMR adjustment for joint orientation (adapted from Bieniawski, 1989).

Joint orientation assessment for	Very favourable	Favourable	Fair	Unfavourable	Very unfavourable
<i>Tunnels</i>	0	-2	-5	-10	-12
<i>Foundations</i>	0	-2	-7	-15	-25
<i>Slopes*</i>	0	-5	-25	-50	-60

**It is recommended to use slope mass rating (SMR).*

The final index value for the RMR is the algebraic sum of the ratings, previously determined from Table 9 to Table 14, with the correction of the discontinuities orientation on Tables 15 and 16. Thus, it can be translated as the following formula [14]:

$$RMR = \sum(\text{Parameter ratings}) + \text{adjustment due to discontinuity orientation} \quad [14]$$

There are five different classes with different geotechnical meaning explained in Table 17. Therefore, a rock mass classified as Very Good (Class I) will be hard, slightly jointed, with no important seepage and slightly weathered, and so will present very few problems of strength and stability. It can be inferred that its bearing capacity will be high, it will allow excavation of steep slopes and no support or reinforcement measures will be needed in tunnels. This classification also describes the stand-up time and unsupported tunnel span characteristics of the rock mass.

Table 17 – Design parameters and engineering properties of rock mass (adapted from Bieniawski, 1989).

S. No.	Parameter/properties of rock mass	RMR (rock class)				
		100 – 81 (I)	80 – 61 (II)	60 – 41 (III)	40 – 21 (IV)	<20 (V)
1	Classification of rock mass	Very good	Good	Fair	Poor	Very poor
2	Average stand-up time	20 years for 15m span	1 year for 10m span	1 week for 5m span	10 hours for 2.5m span	30 minutes for 1m span
3	Cohesion of rock mass (MPa)*	> 0.4	0.3 – 0.4	0.2 – 0.3	0.1 – 0.2	< 0.1
4	Angle of internal friction of rock mass	> 45°	35° – 45°	25° – 35°	15° – 25°	< 15°
5	Allowable bearing pressure (T/m ²)	600 – 440	440 – 280	280 – 135	135 – 45	45 – 30
6	Safe cut slope (°) (Waltham, 2002)	> 70	65	55	45	< 40

**These valuables are applicable to slopes only in saturated and weathered rock mass.*

Bieniawski (1989) published a set of guidelines for the selection of support in tunnels in rock for which the value of RMR has been determined. These guidelines are reproduced in Table 18.

Table 18- Guidelines for excavation and support of 10 m span rock tunnels in accordance with the RMR system (after Bieniawski, 1989). Hoek et al. (1998) reported that these guidelines have been published for a 10 m span horseshoe shaped tunnel, constructed using drill and blast methods, in a rock mass subjected to a vertical stress <25 MPa (equivalent to a depth below surface of <900 m). It should be noted also has not had a major revision since 1973. In many mining and civil engineering applications, steel fibre reinforced shotcrete may be considered in place of wire mesh and shotcrete.

Rock Mass Class	Excavation	Supports		
		Rock bolts (20mm diameter, fully grouted)	Conventional shotcrete	Steel sets
I - Very Good rock RMR: 81-100	Full face; 3 m advance	Generally no support required except spot bolting		
II - Good rock RMR: 61-80	Full face; 1.0 - 1.5 m advance complete support 20m from face	Locally, bolts in crown 3 m long, spaced 2.5 m with occasional wire mesh	50 mm in crown where required	None
III - Fair rock RMR: 41-60	Top heading and bench; 1.5 - 3 m advance in top heading; commence support after each blast; complete support 10 m from face	Systematic bolts 4 m long, spaced 1.5 - 2m in crown and walls with wire mesh in crown	50 - 100 mm in crown and 30 mm in sides	None
IV - Poor rock RMR: 21-40	Top heading and bench; 1.0 - 1.5 m advance in top heading; install support currently with excavation, 10m from face	Systematic bolts 4 - 5m long, spaced 1 - 1.5m in crown and wall with wire mesh	100 - 150 mm in crown and 100 mm in sides	Light to medium ribs spaced 1.5 m where required
V - Very poor rock RMR: <20	Multiple drifts; 0.5 - 1.5 m advance in top heading; install support currently with excavation; shotcrete as soon as possible after blasting	Systematic bolts 5 - 6m long, spaced 1 - 1.5 in crown and walls with wire mesh; bolt invert	150 - 200 mm in crown, 150 mm in sides and 50 mm on face	Medium to heavy ribs spaced 0.75 m with steel lagging and forepoling if required; close invert

The RMR classification can be used to obtain geomechanical properties of rock mass as shown in Table 19.

Table 19 - Direct relations between rock mass classification and properties of rock mass (adapted from Aydan et al., 2014, In: Abbas and Konietzky, 2015).

Property	Empirical relation	Proposed by
Deformation modulus, E_m	$E_m = 2RMR - 100$ (GPa) (for $RMR > 50$)	Bieniawski (1978)
	$E_m = 10^{((RMR-10)/40)}$ (GPa)	Serafim and Pereira (1983)
	$E_m = e^{(4.407+0.081 \cdot RMR)}$ (GPa)	Jasarevic and Kovacevic (1996)
	$E_m = 0.0097RMR^{3.54}$ (MPa)	Aydan et al. (1997)
	$E_m = 25 \log Q$ (GPa)	Grimstad and Barton (1993)
	$E_m = (1 - \frac{D}{2}) \sqrt{\frac{\sigma_{ci}}{100}} 10^{((GSI-10)/40)}$ (GPa) (for $\sigma_{ci} < 100$ MPa)	Hoek et al. (2002)
	$E_m = 100 \frac{(1-0.5D)}{1+e^{\frac{25+250 \cdot GSI}{11}}}$ (GPa)	Hoek and Diederichs (2006)
	$E_m = 0.135 \left[E_i + \frac{1}{WD} \frac{RQD}{100} \right]^{1.1811}$ (GPa)	Kayabasi et al. (2003)
	$E_m = 5.6RMI^{0.3}$ (GPa) (for $RMI > 0.1$)	Palmstrom (1996)
	$E_m = 0.1 \left(\frac{RMR}{10} \right)^3$	Mitri et al. (1994)
	$E_m = 7(\pm 3) \sqrt{10^{(RMR-44)/21}}$ (GPa)	Diederichs and Kaiser (1999)
	$E_m = 10Q^{1/3}$ (GPa)	Barton (1995)
	$E_m = 10 \left(Q \frac{\sigma_{ci}}{100} \right)^{1/3}$ (GPa)	Barton (2002)
	$E_m = 10^{(\frac{GSI-10}{40})} \sqrt{\frac{\sigma_{ci}}{100}}$ (GPa)	Hoek and Brown (1997)
	$E_m = 0.0876RMR$ (GPa) (for $RMR > 50$)	Galera et al. (2005)
	$E_m = 0.0876RMR + 1.056(RMR-50) + 0.015(RMR-50)^2$ (GPa) (for $RMR \leq 50$)	Galera et al. (2005)
Uniaxial compressive strength, σ_{cm} (MPa)	$\sigma_{cm} = 0.0016RMR^{25}$	Aydan et al. (1997)
	$\sigma_{cm} = 5\gamma \left(Q \frac{\sigma_{ci}}{100} \right)^{1/3}$	Barton (2002)
Friction angle, φ_m ($^\circ$)	$\varphi_m = 20 + 0.5RMR$	Aydan and Kawamoto (2001)
	$\varphi_m = 20 \sigma_{cm}^{0.25}$	Aydan et al. (1993)
	$\varphi_m = \tan^{-1} \left(\frac{J_r}{J_a} \times \frac{J_w}{1} \right)$	Barton (2002)
Cohesion, c_m (MPa)	$c_m = \frac{\sigma_{cm} (1 - \sin \varphi_m)}{2 \cos \varphi_m}$	Aydan and Kawamoto (2001)
	$c_m = \left(\frac{RQD}{J_n} \times \frac{1}{SRF} \times \frac{\sigma_{ci}}{100} \right)$	Barton (2002)
Poisson's ratio, ν_m	$\nu_m = 0.25(1 + e^{-\sigma_{cm}/6})$	Aydan et al. (1993)
	$\nu_m = 0.5 - 0.2 \frac{RMR}{RMR + 0.2(100 - RMR)}$	Tokashiki and Aydan (2010)

E_m deformation modulus of rock mass, E_i Young's modulus of intact rock, RMR rock mass rating, Q rock mass quality, GSI Geological Strength Index, D Disturbance factor, σ_{ci} uniaxial compressive strength of intact rock, σ_{cm} uniaxial compressive strength of rock mass, RQD Rock Quality Designation, RMI Rock Mass Index, WD weathering degree, φ_m friction angle of rock mass, c_m cohesion of rock mass, ν_m Poisson's ratio of rock mass, J_n joint set rating, J_r joint roughness rating, J_w joint water rating, J_a joint alteration rating, SRF stress reduction factor, γ rock density (t/m^3)

2.4.5. Rock Mass Quality Q-system by Barton et al. (1974, 1977, 1980) and updated by NGI (2013)

After studying over 210 different case histories of hard-rock tunnels and caves from Scandinavia, N. Barton, R. Lien and J. Lunde, at the Norwegian Geotechnical Institute (NGI), proposed in 1974 the so-called Q-system classification for rock masses (Barton et al., 1974). Since 1974, the number of cited case histories evaluated has increased to over 1260 (Barton, 2002). The relevant bibliography related to Q-system is the following: Barton et al. (1974, 1977, 1980, 1985), Barton and Choubey (1977), Grimstad and Barton (1993), Barton and Quadros (2002), Barton and Bieniawski (2008), Barton (2000, 2002, 2006, 2007, 2012), NGI (2013). RMR and Q-System use essentially the same approach but use different log-scale ratings as, Q-system is a product of ratio of parameters while, RMR is the sum of parameters (Hoek et al., 1998; Hoek, 2007). The recommended applications for this classification are mainly for tunnels and caves with dome ceilings (Barton et al., 1974; Bieniawski, 1989; Singh and Goel, 1999, 2011; NGI, 2013). The numerical values of the Q-system varies in a logarithmic scale from 0,001 (poor rock masses quality) until 1000 (exceptional rock mass quality).

The rock mass quality classification (Q-system) is defined by the following factors (Barton et al., 1974, 1980):

$$Q = \left[\frac{RQD}{J_n} \right] * \left[\frac{J_r}{J_a} \right] * \left[\frac{J_w}{SRF} \right] \quad [15]$$

Where:

- RQD – Rock Quality Designation;
- J_n – Number of discontinuities sets;
- J_r – Joint roughness;
- J_a – Joint alteration factor;
- J_w – Joint water reduction factor;
- SRF – Stress reduction factor to consider in situ stresses.

It is possible to split the previous formula [15] as three different quotients (Barton et al., 1974, 1980; Hoek et al., 1998): rock mass structure (RQD/J_n), inter-block shear strength (J_r/J_a) and active tension (J_w/SRF). The first quotient (RQD/J_n) represents the structure of the rock mass and is a measure of the matrix block unit. The second quotient (J_r/J_a) concerns the friction occurring in the joint walls and relates the joint roughness with its alteration factor and materials contained within it. It will increase with the presence of more rough walls and decreases with higher alteration values. The third quotient (J_w/SRF) is an empirical factor that describes an active stress condition.

RQD and number of discontinuities sets (J_n)

The RQD value (Deere et al., 1967), in percentage, is the rating of RQD used for the Q-system (Table 20). When the rock mass has poor quality, a RQD rating of less than 10%, a minimum value of 10 should be used to evaluate Q. The number of discontinuities sets (J_n) can be affected by existing foliations, schistosity, slaty cleavage, among others. If these occurrences on the rock mass are frequent, they should be counted as a complete discontinuity set. If they only occur randomly and with occasional appearances they should be counted as a random joint set, while evaluating this parameter in Table 21.

Table 20 - Rock Quality Designation (adapted from Barton et al., 1974, 1980).

	RQD %	Condition
A	<25	Very poor
B	25-50	Poor
C	50-75	Fair
D	75-90	Good
E	90-100	Very good

Table 21 – Number of discontinuities sets (J_n) (adapted from Barton et al., 1974, 1980).

	Condition	J_n
A	Massive, no or few joints	0.5 – 1.0
B	One joint set	2
C	One joint set plus random	3
D	Two joint sets	4
E	Two joint sets plus random	6
F	Three joint sets	9
G	Three joint sets plus random	12
H	Four or more joint sets, random, heavily jointed, "sugar cube", etc.	15
I	Crushed rock, earth-like	20
	For intersections use, $3 * J_n$ For portals use $2 * J_n$.	

Joint roughness (J_r) and alteration factor (J_a)

Table 22 and 23, respectively, represent the roughness and degree of alteration of joint walls or filling materials. These parameters should be obtained from the weakest or clay-filled discontinuity set. If the relation of these parameters is calculated with a set oriented for stability, then a second set less favorably may be of greater significance with a different value for (J_r/J_a) and shall be used on equation [15].

Table 22 - Discontinuities wall roughness (J_r) (adapted from Barton et al., 1974, 1980).

Condition		J_r
(a) Rock wall contact and (b) Rock wall contact before 10 cm shear		
A	Discontinuous joint	4.0
B	Rough or irregular, undulating	3.0
C	Smooth, undulating	2.0
D	slicken sided, undulating	1.5
E	Rough or irregular, planar	1.5
F	Smooth, planar	1.0
G	Slicken sided, planar	0.5
Note: i) Description refers to small scale features and intermediate scale features, in that order		
(c) No rock wall contact when sheared		
H	Zone containing clay minerals thick enough to prevent wall contact	1.0
Note: ii) Add 1.0 if the mean spacing of the relevant joint set is greater than 3m (dependant on the size of the underground opening)		
iii) $J_r = 0.5$ can be used for planar, slicken sided joints having lineation, provided the lineations oriented in the estimated sliding direction		

Table 23 – Discontinuities alteration factor (J_a) (adapted from Barton et al., 1974, 1980).

Condition		Φ , approx. (degree)	J_a
(a) Rock wall contact (no material filling, only coating)			
A	Tightly healed, hard, non-softening, impermeable filling, i.e., quartz or epidote		0.75
B	Unaltered joint walls, surface staining only	25 – 35	1.0
C	Slightly altered joint walls; non-softening mineral coatings, sandy particles, clay-free disintegrated rock, etc.	25 – 30	2.0
D	Silty or sandy clay coatings, small clay fraction (non-softening)	20 – 25	3.0
E	Softening or low friction clay mineral coatings, i.e., kaolinite and mica; also chlorite, talc, gypsum, and graphite, etc., and small quantities of swelling clays (discontinuous coatings, 1–2 mm or less in thickness)	8 – 16	4.0
(b) Rock wall contact before 10 cm shear (thin mineral fillings)			
F	Sandy particles, clay-free disintegrated rock, etc.	25 – 30	4.0
G	Strongly over-consolidated, non-softening clay mineral fillings (continuous, <5 mm in thickness)	16 – 24	6.0
H	Medium or low over-consolidation, softening, clay mineral fillings (continuous, <5 mm in thickness)	12 – 16	8.0
J	Swelling clay fillings, i.e., montmorillonite (continuous, <5 mm in thickness); value of J_a depends on percent of swelling clay-size particles, and access to water, etc.	6 – 12	8 – 12

It has been found that $\tan^{-1}(J_r/J_a)$ is a fair approximation of the actual peak sliding angle of friction along the clay-coated joints. So, another way to estimate the internal friction angle (Table 24) was proposed by Barton and Bieniawski (2008).

Table 24 – Estimation of Angle of Internal Friction from the parameters J_r and J_a (Barton and Bieniawski, 2008)

Description		$\tan^{-1}(J_r/J_a)$					
		<i>(thin coatings)</i>					
(a) Rock wall contact		J_r	$J_a = 0.75$	1.0	2.0	3.0	4.0
	A. Discontinuous joints	4.0	79°	76°	63°	53°	45°
	B. Rough, undulating	3.0	76°	72°	56°	45°	37°
	C. Smooth, undulating	2.0	69°	63°	45°	34°	27°
	D. Slicken sided, undulating	1.5	63°	56°	37°	27°	21°
	E. Rough, planar	1.5	63°	56°	37°	27°	21°
	F. Smooth, planar	1.0	53°	45°	27°	18°	14°
	G. Slicken sided, planar	0.5	34°	27°	14°	9.5°	7.1°
(b) Rock wall contact when sheared		<i>(Thin filling)</i>					
		J_r	$J_a = 4.0$	6	8	12	
	A. Discontinuous joints	4.0	45°	34°	27°	18°	
	B. Rough, undulating	3.0	37°	27°	21°	14°	
	C. Smooth, undulating	2.0	27°	18°	14°	9.5°	
	D. Slicken sided, undulating	1.5	21°	14°	11°	7.1°	
	E. Rough, planar	1.5	21°	14°	11°	7.1°	
	F. Smooth, planar	1.0	14°	9.5°	7.1°	4.7°	
	G. Slicken sided, planar	0.5	7°	4.7°	3.6°	2.4°	
(c) No rock wall contact when sheared		<i>(Thick filling)</i>					
		J_r	$J_a = 5$	6	8	12	
	Nominal roughness of discontinuity rock walls	1.0	11.3°	9.5°	7.1°	4.8°	
		J_r	$J_a = 13$	16	20	–	
		1.0	4.4°	3.6°	2.9°	–	
(c) No rock wall contact when sheared (thick mineral fillings)							
K, L, M	Zones or bands of disintegrated or crushed rock and clay (see G, H, J for description of clay condition)				6 – 24		6, 8 or 8 – 12
N	Zones or bands of silty or sandy clay, small clay fraction (non-softening)				–		5.0
O, P, R	Thick, continuous zones or bands of clay (see G, H, J for description of clay condition)				6 – 24		10, 13 or 13 – 20

Joint water reduction factor (J_w) and Stress Reduction Factor (SRF)

The presence of water along joint walls will reduce the effective normal stress of the shear strength of joints. The water may cause the softening and possible wash-out of joint filling material thus, reducing the joint shear strength. The ratings for the water reduction factor (J_w) are presented in Table 25.

Table 25 - Joint water reduction factor J_w (adapted from Barton et al., 1974, 1980).

Condition	Approx. water pressure (MPa)	J_w
A Dry excavation or minor inflow, i.e., 5 lt./min locally	< 0.1	1
B Medium inflow or pressure, occasional outwash of joint fillings	0.1 – 0.25	0.66
C Large inflow or high pressure in competent rock with unfilled joints	0.25 – 1.0	0.5
D Large inflow or high pressure, considerable outwash of joint fillings	0.25 – 1.0	0.33
E Exceptionally high inflow or water pressure at blasting, decaying with time	> 1.0	0.2 – 0.1
F Exceptionally high inflow or water pressure continuing without noticeable decay	> 1.0	0.1 – 0.05

Factors C to F are crude estimates. Modify J_w if drainage measures are installed. Special problems caused by ice formation are not considered. For general characterization of rock masses distant from excavation influences, the use of J_w ¼ 1.0, 0.66, 0.5, 0.33, etc., as depth increases from, say, 0–5, 5–25, 25–250 to > 250 m is recommended, assuming that RQD/J_n is low enough (e.g., 0.5–25) for good hydraulic conductivity. This will help to adjust Q for some of the effective stress and water softening effects in combination with appropriate characterization values of SRF. Correlations with depth-dependent static modulus of deformation and seismic velocity will then follow the practice used when these were developed.

The stress reduction factor (SRF) parameter (Table 26) is a measure of loosening pressure during an excavation through, shear zones and clay-bearing rock masses. Rock stress, q_c/σ_1 , in a competent rock mass where, q_c is the uniaxial compressive strength (UCS) of rock material and σ_1 is the major principal forces before excavation. *SRF* can also be regarded as a total stress parameter.

When creating this classification, Barton et al. (1974) did not considered the influence of joint orientation due to the fact that, many types of excavations can be, and normally are, adjusted to avoid the maximum effect of unfavourably oriented major joints. He also stated that the parameters J_n , J_r and J_a played a more important role than joint orientation because, the number of joint sets determines the degree of freedom for block movement; the frictional and dilatational characteristics (J_r) can counterbalance the down-dip gravitational component of weight of wedge formed by the unfavourably oriented joints (Singh and Goel, 2011).

After retrieving the Q-system value, there are several parameters that can be designed, such as an estimation of the support pressure (Barton et al., 1974, 1980), a vertical or roof support pressure and consequently, a horizontal or wall support pressure (Singh et al., 1992), an estimation of deformation or closure and finally the unsupported span.

Table 26 - Stress Reduction Factor (adapted from Barton et al., 1974, 1980).

Condition	SRF			
(a) Weakness zones intersecting excavation, which may cause loosening of rock mass when tunnel is excavated				
A Multiple occurrences of weakness zones containing clay or chemically disintegrated rock, very loose surrounding rock (any depth)	10.0			
B Single-weakness zones containing clay or chemically disintegrated rock (depth of excavation \leq 50 m)	5.0			
C Single-weakness zones containing clay or chemically disintegrated rock depth of excavation \geq 50 m)	2.5			
D Multiple-shear zones in competent rock (clay-free), loose surrounding rock (any depth)	7.5			
E Single-shear zones in competent rock (clay-free) (depth of excavation \leq 50 m)	5.0			
F Single-shear zones in competent rock (clay-free) (depth of excavation \geq 50 m)	2.5			
G Loose, open joints, heavily jointed or "sugar cube," etc. (any depth)	5.0			
(b) Competent rock, rock stress problems				
	q_c/σ_1	σ_θ/q_c	SRF (old)	SRF (new)
H Low stress, near surface, open joints	> 200	< 0.01	2.5	2.5
J Medium stress, favorable stress condition	200 – 10	0.01 – 0.3	1.0	1.0
K High stress, very tight structure; usually favorable to stability, may be unfavorable to wall stability	10 – 5	0.3 – 0.4	0.5 – 2.0	0.5 – 2.0
L Moderate slabbing after >1 hour in massive rock	5 – 3	0.5 – 0.65	5 – 9	5 – 50
M Slabbing and rock burst after a few minutes in massive rock	3 – 2	0.65 – 1.0	9 – 15	50 – 200
N Heavy rock burst (strain-burst) and immediate dynamic deformations in massive rock	< 2	> 1	15 – 20	200 – 400
(c) Squeezing rock; plastic flow of incompetent rock under the influence of high rock pressures				
O Mild squeezing rock pressure				1 – 5 5 – 10
P Heavy squeezing rock pressure				> 5 10 – 20
(d) Swelling rock; chemical swelling activity depending on presence of water				
Q Mild swelling rock pressure				5 – 10
R Heavy swelling rock pressure				10– 15
Considerations:				
Reduce these SRF values by 25–50% if the relevant shear zones only influence but do not intersect the excavation. This will also be relevant for characterization;				
For strongly anisotropic virgin stress field (if measured): when $5 < \sigma_1/\sigma_3 < 10$, reduce q_c to 0.75 q_c ; when $\sigma_1/\sigma_3 > 10$, reduce q_c to 0.50 q_c (where q_c is unconfined compressive strength). σ_1 and σ_3 are major and minor principal stresses, and σ_θ is the maximum tangential stress (estimated from elastic theory);				
Few case records available where depth of crown below surface is less than span width; suggest SRF increase from 2.5 to 5 for such cases;				
Cases L, M, and N are usually most relevant for support design of deep tunnel excavation in hard massive rock masses, with RQD/J_n ratios from about 50–200;				
For general characterization of rock masses distant from excavation influences, the use of SRF = 5, 2.5, 1.0, and 0.5 is recommended as depth increases from, say, 0–5, 5–25, 25–250, >250 m. This will help to adjust Q for some of the effective stress effects, in combination with appropriate characterization values of J_w . Correlations with depth-dependent static modulus of deformation and seismic velocity will then follow the practice used when these were developed.				

The unsupported span is the parameter that concerns the behaviour of the excavation and the required support for it. The equivalent dimension (D_e), takes in consideration the size and the

purpose of the excavation by relating the span (or excavation diameter or height) with a safety index, the Excavation Support Ratio (ESR) and it is calculated using the following equation [16]:

$$D_e = \frac{\text{span, diameter, or height (m)}}{ESR} \quad [16]$$

The ESR value is related with the purpose of the excavation and the degree of safety demanded by the support system installed to keep its stability. Barton et al. (1974) proposes the values observed in Table 27.

Table 27 - Values of Excavation Support Ratio (Barton, 2008).

Type of excavation		ESR
A	Temporary mine openings, etc	2 – 5
B	Permanent mine openings, water tunnels for hydro power (excluding high pressure penstocks), pilot tunnels, drifts and headings for large openings, surge chambers	1.6 – 2.0
C	Storage caverns, water treatment plants, minor road and railway tunnels, access tunnels	1.2 – 1.3
D	Power stations, major road and railway tunnels, civil defense chambers, portals, intersections	0.9 – 1.1
E	Underground nuclear power stations, railway stations, sports and public facilities, factories, major gas pipeline tunnels	0.5 – 0.8

When using Tunnel Boring Machines (TBM) to excavate tunnels, this values suffers a minor update, as described on the Table 28.

Table 28 – ESR values when considering the excavation for tunnels by Tunnel Boring Machines (TBM) (Barton, 2000). When calculating car traffic tunnels or high velocity train tunnels the used value shall be 0.5 (Hoek, 2007).

Type of excavation		ESR
A	Pilot tunnel	2
B	Tunnels for water and sewer	1.5
C	Traffic tunnels	0.5 – 1.0

Using the Q-system ratings and the equivalent dimension (D_e) values, it is possible to retrieve the category of the definitive reinforcement from the rock support chart (see details in NGI, 2013), Figure 19

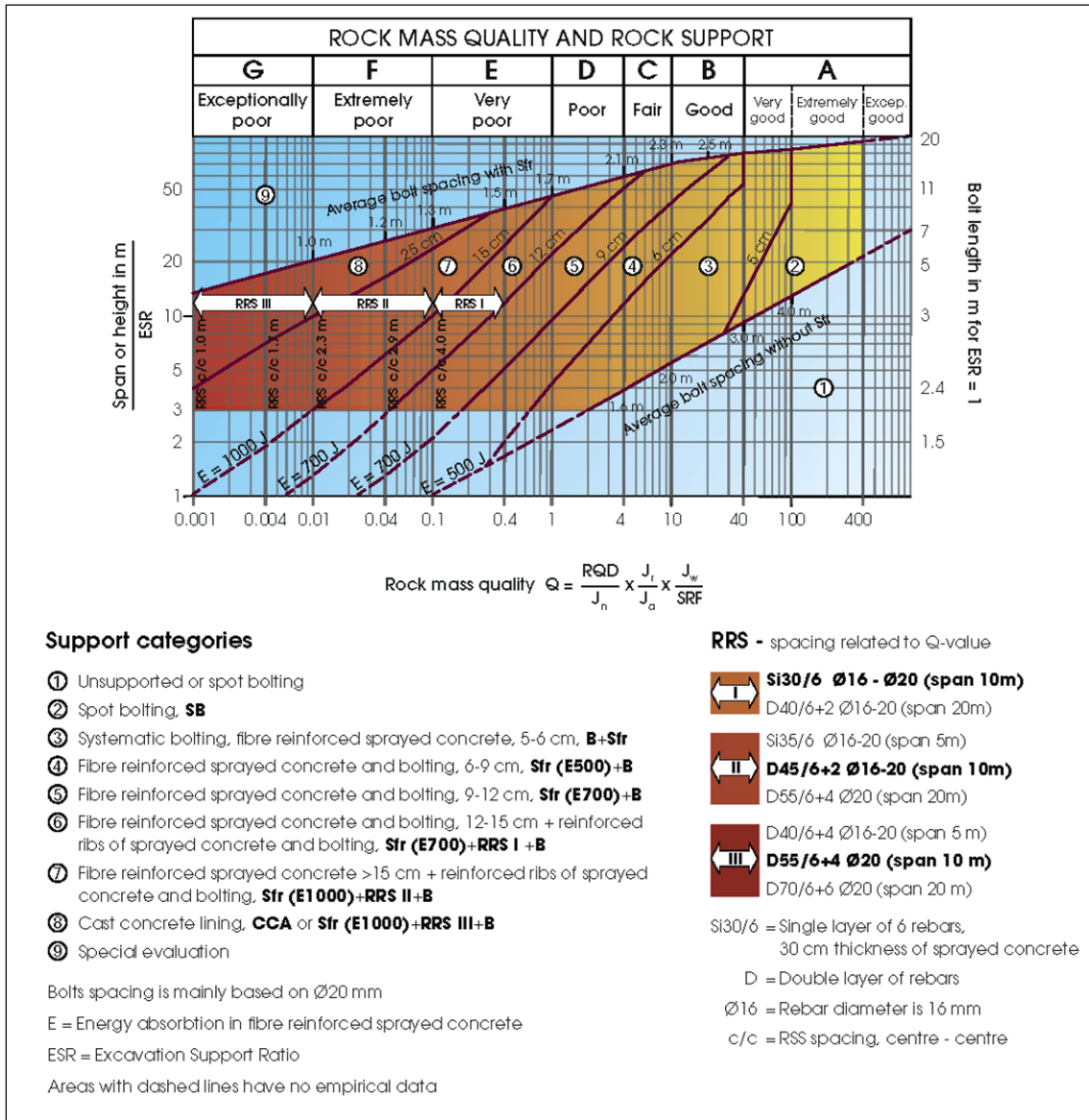


Figure 19 - Q-system classification and rock support chart for retrieving the reinforcement category (adapted from Barton et al., 1974, 1980). After: NGI (2013).

The ESR (Excavation Support Ratio) value allows also the attainment of other parameters (see Figure 19).

Barton et al. (1974) proposed the equation [17], for obtaining the maximum span (L) for a self-supporting rock mass:

$$L = 2 * RSR * Q^{0,4} \tag{17}$$

2.4.6. RMR-Q-system correlation: updated support chart

The geomechanical classifications previously refereed, RMR and Q-system (Bieniawski, 1973, 1989; Barton et al., 1974, 1980, and references therein), were developed with a common goal of evaluating rock masses based on parametric descriptions of the rock-masses and geomechanical quantitative testing (ISRM, 2007, 2015). Barton and Bieniawski (2008) stated an important issue: the essence of both schemes was to quantify rock mass characteristics previously based on qualitative geological descriptions. With its wide popularity and persistent usage, Barton and Bieniawski (2008) agreed when saying that: *“(...) after 35 years of use throughout the world in tunnelling and mining, the record of the RMR and Q systems in geological and engineering practice speaks for itself. These two systems have become entrenched as the most effective empirical design tools for determination of rock mass quality and estimating rock mass properties and tunnel support measures”*. Meaning that, throughout the engineering project, it is essential the usage of at least one classification, quantifying the new rock mass conditions found and adapting the reinforcement methods within each classification.

A few differences between the two classifications can be pointed out, such as: the Q-system does not consider the uniaxial compression strength (UCS), while the RMR does not relate the in-situ rock stress conditions. Both classifications consider the geology and structure of the rock although in different ways. This way, the correct approach is using the ISRM procedures (ISRM, 2007, 2015) to the geological and geotechnical assessment.

The comparison and correlation between these two classification systems was established with more than 100 different cases from different continents (Bieniawski, 1989). Regarding this approach, Table 29 shows the different expressions along the years, by diverse authors.

Table 29 - Correlation proposal for the RMR - Q-system from different authors (Bieniawski, 1989; Barton, 2006).

Correlation proposal for RMR – Q-system	Author
$RMR = 5,9 \ln Q + 43$	Rytledge & Preston (1978)
$RMR = 5,4 \ln Q + 55,2$	Moreni (1980)
$RMR = 5 \ln Q + 60,8$	Cameron-Clarke & Budavari (1981)
$RMR = 10,5 \ln Q + 41,8$	Abad et al. (1984)
$RMR = 9 \ln Q + 44$	Bieniawski (1989)
$RMR = 15 \ln Q + 50$	Barton (1995)

Based on some previous Barton’s works (e.g., Barton et al., 1974, 1980; Grimstad and Barton, 1993; Barton, 2000) a support chart identical to the one previously made for the Q-system was

proposed (Figure 20). In that updated chart, Barton and Bieniawski (2008) proposed the addition of alternate correlations between RMR and Q-system.

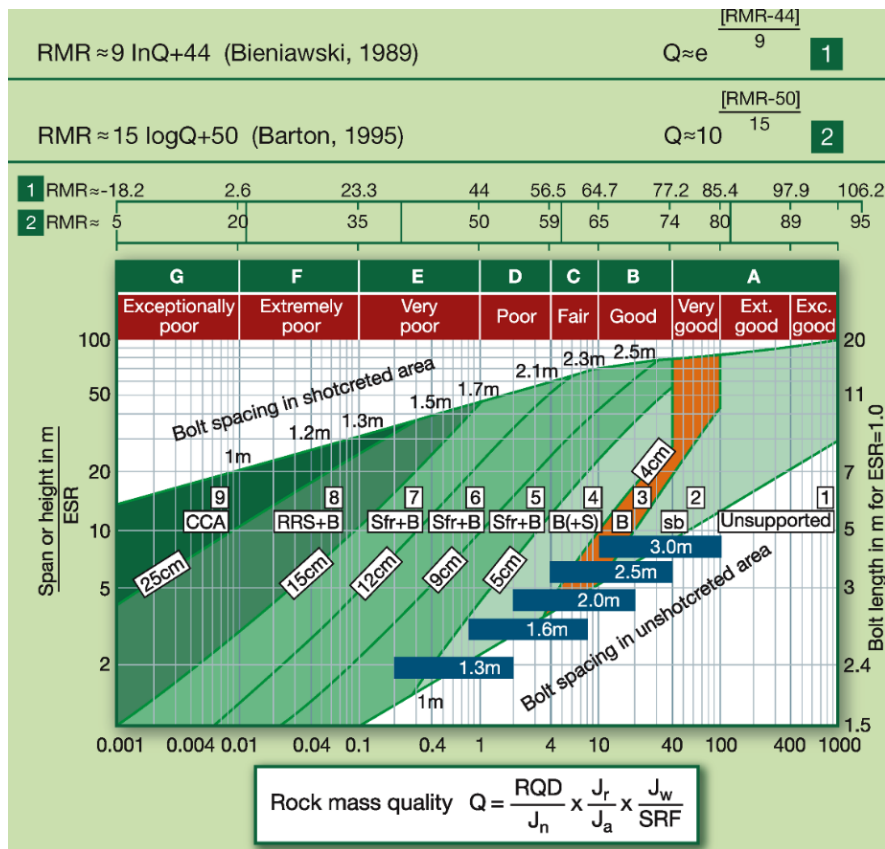


Figure 20 - The support selection chart, with the addition of alternate correlations between RMR and Q (after Barton and Bieniawski, 2008).

However, for the correct application of these classifications it is necessary to pay attention to the following topics, such as (Barton and Bieniawski, 2008):

- i) Ensure that the classification parameters are quantified (measured, not just described), from standardised tests, for each geotechnically zone, employing boreholes, exploration adds and surface mapping, plus applied geophysics;
- ii) Follow the established procedures by the Q-system and RMR classifications and properly determining their typical ranges and the average values;
- iii) Use both systems and confirm with at least two correlations proposed by Bieniawski and Barton;
- iv) Assess the support and reinforcement requirements, in accordance to the rock mass to be applied;
- v) Estimate stand-up time and rock mass modulus for preliminary modelling purposes (Figure 21).

- vi) If sufficient information is not available, recognising the iterative design process, request further geological exploration and parameter testing, e.g. stress measurements, if necessary;
- vii) Apply numerical modelling, where it is possible and confirm if the information available is enough;
- viii) Perform RMR and Q-system mapping as the construction proceeds so that comparisons can be made of expected and encountered conditions, leading to design verification or appropriate changes.

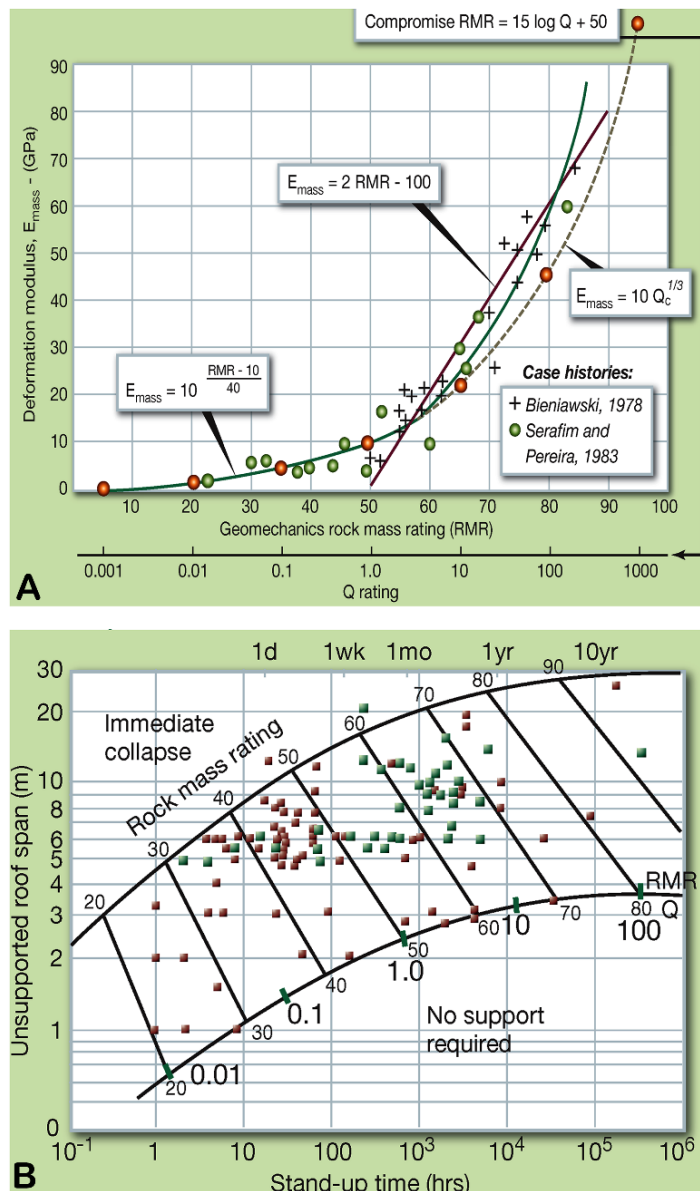


Figure 21 - A) Static modulus of deformation E_m versus RMR and Q-system; B) Stand-up time data versus RMR from case histories, where red dots represents tunnel, and green signifies mine results (case histories and RMR data compiled by Bieniawski, 1989; Q-system relationship by Barton, 2002).

2.4.7. Geological Strength Index (GSI)

The Geological Strength Index (GSI) resulted from combining observations of the rock mass conditions (Terzaghi's descriptions; Terzaghi, 1946) with relationships, developed from the experience achieved using the RMR-system (Singh and Goel, 2011). GSI is a simple, fast and reliable system to characterise rock masses. It is based on the rock mass geostructure and classifies the geological-geotechnical quality of rock masses through the definition of diverse rock classes. The key publications related to the GSI Index are the following: Hoek (1994, 1998, 2007), Hoek et al. (1998), Hoek and Marinos (2000), Marinos and Hoek (2000, 2001), Cai et al. (2004), Marinos et al. (2005, 2006, 2007), Hoek et al. (2013).

The original criterion for jointed rock masses used by Hoek and Brown (1980a,b) — the so-called Hoek-Brown criterion — assumes that the rupture of the rock mass is due to dynamic processes (translation or rotation) affecting the intact rock blocks separated by joints. Equation [18] presents its mathematical formula:

$$\sigma'_1 = \sigma'_3 + \sigma_c * \left(m_i * \frac{\sigma'_3}{\sigma_c} + 1 \right)^{1/2} \quad [18]$$

where:

- σ'_1 – Maximum effective principal stress;
- σ'_3 – Minimum effective principal stress;
- σ_c – Uniaxial compressive stress (UCS) of intact rock material;
- m_i – Hoek-Brown rock material constant.

Along the years, the equation stated above [18] suffered some changes and improvements, becoming the generalised strength criterion (e.g., Hoek et al., 1992, 2002; Hoek and Marinos, 2007 and references therein), as equation [19] shows:

$$\sigma'_1 = \sigma'_3 + \sigma_c * \left(m_b * \frac{\sigma'_3}{\sigma_c} + s \right)^a \quad [19]$$

Where:

- m_b – reduced value of material constant m_i ;
- s, a – constant values depending on the rock material.

While the parameters of the equation [19] are obtained via tests, the m_b, s and a values are described via correlations, using the GSI value, that varies between 0 and 100. The rock mass quality from the GSI classification can be evaluated through Table 30.

Table 30 - GSI rock mass qualitative classification (adapated from Hoek, 2007)

GSI	> 75	55 – 75	35 – 55	20 – 35	< 20
Rock mass quality	Very good	Good	Fair	Poor	Very poor

The GSI index can also be obtained by the previously described classifications: the RMR and Q-system. According to Hoek (2007), the GSI index is defined by the following equation [20] taking into consideration that its application can only be applicable with values of RMR > 23. Moreover, the orientation of the joints does not affect the excavation, therefore it is very favourable to it and the rating related to the presence of water is 15 (e.g., dry rock mass). This way, the relation between the two classifications is the following:

$$GSI = RMR - 5 \quad [20]$$

For Barton (2011), the previous algebraic relation, due to its simple and reducing nature, it is not usable in the current days with the actual knowledge of the geomechanical classifications and should be neglected. However, some authors refer this relation as valid and plausible to do a provisional evaluation of the GSI index (e.g., Hoek, 2007; Singh and Goel, 2011).

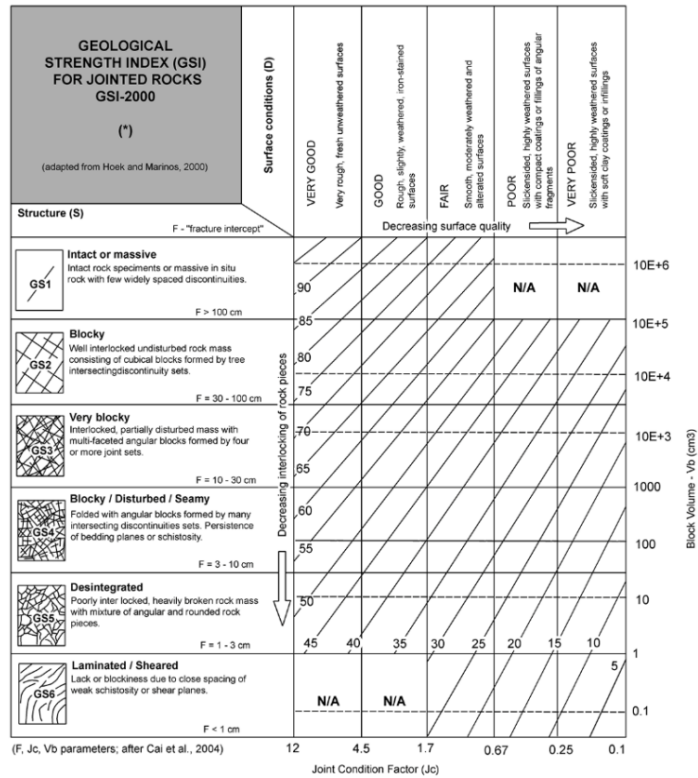
Additionally, it is possible to estimate the GSI index by means of the Q-value. Before estimating the GSI through Q, it is necessary to calculate an adapted Q' , as shown on equation [21]. In this case, there is a consideration to make as the active tension in the rock mass is not considered.

$$Q' = \frac{RQD}{J_n} * \frac{J_r}{J_a} \quad [21]$$

Hence, the GSI index will be estimated through equation [22]:

$$GSI = \ln(Q') + 44 \quad [22]$$

For a more direct approach, it is possible to use the GSI chart (e.g., Hoek and Marinos, 2000; Marinos and Hoek, 2001; Marinos et al., 2005, 2007; Hoek et al., 2013) that describes the geostructure characteristics of the rock mass, according to the rock discontinuities and the discontinuity surface conditions (Figure 22 and Figure 23). The relationship between rock mass structure (geostructural conditions) and rock discontinuity surface conditions (geotechnical conditions) is used to estimate an average GSI value represented in the form of diagonal contours. It is recommended to use a range of values of GSI preferably to a single value (Hoek, 1998).



* From the lithology, structure and surface conditions of the discontinuities, estimate the average value of GSI. Do not try to be too precise. Quoting a range from 33 to 37 is more realistic than stating that GSI = 35. Note that the table does not apply to structurally controlled failures. Where weak planar structure planes are present in an unfavourable orientation with respect to the excavation face, these will dominate the rock mass behaviour. The shear strength of surfaces in rocks that are prone to deterioration as a result of changes in moisture content will be reduced if water is present. When working with rocks in the fair to very poor categories, a shift to the right may be made for the wet conditions. Water pressure is dealt with by effective stress analysis.

Figure 22 – GSI-2000 chart (adapted from the version Hoek and Marinos, 2000): estimate of GSI based on in-situ geostucture of the rock mass and geotechnical discontinuities conditions (adapted from Hoek and Marinos, 2000; and updated from Cai et al., 2004 in terms of its quantification by block volume and joint condition factor is also shown on the right side).

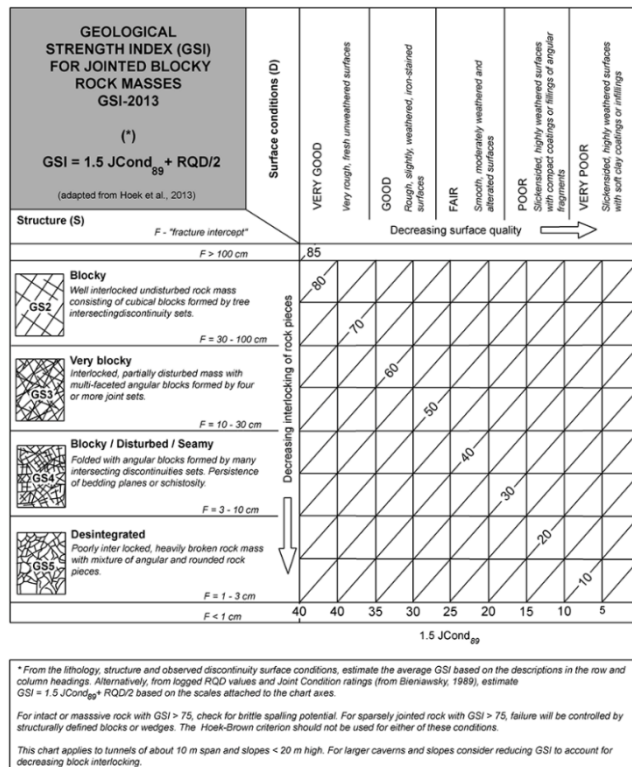


Figure 23 – GSI-2013 chart (adapted from the version Hoek et al., 2013): modified Geological Strength Index chart and the quantification GSI geomechanical classification proposal by Hoek et al. (2013).

2.4.8. Hydrogeomechanical classification

The main goal of hydrogeomechanical classifications is to identify bedrock groundwater conditions through, the location of open fractures with fluid circulation – the fracture network. Groundwater development in mountainous terrains still present challenges since, when doing site-studies for understanding groundwater systems, the surficial aquifers have been largely removed by erosive activity leaving no trace of where to locate fractured bedrock aquifers (Gates, 2003). In order to, understand the role of the bedrock groundwater sources and seepage in engineering works, hydrogeologists and rock engineers employ a blend of investigative techniques, such as, the Hydro-Potential (HP) Value or the rock mass Hydraulic Conductivity (HC-system), to include terrain and fracture analysis coupled with structural mapping and hydrogeotechnical surveys.

Groundwater seepage into excavations for tunnels, mines and other construction sites presents challenging problems for mining and civil engineering projects. Having a hydrogeomechanical tool at the engineer's disposal to predict seepage would aid in planning for construction and design problems. In addition, groundwater flow through fractured bedrock is controlled by several interrelated physical characteristics of the rock mass, including the lithology and rock quality, number, density, roughness, hydraulic conductivity, shape, aperture, and the connectivity of fractures (Gates, 2003).

2.4.8.1. The Hydro-Potential (HP) Value

An important consideration when dealing with engineering projects, such as excavations for tunnels, mines and other constructions sites, is the groundwater seepage found on site. Gates (1995, 1997, 2003) created this technique, mainly, to aid the construction planning and design problems concerning the seepage prediction on rock masses.

Gates (1997, 2003) proposed the so-called Hydro-Potential (HP) value as a new rock mass classification semi-quantitative technique employed to evaluate the potential for developing groundwater in bedrock. This technique may also be adapted to estimate groundwater seepage into excavations in bedrock. The HP-value estimates the rock mass potential to hydraulically transmit groundwater. The method is a simple and quick technique used to evaluate rock outcrop surroundings and within the construction site (Gates, 2003).

The HP-value technique is a modification of the engineering rock mass quality designation (Q-system), originally developed for evaluating rock competency in tunnel design (Barton et al., 1974, 1980) and seismic rock fall susceptibility (Harp and Noble, 1993). The method uses six fracture characteristics of the rock mass and assigns a numerical value (details in Gates, 1997, 2003). For

purposes of estimating the HP-value, the term “joint” is roughly, or non-genetically, used to refer all discontinuities that can act as groundwater conduits, such as foliation, joints, faults, and other cracks (Gates, 2003).

The equation [23] for the Hydro-Potential value is as follows:

$$HP_{value} = \left(\frac{RQD}{J_n}\right) \times \left(\frac{J_r}{(J_k)(J_{af})}\right) \times (J_w) \quad [23]$$

Where:

- RQD – Rock Quality Designation;
- J_n – Joint set number;
- J_r – Joint roughness number;
- J_k – Joint conductivity factor;
- J_{af} – Joint aperture factor;
- J_w – Joint water factor.

The application of the HP-value technique is rather simple and straightforward using the following tables (see details in Gates, 1997, 2003).

Rock Quality Designation – RQD

As it was previously stated, the description and rating for this parameter can be found on Table 31 and it was suggested by Deere (1963) and Deere et al. (1967).

Table 31 – RQD classification (after Deere, 1963; adapted from Gates, 1997, 2003).

	RQD %	Condition
1.	<25	Very poor
2.	25-50	Poor
3.	50-75	Fair
4.	75-90	Good
5.	90-100	Very good

If the drill core is unavailable, one must estimate the average RQD from rock outcrops in the surrounding of the test well site. Palmström (1995) suggested the following relationship [24]:

$$RQD = (115) - (3.3J_v) \quad [24]$$

Where, J_v – total number of joints or fractures per cubic meter of rock mass. For $J_v < 4.5$, RQD = 100 (Palmström, 1995).

Joint Set Number – J_n

The joint set number represents the number of joint sets grouped with the same orientation and density of fractures in the rock mass. It is possible to define it with fracture survey analyses techniques, such as, the Scanline Sampling Technique, coupled with stereonet and rose diagrams. These methods were developed from the measurement of geological attitudes of joints

observed in the rock and the consequent plot in a diagram. The plotted diagram displays the intervals of higher occurrence of the discontinuities orientation in a rock mass. Hence, it is possible to define the discontinuities sets and their orientation. Table 32 shows the description and rating for the Joint Set Number.

Table 32 – Description and ratings for joint set number (after Barton et al., 1974; adapted from Gates, 1997, 2003).

Number	Condition	J_n
1.	Massive, no or few joints	0.5 – 1.0
2.	One joint set	2
3.	One joint set plus random	3
4.	Two joint sets	4
5.	Two joint sets plus random	6
6.	Three joint sets	9
7.	Three joint sets plus random	12
8.	Four or more joint sets, random, heavily jointed, "sugar cube", etc.	15
9.	Crushed rock, earth-like	20
Note: For intersections use ($3*J_n$). For portals use ($2*J_n$).		

Joint Roughness Number – J_r

The joint roughness number represents the smoothness of the plane up unto the absolute roughness of the joint, which, in hydrogeomechanical classifications may be known as the potential flow conduit. This parameter concerns the variation and effective aperture size of the fracture through the channelling of flow between the fracture walls. Louis (1969) demonstrated that fluid flow is dependent on fracture roughness. Joint roughness may be measured using a contour gauge and compared to a set of standard profiles developed by Barton and Choubey (1977). However, it is usually sufficient to estimate the roughness by inspection of the joint planes (Gates, 2003). Table 33 shows the ratings for this parameter.

Table 33 – Description and ratings for joint roughness number, J_r (after Barton et al., 1974; adapted from Gates, 1997, 2003).

No.	Description	Rating
1.	Discontinuous joints	4.0
2.	Rough or irregular, undulating	3.0
3.	Smooth, undulating	2.0
4.	Slicken sided, undulating	2.0
5.	Rough or irregular, planar	1.5
6.	Slicken sided planar	1.5
7.	Smooth, planar, polished	1.0

Joint aperture factor – J_{af}

Aperture size and shape are extremely important in the evaluation of flow characteristics of a fracture. Roughness also controls the effective shape of the fracture aperture. The aperture size of the fractures exposed at the surface outcrop will provide an estimate of maximum width of fracture apertures in the sub-surface bedrock. Table 34 lists the description and ratings for the joint aperture factor, J_{af} described, among others, by Harp and Noble (1993). Gates (1997) has found that is sufficient to report the 90th percentile of the average width of the aperture.

Table 34 – Description and ratings for joint aperture factor, J_{af} (modified from Harp and Noble, 1993; adapted from Gates, 1997, 2003).

No.	Description	Rating
1.	All joints tight, < 0.1 mm	1.0
2.	Joints 90% 0.1 ≤ 1.0 mm	1.2
3.	Joints 90% 1.0 ≤ 5.0 mm	1.4
4.	Joints 90% 5.0 ≤ 10.0 mm	1.8
5.	Joints 90% 10.0 ≤ 20.0 mm	2.5
6.	Joints 90% 20.0 ≤ 50.0 mm	5.0
7.	Joints 90% 50.0 ≤ 100.0 mm	7.5
8.	Joints 90% 100.0 ≤ 200.0 mm	10.0
9.	Joints 90% > 200 mm	15.0

Joint Hydraulic Conductivity Factor – J_k

The hydraulic conductivity of a fracture is a function of the presence or lack of infilling material in the joint. Sterrett (2007) defines hydraulic conductivity as the rate of water flow, expressed in meters per day (m/day), through a cross section of one square meter under a unit hydraulic gradient at the prevailing temperature. A fracture healed with some type of mineral will exhibit a low hydraulic conductivity while an open, clean fracture will have an excellent flow. The description and ratings related to J_k are summarised in Table 35.

Table 35 – Descriptions and ratings for average hydraulic joint conductivity number, J_k (modified from Freeze and Cherry, 1979; adapted from Gates, 1997, 2003).

No.	Description	Rating	Hydraulic Conductivity (m/day)
1.	All joints tight or healed with calcite/ quartz, no flow	1.0	$<10^{-5}$
2.	90% joints clay filled, poor flow	2.0	$10^{-5} - 10^{-2}$
3.	90% joints silty sand filled, moderate flow	3.0	$10^{-2} - 10^{-1}$
4.	90% joints clean sand to gravel filled, moderate to good flow	3.5	$10^{-1} - 10^3$
5.	90% joint walls clean mostly open, good flow	4.0	$10^3 - 10^5$
6.	90% joints open, clean, excellent flow	5.0	$>10^5$

Joint Water Factor – J_w

The HP-value is estimated from the fracture characteristics. Annual precipitation rates, regional or local groundwater flow settings, and/or the impact of reservoirs and large bodies of water in the vicinity of interest do not directly control the HP-value. Nonetheless, the presence of groundwater discharging from joints along the rock outcrop enhances the probability of groundwater occupying the fractures in the subsurface bedrock. Therefore, the occurrence of water in the fracture is a characteristic of the fracture itself. Table 36 lists the description and ratings for the joint water factor (J_w) suggested, among others, by Barton et al. (1974) and updated by Gates (1997, 2003) to include items 2 through 5 (description, drops/min and rating).

Table 36 – Description and rating for joint water factor, J_w (modified from Barton et al, 1974; adapted from Gates, 1997, 2003).

No.	Description	Drops/min	L/sec	Rating
1.	Dry	<1	$< 1 \times 10^{-6}$	1.0
2.	Damp	$1 \leq 10$	$1 \times 10^{-6} \leq 1 \times 10^{-5}$	0.94
3.	Drops	$10 \leq 100$	$1 \times 10^{-5} \leq 1 \times 10^{-4}$	0.86
4.	Dripping	>100	$1 \times 10^{-4} \leq 1 \times 10^{-3}$	0.76
5.	Seeping		$1 \times 10^{-3} \leq 1 \times 10^{-2}$	0.66
6.	Slight flow		$1 \times 10^{-2} \leq 1 \times 10^{-1}$	0.50
7.	Moderate flow		$1 \times 10^{-1} \leq 1$	0.33
8.	High flow		>1	0.20

Note: 1 drop (minim) $\approx 1 \times 10^{-6}$ litre $\approx 2 \times 10^{-5}$ gallon, 1 litre/second = 15.85 gallons/minute.

Gates (2003) states an important issue: “normally, surface rock outcrops surrounding the target basin are dry, therefore a rating value of one is most common for these joints. However, in some cases there may be seeps or perennial springs exiting the joints of the rock outcrop. Joints for this rock would receive a rating less than one depending on the flow discharge”. The numerical HP-

values ranges from 1.33×10^{-3} (for exceptionally poor quality rock) up to 800 (for exceptionally good quality; competent rock mass).

Gates (1997) compared the HP-values to both yield and specific capacities of bedrock wells; the curve displayed a strong inverse relationship between HP-values and seepage. Over than -0.76 for the correlation coefficient, R , which is good for geologic correlations. For the coefficient of determination, R^2 , it suggested that 60% of the HP-values correlate with observed seepage values. When comparing the HP-values of the rock masses to both pumping yields of wells and seepage, it was observed an inverse and even stronger correlation. In this case, the correlation coefficient, R , exceeded -0.92 , which is exceptional for geologic correlations. The coefficient correlation, R^2 , suggested that 86% of the HP-values correlate with both well discharge from bedrock and observed seepage discharge from fractured rock (details in Gates, 1997, 2003). As showed in Figure 24, over 83% of the studied wells indicated higher yields and specific capacities correspond to lower HP-values for outcrops of similar lithology in the vicinity of the local bedrock wells.

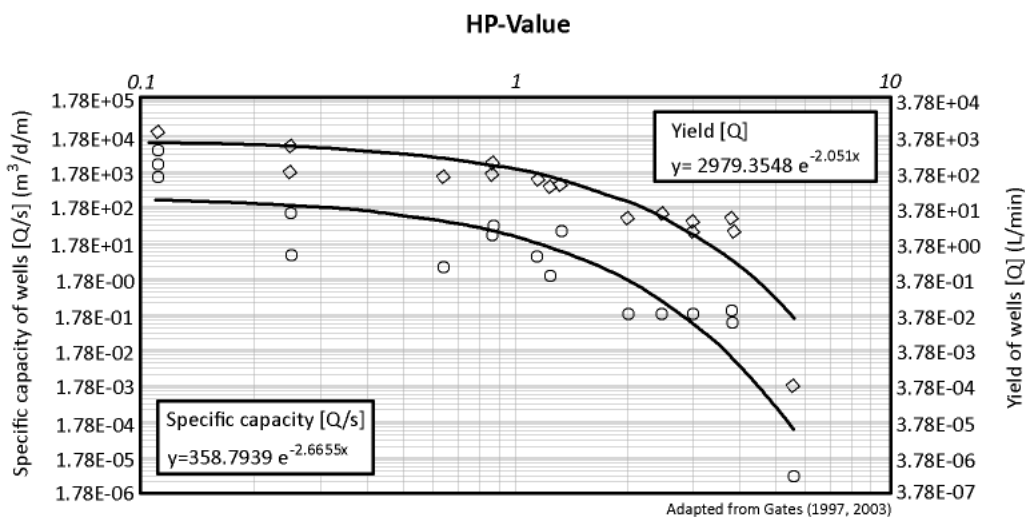


Figure 24 - Comparison of HP-values to yields and specific capacities of local bedrock wells (adapted from Gates, 2003).

Equation 25 provides an estimation of the well and seepage discharge or flow rate (Q), based on observed HP-values for the local rock mass:

$$Q(L/min) = 3,785 \times (919,71 \times e^{-2.3144HP-value}) \quad [25]$$

Wells located in fractured bedrock with very low HP-values (< 1) typically exhibit higher yields. On the other hand, wells located in competent rock with high HP-values exhibit low yields. There is a higher probability of locating producing wells in fractured rock masses and, rock masses that exhibit lower HP-values, may display seepage problems assuming that groundwater is present in

the fractures. As opposed, in competent rocks that exhibit higher HP-values should have less seepage problems (details in Gates, 1997, 2003).

Concluding, Gates (1997, 2003) observed that rock masses which display HP-values < 3 are subject to potential seepage problems assuming groundwater is present in the rock mass geo-structure. Conversely, rock masses that exhibit HP-values > 3 appear to have little seepage problems. The benefits of the HP-value are twofold: this technique increases the probability of locating suitable test well sites in bedrock and the HP-value is a viable tool used to predict seepage problems in rock excavations such as tunnels or mines.

2.4.8.2. The rock-mass Hydraulic Conductivity (HC) classification system

The Hydraulic Conductivity (HC) classification proposed by Hsu et al. (2008, 2011), is another application for estimating hydraulic conductivity on fractured rocks. It is based on the following four parameters: rock quality designation (RQD), depth index (DI), gouge content designation (GCD), and lithology permeability index (LPI). HC-values can be calculated from borehole image data and rock core data. This approach is, slightly, cost effective since there is no need of buying equipment designed to obtain hydraulic properties of fractured rocks, which can be quite expensive, while if, the fractured rock mass is already being studied using rock mass classifications, HC can be estimated quickly without additional in-situ hydraulic tests (Hsu et al., 2008, 2011; Chen and Zhou, 2011).

Components of the HC index

Once more, when analysing hydraulic conductivity on rock masses, one of the mandatory components in the classification parameters is the RQD Index. As it written before, fractures reflect the ability of a formation to transmit water through them. Thus, the degree of fracturing is regarded as a factor in evaluating rock mass permeability. This index can be retrieved by Deere et al. (1967) formula. Typically, RQD is estimated based on the percentage of drill core recovered that exceeds 10 cm (4-inches) long compared to the overall core run (Deere, 1963; Deere et al., 1967; Deere and Deere, 1988).

Another parameter that Hsu et al. (2008, 2011) defined was the Depth Index (DI). Many researchers (e.g.. Snow, 1969; Wei et al., 1995; Caine et al., 1996; Evans et al. 1997, Ingebritsen and Manning, 1999; Ingebritsen et al., 2006; Singhal and Gupta, 2010) pointed out that rock mass permeability is likely to decrease with depth in fractured rocks. The fractures aperture and spacing is reduced due to the increment of geostatic stresses that, consequently, reduces the permeability of fractured rock masses. To assess the influence of this parameter, Hsu et al. (2008, 2011) defined a DI, equation [26]:

$$DI = 1 - \frac{L_C}{L_T} \quad [26]$$

Where, L_C is the depth which is located at the middle of a *double packer* test interval in a borehole and L_T is the total length of the borehole. The value of DI is always greater than zero and less than one. The greater the DI value, the higher the permeability.

Generally, it is known that clay-rich fractures have reduced permeability than any other porous material. However, it is one of the most common materials found in the infillings of fractures. To assess the influence of these materials in permeability, a Gouge Content Designation (GCD) index was defined as the following equation [23]:

$$GCD = \frac{R_G}{R_T - R_S} \quad [27]$$

Where, R_G is the total length of the gouge content. The greater GCD value, the more gouge content will appear in a core run, reducing the permeability of the core run. GCD values are always greater than zero and less than one.

In the section related to the general approach for groundwater circulation, it was stated that porosity is different for different lithologies. Thus, Hsu et al. (2008, 2011) describes that, when studying rock masses, their main porosity and permeability are due to the individual character of the rock itself. While fractures are the most important parameter to study in intact rock masses, grain-size characteristics are the most important in sedimentary formations. To assess the influence of lithology on permeability, a Lithology Permeability Index (LPI) was defined (Table 37). The HC rock mass classification is the product of the four parameters and can be given by the following equation [28]:

$$HC = \left(1 - \frac{RQD}{100}\right) (DI)(1 - GCD)(LPI) \quad [28]$$

The values on each parenthesis are always greater than zero and less than one and the higher the value on each parenthesis, the higher the permeability.

Table 37 – Description and ratings for lithology permeability index (adapted from Hsu et al. 2008, 2011).

Lithology	Hydraulic Conductivity (m/s)				Range of rating	Suggested Rating
	Reference ¹	Reference ²	Reference ³	K average		
Sandstone	$10^{-6}\sim 10^{-9}$	$10^{-7}\sim 10^{-9}$	$10^{-7}\sim 10^{-9}$	$10^{-7.5}$	0,8-1,0	1
Silty Sandstone	-	-	-	-	0,9-1,0	0,95
Argillaceous Sandstone	-	-	-	-	0,8-0,9	0,85
S.S. interbedded with some Sh.	-	-	-	-	0,7-0,8	0,75
Alternations of S.S. & Sh.	-	-	-	-	0,6-0,7	0,65
Sh. Interbedded with some S.S.	-	-	-	-	0,5-0,7	0,6
Alternations of S.S & Mudstone	-	-	-	-	0,5-0,6	0,55
Dolomite	$10^{-6}\sim 10^{-10.5}$	$10^{-7}\sim 10^{-10.5}$	$10^{-9}\sim 10^{-10}$	10^{-8}	0,6-0,8	0,7
Limestone	$10^{-6}\sim 10^{-10.5}$	$10^{-7}\sim 10^{-9}$	$10^{-9}\sim 10^{-10}$	10^{-8}	0,6-0,8	0,7
Shale	$10^{-10}\sim 10^{-12}$	$10^{-10}\sim 10^{-13}$	-	$10^{-10.5}$	0,4-0,6	0,5
Sandy Shale	-	-	-	-	0,5-0,6	0,6
Siltstone	$10^{-10}\sim 10^{-12}$	-	-	10^{-11}	0,2-0,4	0,3
Sandy Siltstone	-	-	-	-	0,3-0,4	0,4
Argillaceous Siltstone	-	-	-	-	0,2-0,3	0,2
Claystone	-	$10^{-9}\sim 10^{-13}$	-	10^{-11}	0,2-0,4	0,3
Mudstone	-	-	-	-	0,2-0,4	0,2
Sandy Mudstone	-	-	-	-	0,3-0,4	0,4
Silty Mudstone	-	-	-	-	0,2-0,3	0,3
Granite	-	-	$10^{-11}\sim 10^{-12}$	$10^{-11.5}$	0,1-0,2	0,15
Basalt	$10^{-6}\sim 10^{-10.5}$	$10^{-10}\sim 10^{-13}$	-	$10^{-11.5}$	0,1-0,2	0,15

¹ B.B.S. Singhal & R.P. Gupta (1999)

² Karlheinz Spitz & Joanna Moreno (1996)

³ Bear (1972)



Chapter 3.

**Coupling hydrogeomechanical classifications and hydrogeotechnical mapping:
importance on hard rock hydrogeology practice**

Synopsis

Throughout the last century, technological developments increased at surprising rates carrying with it an extended scientific knowledge regarding all type of geoengineering issues. One of those areas, focused on development of applied hydrogeology for rock engineering problems, such as groundwater infiltrations, role of water on rock slope stability, hydrogeomechanical assessment of underground excavations, mining tunnels and dams, hydrogeotechnical mapping for engineering geosciences and geotechnics, among others. These advances enhanced the creation of hydrogeomechanical classifications and indexes highlighting the design for a specific geoengineering scenario. It has been carried out a study regarding the role of groundwater on fractured rock masses of the Caldas da Cavaca hydromineral system site (Aguiar da Beira, Central Portugal) which, has a thermal tradition that dates back to the late 19th century.

3.1. General remarks

During the development of rock mass classifications, rare schemes were proposed for groundwater content and flow rate achievement in a given rock mass. The hydro-potential (HP) value technique by Gates (1995, 1997, 2003), the hydraulic conductivity (HC) classification system by Hsu et al. (2008, 2011) and the Joint Water Factor (J_w) from the HP-value (modified from Barton et al, 1974; adapted from Gates, 1997, 2003) may give interesting inputs to a comprehensive analysis on hydraulic behaviour of rock masses. This study case focuses on three different rock slopes and integrates borehole core data of the site in order to achieve a broader array of results.

While the slopes are located in the same geographical area, their geological and geomechanical characteristics have a different weight on their overall groundwater behaviour. This way, the final remarks show diverse perspectives evaluating a wider but a more comprehensive hydrogeomechanical data set. Finally, the main aim of this study is to demonstrate the importance of coupling hydrogeomechanical classification schemes and indexes and hydrogeotechnical mapping for the assessment of hard-rock hydrogeology and rock engineering practice.

The organisation of the case study chapter is based on a general paper layout structure of an extended version from any international journal in the field of engineering or applied science. The present section follows the general layout of an original paper (extended version), which will be summarised, in near future, to a shorten version (typically, with 8,000 words; 8 figures and 3 tables; and supplementary material) to be submitted, in co-authorship, to an indexed international journal.

3.2. Regional and local framework

The study site is located in Central Portugal, in the municipality of Aguiar da Beira, Guarda district, covering an area of about 10 km². It places between 7°34'W–7°35'W longitude and 40°44'N–40°47'N latitude (WGS84 coordinate system), belonging to the river Dão catchment, which is a part of the Mondego drainage basin. The Caldas da Cavaca area situates on the so-called Beiras Variscan granitic belt (Dão complex granite, Central-Iberian Zone; Boorder, 1965), near the Western border of the deep crustal megastructure Bragança–Vilariça–Manteigas fault zone, with a general trend of NNE-SSW (Ribeiro et al., 2007), belonging to the Iberian Massif. The main regional tectonic structure, responsible for the thermal water occurrence, is the NE-SW Dão fault zone and its related deep fracture network system. All these structures have a great influence in the regional drainage network. The main hydrogeological division of Northern Portugal is determined by the mountain range associated to the major Verin-Régua-Penacova fault zone (Figure 25), the Western Mountains (Ribeiro, 1949).

In a local perspective, the main morphologic features covering the study site are the NNE-SSW Ribeira da Coja valley (bottom c. 521 m), with an altitude difference, between top and bottom, of about 170 m, and several steeping slopes (Teixeira et al., 2015). The study area is mainly composed of coarse grained porphyritic granite, alluvial deposits and dolerite dykes (Boorder, 1965). The mafic dykes are mostly exposed over distances of less than 30 m and often weathered to fresh.

The study area has a Köppen–Geiger *Csb* climate (McKnight and Hess, 2000; Peel et al., 2007), which corresponds to a temperate climate, with a dry and warm summer. The mean annual temperature is 13°C, ranging from 6,2°C in January to 20,1°C in July. The average annual precipitation is 1252,4 mm/year, but not constant throughout the year. January has a mean rainfall reaching 189 mm while, July only has 16 mm.

According to the Thornthwait and Mather (1955) method, the annual water balance was calculated, with a field capacity of 150 mm. From June to September, the region has a water deficit, especially in July and August, with a total deficit in the four months of 117,4 mm. The full field capacity is only achieved in November, and from December to May, a total water surplus of 742,8 mm is registered (Teixeira et al., 2015). The estimative recharge rate is around 14% of mean annual rainfall (Carvalho et al., 2005a) and the landscape is mainly dominated by rocky outcrops, *Pinus pinaster* forest, and agricultural areas (Teixeira, 2011).

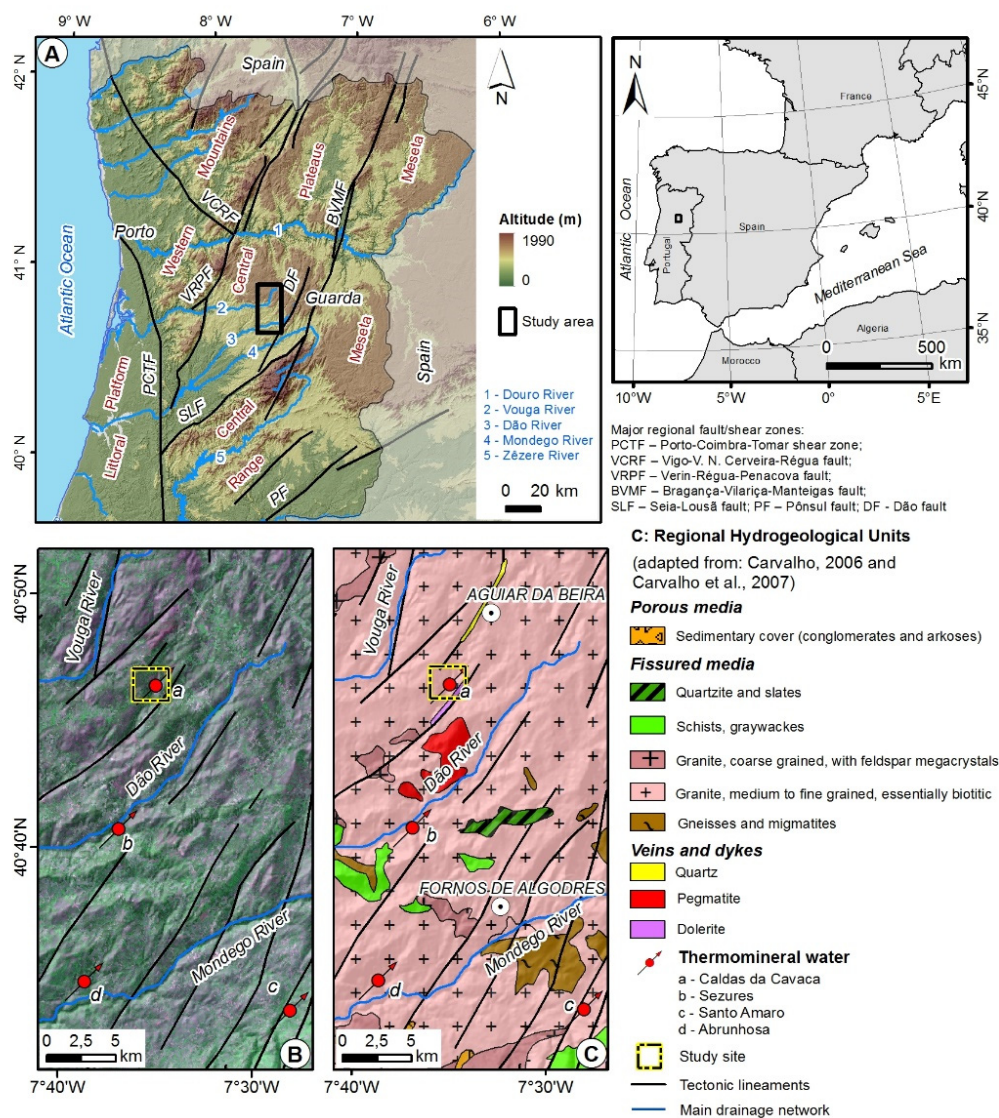


Figure 25 - Regional framework of the Caldas da Cavaca hydromineral system, Aguiar da Beira municipality: **A** location of study area; **B** satellite image (compiled from Landsat 7 ETM+ data, 2000/01; all IR colour, bands 7-4-5 = RGB; adapted from Global Land Cover Facility); **C** shaded relief, regional geology (adapted from Oliveira et al., 1992) and hydrogeology (adapted from Carvalho, 2006; Carvalho et al., 2007) and main hydromineral springs (adapted from Carvalho, 2006). After: Teixeira et al. (2015).

According to Teixeira et al. (2015), Caldas da Cavaca hydromineral system is characterised by (details in Carvalho et al., 2005b; Teixeira, 2011): i) water output temperatures around 29.8°C, ii) relatively high pH values (c. 8.3), iii) TDS contents in the range of 262–272 mg/L, iv) presence of reduced sulphur species (HS, c. 0.9 mg/L), v) high silica contents around 55 mg/L which represent a considerable percentage of total mineralisation (around 21 %); vi) electrical conductivity (EC) measurements ranging 353–427 μScm^{-1} indicating the presence of medium mineralised waters, and, vii) high fluoride concentrations up to 14 mg/L. These waters belong to $\text{HCO}_3\text{-Na}$ facies.

The groundwater path flow and its hydraulic conductivity are governed mainly by geometric discontinuity patterns and weathering, resulting on non-continuous productive zones. Nevertheless, it is clear that in the Variscan Iberian Massif, lithology plays a major role on the productivity of regional geological units and related water wells (e.g., Carvalho et al., 2005a; Carvalho, 2006; Carvalho et al., 2007).

Caldas da Cavaca site is recognised within the region, for its thermal spa tradition, which dates back to the late nineteenth century (e.g. Freire de Andrade, 1937; Acciaiuoli, 1952/53; Carvalho, 1996). Lately, an entire rehabilitated thermal centre has re-opened, after many years of inactivity. The former thermal spring and shallow well (Freire de Andrade, 1935, 1938) used for therapeutic purposes at the old spa, were replaced by two new wells (Teixeira et al., 2015). Their placement resulted from geological, geomorphological and hydrogeological studies carried out in the last years (Carvalho et al., 2005b; Teixeira et al., 2010; Teixeira, 2011; Teixeira et al., 2015, and references therein).

This introductory section, outlining the regional geomorphological and geological constraints, followed closely the works of Carvalho et al. (2005b), Teixeira (2011) and Teixeira et al. (2010, 2015).

3.3. Materials and methods

Accordingly to Figure 7 (Chapter 1), the present dissertation follows a combined workflow of four major steps. These steps have the purpose of portraying the advantage of coupling hydrogeomechanical data with GIS-based mapping for a better understanding of the hydrogeological conceptual model of Caldas da Cavaca rock mass.

The collection of field mapping data (such as, topographic information, remote sensing studies, hydrological and climatological data, field surveys) together with hydrogeological published papers, technical reports of the area and old maps provide an overview of the regional and/or local framework. Geological, hydrogeological, geotechnical and geomechanical parameters of Caldas da Cavaca rock mass are characterised by field and laboratory techniques, such as, rock sampling surveys on outcrop rock mass exposures to study the fracturing degree and geomechanical parameters (e.g., Dinis da Gama, 1995; ISRM, 2007, 2015; Chaminé et al., 2015). After collecting and synthesising all the field and laboratory data, the third stage follows up with the application and evaluation of the gathered information on rock mass classifications, particularly, on the application of the hydrogeomechanical classification schemes and indexes. This stage involves the determination of several parameters that characterise Caldas da Cavaca site, according to its geotechnical, geomechanical (RQD, GSI, W, F, S – see ISRM, 1981; GSE, 1995) and hydrogeomechanical (Jw, Q, [Q/s], K, T, HP-Value, HC – see CFCFF, 1996) parameters. As

referred before, integrating these parametric data with GIS-based mapping reasoning, assembles all the hydrogeomechanical data required for designing a more robust hydrogeological conceptual site model.

3.4. Data and results

Three heterogeneous slopes (mainly rock mass exposures with, a few soil mass short sections) were assigned for the hydrogeomechanical study. The studied rock slope sections (Amores slope, A; Lagoa slope, L, and Cancela slope, C) surrounding Caldas da Cavaca hydromineral system site provide a diversity of data required for the main goal of this research. Figure 26 shows the location of Amores, Lagoa and Cancela slopes within Caldas da Cavaca study site. The total slope length has an extension of 484 m and a height that varies from 1 to 7 m above the road, oriented mainly N45°E/N60°E (slopes A and L, respectively) and N80°E/N110°E (slope C).

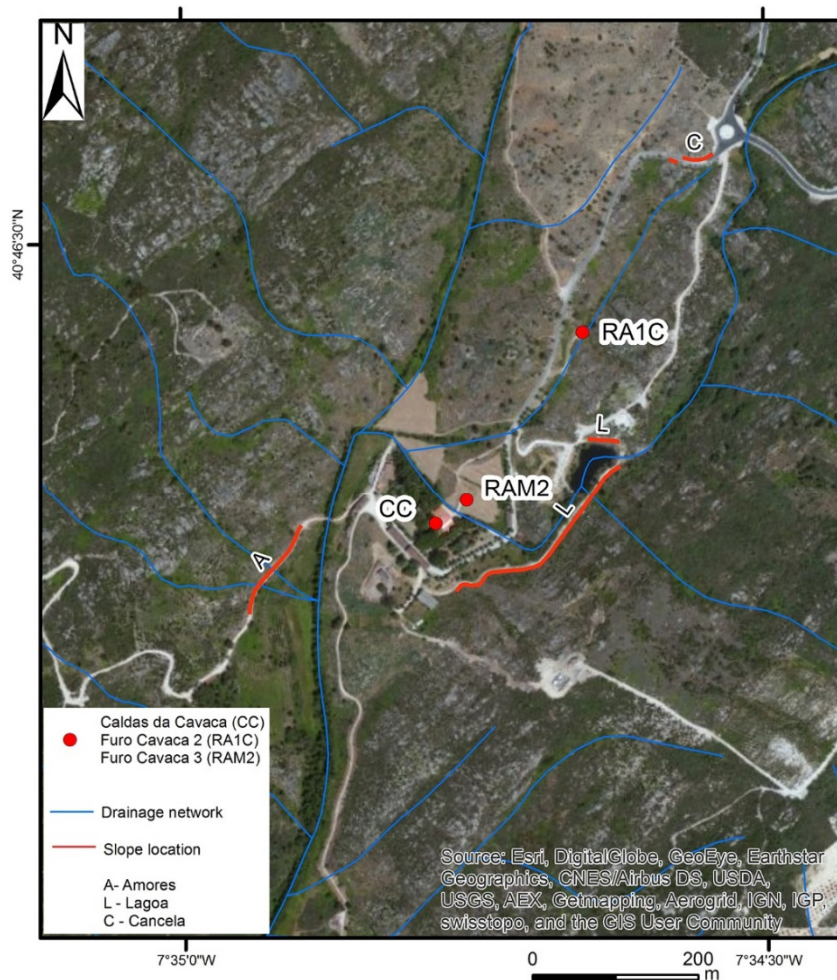


Figure 26 – Location of the three studied slopes according to the scanline sampling technique (Caldas da Cavaca site, Aguiar da Beira).

Since, groundwater research wells with, its respective data, were requested by Carvalho J. M. and executed by Azenha R. L. (2007), borehole RA1C and RAM2 were also study subjects.

3.4.1. Geomechanical rock mass description

The studied slopes are within the same area, so, as expected, the geomechanical rock mass characteristics did not differ much from one another. Nevertheless, in this first study stage (see Figure 7) and using scanline sampling surveys, the general data from the slopes was gathered and organised according to: Lagoa slope 1 & 2, Cancela slope 1 & 2 and Amores slope.

The main type of discontinuities present in Caldas da Cavaca rock mass area are joints, being a small percentage faults and, in all slopes, their orientation tend to the same quadrants. The first and dominant set of joints as a major joint orientation of N120°-150°E (dipping 75°NE/SW to 90°NE/SW). The second set of joints has a general orientation trending N20°-80°E (dipping 55°-90°SE).

Considering the weathering grade, these slopes exhibit, mainly, a moderate weathering (W_3) with occurrences of highly to completely weathered (W_{4-5}) rock and, some punctual occurrences of fresh to slightly weathered rock (W_{1-2}) on Amores and Lagoa slopes.

A parameter of great importance regarding this study, when considering rock engineering slope stability problems, surface and underground mining and an influential parameter on fracture interconnectivity is the fracturing degree (ISRM, 1981). This fracture interconnectivity takes a huge roll on water flow in fractured medium since, a more frequent fracturing degree increases the chance of fracture interconnectivity thus, providing more paths for the water flow. In this work, the resultant fracturing degree tendency showed a higher occurrence of wide spacing (F_{1-2}) discontinuities, to discontinuities with moderate spacing (F_3) and, a small percentage of close spacing discontinuities (F_{4-5}).

Roughness also plays an important role on water flow in fractured media. When water flows through smooth and plain surfaces, it is able to flow without the need of outlining obstacles, having a more linear and direct path. On the contrary, if surfaces are rougher with stepped profiles, water finds many obstacles along its way, which reduce the yield and transmissivity of the aquifer. Concerning the *Lagoa* slope, more than 50% of the discontinuities walls appeared smooth (R_{1-2}), with the remaining being mostly rough (R_3) than very rough (R_{4-5}). Amores and Cancela slopes had a major occurrence of rough (R_3) walls, while 30% were smooth (R_{1-2}).

Two more significant properties of joint walls are aperture and the occurring filling material. These properties have an easy understanding influence on water flow since, it is impossible for any fluid to flow if there is no space for it or if it is blocked by any material. Yet, there are several materials that, even though they are present in joint walls, they let water flow, such as,

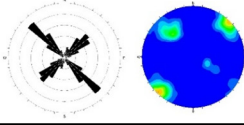
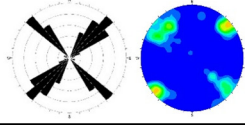
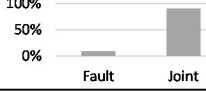
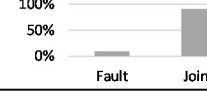
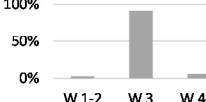
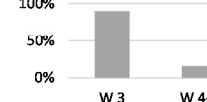
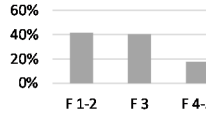
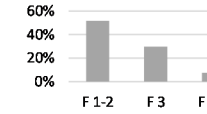
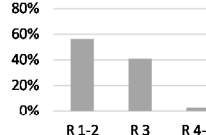
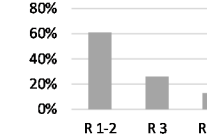


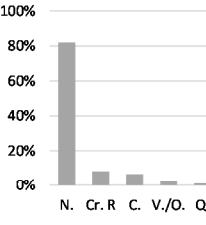
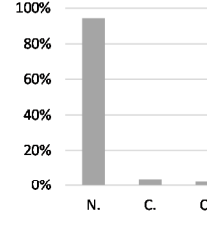
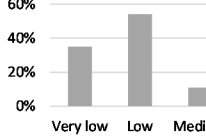
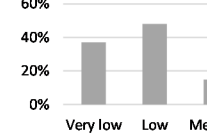
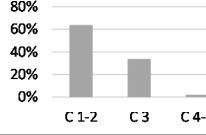
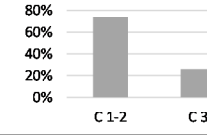
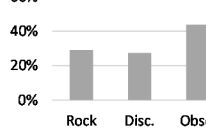
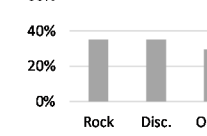
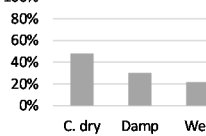
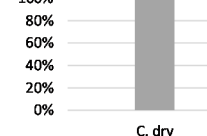
vegetation or organic material and weathered rock material. In this study, all the joints were closed ($<0,5$ mm) with, punctual occurrences of gapped walls (0,5 – 10 mm). Lagoa slope had a small percentage of filling occurrence but showed a wide variety of filling materials, ranging from crushed rock to quartz, clay and vegetation or organic material. Cancela and Amores slopes had a tiny fraction of filling material, being it clay, crushed rock and vegetation or organic material.

Joint continuity or persistence is another important geometrical parameter that, when its dimension increases, the fracture interconnectivity also increases. Most of the discontinuities were classified with a low (1 – 3 m) to very low (< 1 m) continuity, with values ranging, mostly, from 1,5 m to 2,5 m and, in a few cases, medium (3 – 10 m) continuity was found.

Termination parameter ranges from obscure, other discontinuities or rock. An obscure termination has a great value for this study, as it states that, the joint can have an expanded profile behind the observed surface view. The higher it expands along the rock mass, the higher the fracture interconnectivity is possible. Lagoa slope presented a balanced distribution along its joint terminations, being them on rock, other discontinuities or obscure. On Amores and Cancela slopes, obscure termination took the first place, followed by discontinuity termination and, lastly, ending on the rock surface.

Regarding the most important factor for this study, water content, is classified according to the amount of water flowing through rock joints. Lagoa slope presented small sections classified as wet ($10 \leq \text{drops/min} < 100$), as well as damp ($1 \leq \text{drops/min} < 10$), while the most part of the slope was dry. A small section of Amores slope was classified as damp ($1 \leq \text{drops/min} < 10$) while Cancela slope was entirely dry. All the previously described joint characteristics, along with a natural, favouring designed fracture interconnectivity allow the possibility of water occurrence along them. Table 38, 39 and 40 show an overview of the geotechnical and geomechanical basic parameters description for the three rock slopes.

Table 38 - Basic geotechnical and geomechanical parameters for Lagoa slope, Caldas da Cavaca.

	Slope 1 (n=183)			Slope 2 (n=54)		
Lithology	Two-mica granite, coarse grained, porphyritic with feldspar megacrystals			Two-mica granite, coarse grained		
Joint sets	N130°-150°E; 75°-85°NE N40°-60°E; 60°-80°SE			N40°-60°E; 60°-80°SE N130°-150°E; 75°-85°NE		
Discontinuity type	Fault	9,3%		Fault	9,3%	
	Joint	90,7%		Joint	90,7%	
Weathering grade, W	W 1-2	2,7%		W 3	90,2%	
	W 3	91,3%		W 4-5	15,7%	
	W 4-5	6,0%				
Fracturing degree, F	F 1-2	41,7%		F 1-2	51,9%	
	F 3	40,5%		F 3	29,6%	
	F 4-5	17,9%		F 4-5	7,4%	
	Average value = 65,3cm			Average value = 73,6cm		
Roughness	R 1-2	56,3%		R 1-2	61,1%	
	R 3	41,0%		R 3	25,9%	
	R 4-5	2,7%		R 4-5	13,0%	
Aperture	Closed	94,5%		Closed	87,0%	
	Gapped	5,5%		Gapped	13,0%	
	Average value = 0,46mm			Average value = 0,95mm		
Filling	None (N.)	82,0%		None (N.)	94,4%	
	Crushed Rock (Cr. R.)	8,2%		Clay (C.)	3,7%	
	Clay (C.)	6,6%		Quartz (Q.)	1,9%	
	Vegetation/Organic material (V./O.)	2,2%				
	Quartz (Q.)	1,1%				
Persistence/Continuity	Very low	35,0%		Very low	37,0%	
	Low	54,1%		Low	48,1%	
	Medium	10,9%		Medium	14,8%	
	Average value = 1,5 m			Average value = 1,5 m		
Curvature	C 1-2	63,9%		C 1-2	74,1%	
	C 3	33,9%		C 3	25,9%	
	C 4-5	2,2%				
Termination	Rock	29,0%		Rock	35,2%	
	Discontinuity (Disc.)	27,3%		Discontinuity (Disc.)	35,2%	
	Obscure (Obsc.)	43,7%		Obscure (Obsc.)	29,6%	
Water content	Completely dry (C. dry)	48,1%		Completely dry (C. dry)	100,0%	
	Damp	30,1%				
	Wet	21,9%				

LAGOA SLOPE: GEOMECHANICAL JOINT CHARACTERISTICS

Table 39 - Basic geotechnical and geomechanical parameters for Amores slope, Caldas da Cavaca.

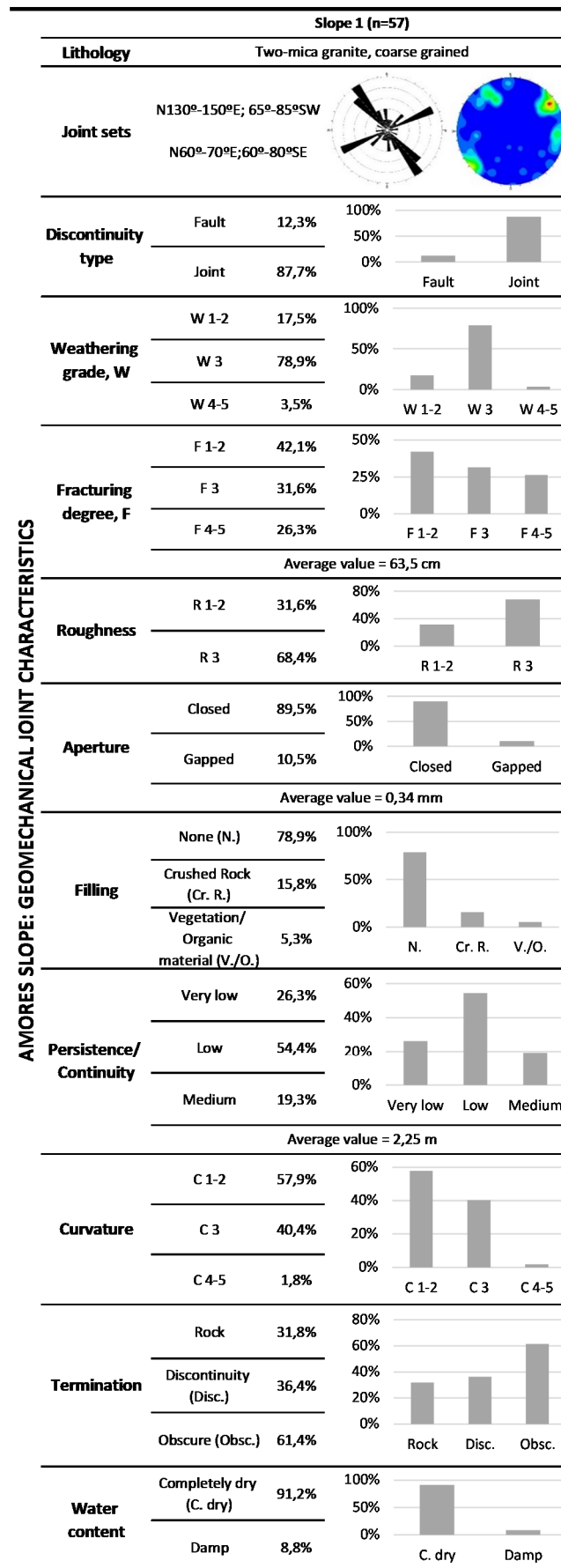


Table 40 - Basic geotechnical and geomechanical parameters for Cancela slope, Caldas da Cavaca.

	Slope 1 (n=44)			Slope 2 (n=19)		
Lithology	Two-mica granite, coarse grained			Two-mica granite, coarse grained		
Joint sets	N120°-140°E; 70°-90° NE N20°-40°E; 55°-75° SE			N140°-150°E; 80°-90° NE N60°-80°E; 80°-90° SE		
Discontinuity type	Fault	4,5%		Joint	100,0%	
	Joint	95,5%				
Weathering grade, W	W 3	88,6%		W 3	100,0%	
	W 4-5	11,4%				
Fracturing degree, F	F 1-2	50,0%		F 1-2	36,8%	
	F 3	31,8%				
	F 4-5	18,2%				
Average value = 71,7cm			Average value = 63,8cm			
Roughness	R 1-2	31,8%		R 1-2	15,8%	
	R 3	65,9%				
	R 4-5	2,3%				
Aperture	Closed	100,0%		Closed	68,4%	
	Gapped					
Average value = 0,1mm			Average value = 1,5mm			
Filling	None (N.)	100,0%		None (N.)	68,4%	
	Crushed rock (Cr. R.)					
	Clay (C.)					
Persistence/Continuity	Very low	37,0%		Very low	36,8%	
	Low	48,1%				
	Medium	14,8%				
Average value = 2,5m			Average value = 1,6m			
Curvature	C 1-2	68,2%		C 1-2	42,1%	
	C 3	22,7%				
	C 4-5	9,1%				
Termination	Rock	18,2%		Rock	26,3%	
	Discontinuity (Disc.)	15,9%				
	Obscure (Obsc.)	65,9%				
Water content	Completely dry (C. dry)	100,0%		Completely dry (C. dry)	100,0%	

CANCELA SLOPE: GEOMECHANICAL JOINT CHARACTERISTICS

3.4.2. Hydrogeomechanical zoning

All the geotechnical, geomechanical and hydrogeomechanical surface data allowed a division of the slopes in zones, grouping them by their similarity. The major consideration taking part on this distinction was the respective joint water content, separating, within each slope, zones containing equivalent water flowing values. This zone distinction allowed the creation of different seepage content zones called hydrogeomechanical zones (HGMZ). The geological, geomechanical and hydrogeomechanical data of each zone was collected and synthesised for later application on rock mass classifications (RQD, RMR, SMR and GSI) and hydrogeomechanical schemes or indexes (joint water factor, J_w , HP-value and HC system).

Table 41 represents the hydrogeomechanical zoning considered for the three slopes.

3.4.2.1. Lagoa slope zoning

In the Lagoa slope, three zones were identified according to its water content: i) Hydrogeomechanical zone (HGMZ) 1, which includes the two sections that had the higher flowing water on all the slope length, with water drops ranging from 10 drops/min to 100 drops/min; ii) HGMZ 2, less humid, with a flowing yield that ranges from 1 drop/min to 10 drops/min; iii) HGMZ 3 includes only dry sections; iv) HGMZ 4 comprises sections completely weathered where, it was not possible to retrieve parameters.

Regarding the uniaxial compressive strength parameter, HGMZ 3 comprised the sections with higher values, from 35,8 MPa to 108,9 MPa (S_3 to S_2), showing a better rock quality, from weathered to fresh to slightly weathered (W_3 to W_{1-2}). These parameters, along with an aperture value of 0,34 mm explain the difficulty of water infiltration along this zone. HGMZ 1 exhibits an aperture value really close to the aperture value of HGMZ 3, 0,35 mm, and yet this zone has water seepage. The rock mass weathering degree of the zone HGMZ 1 supports the possibility of water seepage and infiltration, as, it is mostly weathered to highly weathered (W_3 to W_4). This weathering degree reflects the uniaxial compressive strength with, its fairly low value of 39,8 MPa (S_3).

Regarding fracture intercept, HGMZ 1 had the lowest value in Caldas da Cavaca study site, 49,2cm (F_3). HGMZ 2 and HGMZ 3 have values of, respectively, 60 cm and 72 cm (F_2). All the zones have similar roughness degrees being it mostly smooth to rough (R_{1-2} to R_3) and, although generally, no filling material is present in discontinuities, punctual occurrences of crushed rock, hard clay and, rarely, vegetation appear.

3.4.2.2. Amores slope zoning

In this slope two zones were identified, HGMZ 1 and HGMZ 2.

Considering HGMZ 1, although, there were some joints, conveying water to the outcrop surface, they were minimal and mostly wet, so this slope was considered mainly dry with a few spontaneous drops, varying from 1 drop/min to 10 drops/min. The uniaxial compressive strength (UCS) is high to moderate (S_2 to S_3), ranging from 100 MPa to 40 MPa and, the rock mass is moderately weathered (W_3) with sections of fresh to slightly weathered (W_{1-2}). The average aperture values were low with, a mean of around 0,34 mm and, since most of the discontinuities were closed, no filling material was found, apart from punctual occurrences of crushed rock and some vegetation. In this zone, the average fracture intercept value is 73,7 cm (F_2) with a maximum value of 270 cm (F_1). Most joints are rough to smooth (R_3 to R_{1-2}).

HGMZ 2 is a completely weathered zone, acting like a soil mass, where it was not possible to identify discontinuities.

3.4.2.3. Cancela slope zoning

In this slope, the collected data was from two separated slopes and only one zone was identified, corresponding to a dry zone. Both of the slopes have a low to moderate uniaxial compressive strength (S_4 to S_3), ranging from 15 MPa to 45 MPa and the rock mass appeared to be moderately weathered (W_3) on both slopes, but sometimes highly to completely weathered (W_{4-5}) on slope 1. The average fracture intercept value for slope 1 was 71,7 cm having it, mostly, a wide to moderate spacing (F_2 to F_3). For slope 2 the average value of fracture intercept is 63,8 cm having a moderate to wide spacing (F_3 to F_2). On slope 1, joints are mostly closed and thus, presenting no filling material. Slope 2 has an average aperture of 1,5 mm and, mostly, no filling material was found, with exceptions of hard clay and crushed rock. On both slopes, the joints were considered smooth to rough (R_{1-2} to R_3).

Table 41 - Summary of the basic hydrogeomechanical parameters from the studied rock slopes, Caldas da Cavaca.

HYDROGEOMECHANICAL ZONING

Hydrogeomechanical Zone	Scanline section (Extension, m)	Joint Sets	Weathering grade, W	Fracture intercept, F	Roughness	Aperture	Filling	Seepage	Weathering t	
									Low (0 - 5m)	Medium (5 - 10m)
1	0 - 13,9	N140°-150°E; 80°-90° NE; N30°-60°E; 75-80° SE;	Moderately weathered (W ₃) to highly weathered (W ₄)	Moderate to wide spacing (F ₃ to F ₂) but, sometimes, closed spacing (F ₄); min: 10 cm, max: 130 cm; average value = 49,2 cm	Mostly smooth (R _{1,2}) to rough (R ₃)	Closed (<0,5 mm) to gapped (0,5 - 10 mm); average value = 0,35 mm	Mostly none but, sometimes, crushed rock and hard clay	Drops; 10<drops/min	-	-
	61,1 - 70,8			Wide to moderate spacing (F ₂ to F ₃) but, sometimes, closed spacing (F ₄); min: 10 cm, max: 170 cm; average value = 68,7 cm	Mostly smooth (R _{1,2}) to rough (R ₃)	Closed (<0,5 mm) to gapped (0,5 - 10 mm); average value = 0,74 mm	Mostly none but, sometimes, crushed rock and hard clay	Damp; 1<drops/min		
2	133,0 - 161,9	N0°-10°E; 50°-80° NW	Moderately weathered (W ₃) to highly weathered (W ₄)	Moderate to wide spacing (F ₃ to F ₂) but, sometimes, closed spacing (F ₄); min: 10 cm, max: 170 cm; average value = 68,7 cm	Mostly smooth (R _{1,2}) to rough (R ₃)	Closed (<0,5 mm) to gapped (0,5 - 10 mm); average value = 0,74 mm	Mostly none but, sometimes, crushed rock and hard clay	Damp; 1<drops/min	-	-
	192,0 - 230,0									
3	13,9 - 34,5	N130°-150°E; 70°-80° NE; N10°-20°E; 30°-40° NW	Moderately weathered (W ₃) to fresh-rock to slightly weathered (W _{1,2})	Moderate to wide spacing (F ₃ to F ₂) and rarely, closed spacing (F ₄); min: 10 cm, max: 180 cm; average value = 60,1 cm	Mostly smooth (R _{1,2}) to rough (R ₃)	Closed (<0,5 mm) to gapped (0,5 - 10 mm); average value = 0,34 mm	Mostly closed but, sometimes, crushed rock and hard clay and, rarely, vegetation	Dry	X	-
	86,5 - 98,0									
4	161,9 - 186,1	N130°-150°E; 70°-80° NE; N10°-20°E; 30°-40° NW	Moderately weathered (W ₃) to highly weathered (W ₄)	Wide to moderate spacing (F ₂ to F ₃); min: 10 cm, max: 200 cm; average value = 72,1 cm	Mostly smooth (R _{1,2}) to rough (R ₃)	Closed (<0,5 mm) to gapped (0,5 - 10 mm); average value = 0,95 mm	Mostly closed but, sometimes, crushed rock and hard clay and, rarely, crushed rock	Dry	X	-
	242,0 - 268,3									
5	0 - 39,0	Non available	Completely weathered rock (W ₅)	Non available	Non available	Non available	Non available	Dry to minor inflow	-	-
	34,5 - 61,1									
6	70,8 - 86,5	N130°-150°E; 65°-85°SW; N60°-70°E; 60°80°SE	Moderately weathered (W ₃) to fresh-rock to slightly weathered (W _{1,2})	Wide to moderate spacing (F ₂ to F ₃) but, sometimes, closed spacing (F ₄); min: 5cm, max: 270 cm; average value = 73,7 cm	Mostly rough (R ₃) to smooth (R _{1,2})	Closed (<0,5 mm) to gapped (0,5 - 10 mm); average value = 0,34 mm	Mostly closed but, sometimes, crushed rock and vegetation	Mostly dry to damp (1<drops/min<10)	X	-
	98,0 - 133,0									
7	186,1 - 192,0	Non available	Completely weathered rock (W ₅)	Non available	Non available	Non available	Non available	Dry to minor inflow	-	-
	230,0 - 242,0									
8	0 - 32,6	N130°-150°E; 65°-85°SW; N60°-70°E; 60°80°SE	Moderately weathered (W ₃) to fresh-rock to slightly weathered (W _{1,2})	Wide to moderate spacing (F ₂ to F ₃) but, sometimes, closed spacing (F ₄); min: 5cm, max: 270 cm; average value = 73,7 cm	Mostly rough (R ₃) to smooth (R _{1,2})	Closed (<0,5 mm) to gapped (0,5 - 10 mm); average value = 0,34 mm	Mostly closed but, sometimes, crushed rock and vegetation	Mostly dry to damp (1<drops/min<10)	X	-
	85,4 - 125,8									
9	32,6 - 85,4	Non available	Completely weathered rock (W ₅)	Non available	Non available	Non available	Non available	Dry to minor inflow	-	-
	85,4 - 125,8									

LAGOA SLOPE

AMORES SLOPE

3.4.3. Rock mass classification or indexes

3.4.3.1. Rock Mass Rating (RMR)

This geomechanical classification is based on the parameters established by Bieniawski (1989) and, is mostly used for assessing the rock mass quality of a site with, the final purpose of excavation of tunnels, temporary mine openings, storage caverns, rock slopes and foundations, among others. In this work, it is considered mostly as a reference for the general rock mass quality since it does not study the water flow in a specific way. The RMR classification comparison with other classifications permits a better understanding of the rock mass quality of Caldas da Cavaca site.

Therefore, according to the parameters previously assessed on Table 41, it is possible to move onto Table 42, concerning the RMR classification for the Lagoa slope. As it is noticeable on Table 42, the global rock mass quality for this slope is poor to fair (rock class IV to III). However, with a more detailed analysis it is possible to verify a few particularities:

- HGMZ 1 had the lowest rock mass classification (25), defining this zone as the one with the worse quality. This low characterisation is a function of the low uniaxial compressive strength, low RQD, low spacing, the geological-geotechnical conditions, combined with the presence of water;
- Even though HGMZ 2 also has water flowing in its joints, the flow is smaller, giving it a higher value concerning the groundwater conditions parameter. Besides, in the overall geological-geotechnical parameters, this zone scored higher values, achieving a higher final value (40);
- In HGMZ 3, the study is distinguished within its sections, due to, different uniaxial compressive strength values. These values, combined with its low weathering, dry joints and higher overall parameter values rated the better rock mass classification values (36 to 44);
- The P6 parameter considers a slope configuration resulting in a decreasing of the rock mass quality in an evident way.

Table 42 - Synthesis of the geomechanical parameters for Lagoa slope rock mass rating (version 1989 – RMR₈₉; Bieniawski, 1989).

HGMZ	3													
	1	Value	2	Value	Slope 1				Slope 2	Value				
					Section 1	Value	Section 2	Value			Section 3	Value	Section 4	Value
P1 - UCS (MPa)	39,8	4	70	7	35,8	4	46,9	4	108,9	12	72,2	7	41,8	4
P2 - RQD (%)	42	8	60	13	ZHGM3 - Slope 1				60	13				
P3 - Spacing (m)	0,49	10	0,69	15	50	0,6	12	0,72	15	Continuity: 1-3 m; aperture: 0.35 mm; smooth to rough surfaces; no infillings; weathered to highly weathered				
P4 - Geological- geotechnical conditions	18	18	18	18	Continuity: 1-3 m; aperture: 0.74 mm; smooth to rough surfaces; no infillings; weathered to highly weathered	20	20	Continuity: 1-3 m; aperture: 0.34 mm; smooth to rough surfaces; no infillings; weathered to fresh-rock	18	18	Continuity: 1-3 m; aperture: 0.95 mm; smooth to rough surfaces; no infillings; weathered to highly weathered			
P5 - Groundwater conditions	10	10	Damp (<10 L/min)	12	10	10	12	15	15	Completely dry	15	15	Completely dry	
P6 - Value correction due to discontinuities orientation	-25	-25	Strike perpendicular to excavation axis; drive against dip - Fair	-25	Strike perpendicular to excavation axis; drive against dip - Fair	-25	Strike parallel to excavation axis; 45° - 90° - Fair	-25	Strike parallel to excavation axis; dip 45° - 90° - Fair	-25	Strike parallel to excavation axis; dip 45° - 90° - Fair	-25	Strike parallel to excavation axis; dip 45° - 90° - Fair	
Classification of rock mass	Poor	25	Poor	40	Poor	36	Poor	36	Fair	44	Poor	39	Poor	40
RMR (Rock class)	IV	IV	IV	IV	IV to III	IV to III	IV to III	IV to III	IV to III	IV to III	IV to III	IV to III	IV to III	IV

LAGOA SLOPE: ROCK MASS RATING

Table 43 synthesises the geomechanical parameters for Amores slope. The overall parameters are similar to the Lagoa slope, although water has a low appearance on this slope. Regarding the P6 parameter, the previous situation is also verified. Although the joint sets orientation, regarding the slope orientation, are fair, the reduction of the P6 parameter, on the RMR classification is noticeable.

Table 43 – Synthesis of the geomechanical parameters for Amores slope rock mass rating (version 1989 – RMR₈₉; Bieniawski, 1989).

AMORES SLOPE: ROCK MASS RATING	HGMZ	1	Value
	P1 - UCS (MPa)		86,2
P2 - RQD (%)		60	13
P3 - Spacing (m)		0,74	15
P4 - Geological-geotechnical conditions		Continuity: 1-3 m; Aperture: 0.35 mm; Rough to smooth surfaces; No infillings; Weathered to fresh-rock	21
P5 - Groundwater conditions		Completely dry to damp (None to <10)	14
P6 - Value correction due to discontinuities orientation		Strike perpendicular to excavation axis; drive against dip - Fair	-25
Classification of rock mass		Fair	45
RMR (Rock class)		III	

Even though, Cancela slope is dry, it has a global rock mass quality slightly better than the Amores slope and similar to HGMZ 2 and 3 in Lagoa slope (Table 44). This level of rock mass quality is due to its low uniaxial compressive strength values and poor geological-geotechnical conditions.

Table 44 - Synthesis of the geomechanical parameters for Cancela slope rock mass rating (version 1989 – RMR₈₉; Bieniawski, 1989).

CANCELA SLOPE: ROCK MASS RATING	HGMZ	1			
		Slope 1	Value	Slope 2	Value
P1 - UCS (MPa)		22	2	32,1	4
P2 - RQD (%)		60	13	55	13
P3 - Spacing (m)		0,72	15	0,64	15
P4 - Geological-geotechnical conditions		Continuity: 1-3 m; aperture: 0,097 mm; smooth to rough surfaces; no infillings; weathered to highly weathered	19	Continuity: 1-3 m; aperture: 1,5 mm; smooth to rough surfaces; no infillings; weathered	16
P5 - Groundwater conditions		Completely dry	15	Completely dry	15
P6 - Value correction due to discontinuities orientation		Strike perpendicular to excavation axis; Drive against dip - Fair	-25	Strike perpendicular to excavation axis; Drive against dip - Fair	-25
Classification of rock mass		Poor	39	Poor	38
RMR (Rock class)		IV		IV	

3.4.3.2. Slope Mass Rating (SMR)

The Slope Mass Rating (SMR) classification (Romana, 1985, 1993; Romana et al., 2003) was also performed, in order to, have a better understanding on the influence of joint orientation within the rock slope itself. The value considered for SMR, F3 parameter was the Bieniawski (1976) adjustment rating for joints orientation, equivalent to the P6 parameter of the RMR classification. Table 45 shows that the SMR values are slightly higher and, in some cases, with a significant difference, than the RMR values.

Table 45 - Synthesis of the Slope Mass Rating parameters for the three studied rock slopes.

SLOPE MASS RATING							
HGMZ	1	2	3		HGMZ 1	Slope 1	Slope 2
			Slope 1	Slope 2			
Slope α_s (°)	60				45	80	110
Slope β_s (°)	50 (NW)				70 (SE)	80 (SE)	80 (NE)
Joint α_j (°)	145		40		140	135	145
Joint β_j (°)	85 (NE)		75 (SE)		75 (SW)	80 (NE)	85 (NE)
RMR _b	50		65		57	64	63
F1	0,15	0,15	0,40	0,40	0,15	0,15	0,15
F2	1,00	1,00	1,00	1,00	1,00	1,00	1,00
F3	-25	-25	-25	-25	-25	-25	-25
F4	-8	-8	-8	-8	-8	-8	-8
SMR	38	53	46	47	45	52	51
Classification of rock mass	Bad	Fair	Fair	Fair	Fair	Fair	Fair
Rock class	IVa	IIIa	IIIb	IIIb	IIIb	IIIa	IIIa
RMR	25	40	36 - 44	40	45	39	38

3.4.3.3. Geological Strength Index (GSI)

The geological-geomechanical (GSI) strength index is another measure for obtaining the rock quality and can be achieved by several ways. One of them is a numerical relation between GSI and RMR, as long as, $RMR > 23$, $GSI = RMR - 5$ (Hoek, 2007). However, Barton (2011) argued that this algebraic relation is not suitable according to the actual knowledge of the geomechanical classifications. Thereby, in Table 46, according to Hoek and Marinos (2000), it is presented a synthesis of the rock mass blocking size (geostructural class), the surface conditions (in terms of its geological-geotechnical parameters) and the corresponding achieved interval for each HGMZ of each slope.

Once again, the zone with poorer results was HGMZ 1 of Lagoa slope, followed by the weathered slope 1 of Cancela slope. The rock mass that presented the best results was the Lagoa slope HGMZ 3, slope 1, along with Amores slope.

Table 46 - Synthesis of the Geological Strength Index parameters for the three studied rock slopes.

GEOLOGICAL STRENGTH INDEX								
HGMZ	LAGOA SLOPE				AMORES SLOPE	CANCELA SLOPE		
	1	2	3			1	1	
			Slope 1	Slope 2		Slope 1	Slope 2	
Fracture intercept, F	Average value = 49,2 cm	Average value = 68,7 cm	Average value = 60,1 cm	Average value = 72,1 cm	Average value = 73,7 cm	Average value = 71,7 cm	Average value = 63,8 cm	
Joint sets	Three joint sets				Two joint sets plus random	Two joint sets	Two joint sets	
Geostructural class	Blocky (GS2)				Block (GS2)	Blocky (GS2)	Blocky (GS2)	
Surface conditions	Poor to fair	Poor to fair	Fair to good	Fair	Fair to good	Fair	Fair	
GSI	40 - 50	50 - 60	55 - 65	45 - 55	55 - 65	40 - 50	50 - 60	

3.4.4. Hydrogeomechanical classifications or indexes

Entering the water flow specific classifications, on fractured rock masses, the aim is to achieve data concerning the flow properties of the fractured media. Properties, such as, yield [Q], specific capacity [Q/s], transmissivity [T] and hydraulic conductivity [K] can be achieved. In this type of classifications, a three scenario approach was established, in order to, understand the possible evolution or regression of the slopes and how it would change. The scenario with the more realistic approach (i.e., more conservative and balanced) is the first one (1), followed by a lower quality scenario (2) and lastly, a higher quality scenario (3).

3.4.4.1. Hydro-potential (HP) value

The HP-value is a hydrogeomechanical index based on the parameters proposed by Gates (1997, 2003) although, four of the six parameters are common with the geomechanical classification Q-system (Barton et al., 1974, 1980). As it was defined on the previous chapter, the HP-values range from 1.33×10^{-3} (poor quality rock masses) to 800 (very good quality rock masses) and, according to Gates (1997, 2003) rock masses with HP-values < 3 are subject to potential seepage assuming groundwater is present on the rock mass geo-structure. Rock masses that exhibit HP-values > 3 appear to have little seepage problems thus, the calculus of yield and specific capacity is not valuable.

Table 47, Table 48 and Table 49 synthesise the HP-value parameters defined, respectively, for Lagoa slope, Amores slope and Cancela slope.

Table 47 - Synthesis of the HP-value parameters for the Lagoa slope.

LAGOA SLOPE: HP-VALUE	HGZM	1		2		3			
		Value		Value		Slope 1	Value	Slope 2	Value
						Poor to fair		Fair	
Scenario 1	RQD (%)	Poor	42	Fair	60				60
	Jn	Three joint sets	9	Three joint sets plus random	12	Three joint sets plus random	12	Three joint sets plus random	12
	Jr	Rough or irregular, planar	1,5	Rough or irregular, planar	1,5	Rough or irregular, planar	1,5	Rough or irregular, planar	1,5
	Jk	90% joints silty sand filled, moderate flow	3	90% joints clay filled, poor flow	2	All joints tight or healed with calcite/ quartz, no flow	1	All joints tight or healed with calcite/ quartz, no flow	1
	Jaf	Joints 90% 0.1 ≤ 1.0 mm	1,2	Joints 90% 0.1 ≤ 1.0 mm	1,2	Joints 90% 0.1 ≤ 1.0 mm	1,2	Joints 90% 0.1 ≤ 1.0 mm	1,2
	Jw	Drops	0,86	Damp	0,94	Dry	1	Dry	1
	HP - Value		1,7		2,9		5,2		6,3
Scenario 2	RQD (%)	Poor	35	Poor to fair	50	Poor	40	Poor to fair	50
	Jn	Three joint sets plus random	12	Three joint sets plus random	12	Three joint sets plus random	12	Three joint sets plus random	12
	Jr	Rough or irregular, planar	1,5	Rough or irregular, planar	1,5	Rough or irregular, planar	1,5	Rough or irregular, planar	1,5
	Jk	90% joints silty sand filled, moderate flow	3	90% joints clay filled, poor flow	2	All joints tight or healed with calcite/ quartz, no flow	1	All joints tight or healed with calcite/ quartz, no flow	1
	Jaf	All joints tight, < 0.1 mm	1	Joints 90% 0.1 ≤ 1.0 mm	1,2	Joints 90% 0.1 ≤ 1.0 mm	1,2	Joints 90% 0.1 ≤ 1.0 mm	1,2
	Jw	Drops	0,86	Damp	0,94	Dry	1	Dry	1
	HP - Value		1,3		2,5		4,2		5,2
Scenario 3	RQD (%)	Fair	55	Fair	70	Fair	60	Fair	70
	Jn	Two joint sets plus random	6	Three joint sets plus random	12	Three joint sets plus random	12	Three joint sets plus random	12
	Jr	Rough or irregular, planar	1,5	Rough or irregular, planar	1,5	Rough or irregular, planar	1,5	Rough or irregular, planar	1,5
	Jk	90% joints silty sand filled, moderate flow	3	90% joints clay filled, poor flow	2	All joints tight or healed with calcite/ quartz, no flow	1	All joints tight or healed with calcite/ quartz, no flow	1
	Jaf	Joints 90% 1.0 ≤ 5.0 mm	1,4	Joints 90% 0.1 ≤ 1.0 mm	1,2	All joints tight, < 0.1 mm	1	All joints tight, < 0.1 mm	1
	Jw	Drops	0,86	Damp	0,94	Dry	1	Dry	1
	HP - Value		2,8		3,4		7,5		8,8

Lagoa slope, HGMZ 1, presented the lowest value interval of HP-value – 1,3 to 2,8 – thus having a greater possibility of seepage and infiltration problems. Followed by Lagoa slope, HGMZ 2, with higher values – 2,5 to 3,4 – decreasing the probability of water seepage and infiltrations and, finally, as expected, on Lagoa slope, HGMZ 3, the highest values – 4,2 to 8,8 – in the three scenarios were achieved. Considering Amores slope, only on its lower quality scenario (2), a value of 2,8 was achieved, assessing the possibility of water infiltration. On Cancela slope, all the achieved values – 4 to 35 – were higher than the limit HP-value of 3.

Table 48 - Synthesis of the HP-value parameters for the Amores slope.

	HGMZ	1		Value
Scenario 1	RQD (%)	Fair		60
	Jn	Two joint sets plus random		6
	Jr	Rough or irregular, planar		1,5
	Jk	All joints tight or healed with calcite/ quartz, no flow		1
	Jaf	Joints 90% 0.1 ≤ 1.0 mm		1,2
	Jw	Dry		1
	HP - Value		12,5	
	RQD (%)	Poor to fair		50
	Jn	Three joint sets		9
	Jr	Rough or irregular, planar		1,5
Scenario 2	Jk	90% joints clay filled, poor flow		2
	Jaf	Joints 90% 1.0 ≤ 5.0 mm		1,4
	Jw	Damp		0,94
	HP - Value		2,8	
	RQD (%)	Fair		70
	Jn	Two joint sets		4
Scenario 3	Jr	Rough or irregular, planar		1,5
	Jk	All joints tight or healed with calcite/ quartz, no flow		1
	Jaf	All joints tight, < 0.1 mm		1
	Jw	Dry		1
	HP - Value		26,25	

Table 49 - Synthesis of the HP-value parameters for the Cancela slope.

	HGMZ	1			
		Slope 1	Value	Slope 2	Value
Scenario 1	RQD (%)	Fair	60	Fair	55
	Jn	Two joint sets	4	Two joint sets	4
	Jr	Smooth, undulating	2	Smooth, undulating	2
	Jk	All joints tight or healed with calcite/ quartz, no flow	1	90% joints clay filled, poor flow	2
	Jaf	All joints tight, < 0.1 mm	1	Joints 90% 1.0 ≤ 5.0 mm	1,4
	Jw	Dry	1	Dry	1
	HP - Value		30,0		9,8
	RQD (%)	Poor to fair	50	Poor	45
	Jn	Two joint sets plus random	6	Two joint sets plus random	6
	Jr	Rough or irregular, planar	1,5	Rough or irregular, planar	1,5
Scenario 2	Jk	All joints tight or healed with calcite/ quartz, no flow	1	90% joints clay filled, poor flow	2
	Jaf	All joints tight, < 0.1 mm	1	Joints 90% 1.0 ≤ 5.0 mm	1,4
	Jw	Dry	1	Dry	1
	HP - Value		12,5		4,0
	RQD (%)	Fair	70	Fair	65
	Jn	Two joint sets	4	Two joint sets	4
Scenario 3	Jr	Smooth, undulating	2	Smooth, undulating	2
	Jk	All joints tight or healed with calcite/ quartz, no flow	1	90% joints clay filled, poor flow	2
	Jaf	All joints tight, < 0.1 mm	1	Joints 90% 1.0 ≤ 5.0 mm	1,4
	Jw	Dry	1	Dry	1
	HP - Value		35,0		11,6

3.4.4.2. Hydraulic-Conductivity (HC) System

On the HC System (Hsuo et al., 2008, 2011), the three scenarios approach was maintained but, since this classification was designed for groundwater circulation, an adaptation was required. The major difference to other classifications is the consideration of a depth parameter, the Depth Index (DI) parameter. This parameter states that, when the depth in a subsurface water exploration increases, the aquifer hydraulic conductivity will decrease. Thus, as the exploration depth increases, the DI parameter decreases, decreasing the final HC system value. Since, the available data for this study is from an outcrop surface, this parameter was calculated assuming that the double packer test depth interval was coincident with the correspondent HGMZ section length. Therefore, the L_c considered was the middle point length of the section to be studied and, L_T was the total length of the section. Another parameter that was taken under consideration was the Gouge Content Designation (GCD) index. Since there was a lack of core run information regarding gouge content of clay-rich fractures and, with the adaptation of this classification to outcrop surfaces, the value one (1) was considered for every calculus, therefore stating that, clay-rich fractures did not had influence on the water flow of this rock mass. The considered Lithology Permeability Index (LPI) value was 0,15 since, Caldas da Cavaca study area is mainly composed by granites. Since, the Cancela slope was dry, it was not considered viable for this classification. This classification was also applied on two boreholes, RA1C and RAM2, existent in the area of Caldas da Cavaca study site.

By looking at Table 50, it is possible to conclude that, on the first scenario (1), the higher values of HC system belonged to Lagoa slope HGMZ 1, followed by Amores slope, Lagoa slope HGMZ 2, and finally, RAM2 and RA1C boreholes. When looking at scenario 2, the values of HC increase because the overall geomechanical characteristics decreased. Thus, the possibility of water infiltrations are higher.

Table 50 – Synthesis of the Geological Strength Index parameters for the three studied rock slopes.

HGZM		1		2		1		RA1C	RAM2	
		Section 1	Section 2	Section 1	Section 2	Slope 1	Slope 2			
HC SYSTEM	Scenario 1	RQD	42		60		60		60	60
		DI	0,50	0,07	0,09	0,08	0,50	0,16	0,12	0,17
		GCD	0				0		0	
		LPI	0,15				0,15		0,15	
		HC	4,4E-02	6,0E-03	7,7E-03	5,0E-03	3,0E-02	2,4E-02	7,5E-03	1,0E-02
		RQD	35		50		50		50	50
	Scenario 2	DI	0,50	0,07	0,09	0,08	0,50	0,16	0,12	0,17
		GCD	0				0		0	
		LPI	0,15				0,15		0,15	
		HC	4,9E-02	6,7E-03	6,7E-03	6,2E-03	3,8E-02	1,2E-02	9,3E-03	1,3E-02
		RQD	55		70		70		70	70
		DI	0,50	0,07	0,09	0,08	0,50	0,16	0,12	0,17
Scenario 3	GCD	0				0		0		
	LPI	0,15				0,15		0,15		
	HC	3,4E-02	4,7E-03	6,0E-03	3,7E-03	2,3E-02	7,2E-03	5,6E-03	7,8E-03	
	RQD	55		70		70		70	70	
	DI	0,50	0,07	0,09	0,08	0,50	0,16	0,12	0,17	
	GCD	0				0		0		

3.5. Discussion

3.5.1. Overview

The present work was focused on a comprehensive analysis of the hydrogeomechanical parameters of rock masses which, with the incorporation of a previous collection of selected data set (namely, geological, geotechnical and hydrogeological data), made possible the hydrogeomechanical assessment of Caldas da Cavaca site based on the study of three rock slopes. As described on the previous sections, to understand the overall rock mass quality and the role of the water flow in rock behaviour, several rock mass classifications focused on hydrogeological issues were applied. In order to have a better overview of the studied rock slopes, in the following section, several summary tables about the rock mass classifications for each rock slope are presented. Before the results discussion, it is important to previously consider a few issues. All the conclusions regarding rock mass quality and hydraulic behaviour take in consideration these remarks:

- i) The RMR classification (Bieniawski, 1989 and references therein) is mostly focused on rocky tunnels and/or foundations. For this reason, its tendency is to lower the rock mass quality values for safety purposes. When rock slope study is considered, its approximation is rather simplistic;

-
- ii) The SMR classification (Romana, 1985, 1993; Romana et al., 2003 and references therein), was developed towards a more effective study of rock slope stability. Comparing to the RMR, it provides a more specific analysis over the effect of discontinuities orientation to the excavation direction (P6 parameter). Thus, for the study of rock slopes, it represents a more realistic approach to the rock mass quality rather than RMR classification;
 - iii) The GSI scheme (e.g., Hoek, 1994; Hoek et al., 1998; Hoek and Marinos, 2000 and references therein), due to its practical approach, tends to increment the values of rock mass quality. Recently, a GSI classification approach based on quantification chart was proposed by Hoek et al. (2013), but some issues still remain about its applicability;
 - iv) Lower HP-values (Gates et al., 1997, 2003) denote higher probability of seepage infiltrations;
 - v) Although HC-system classification (Hsu et al., 2008, 2011) is an in-depth hydraulic classification and was designed for groundwater boreholes, in this study it was applied with some restrictions and with an exploratory stage; the outcrop rock scanline surveys from the studied slopes were overlapped as a sub-horizontal borehole, in order to test the practical feasibility;
 - vi) The HC-system does not has a quantifiable scale for its results; therefore, the only consideration regarding its results states that, higher values of HC-system represent higher values of hydraulic conductivity.

3.5.2. Rock mass schemes and hydrogeomechanical classifications or indexes: an outline

Table 51 shows for the Lagoa slope an evident trend regarding the rock mass classifications results for every Hydrogeomechanical Zone (HGMZ). This trend expresses the main rock mass quality qualification for each HGMZ with minor variations.

Table 51 – Synthesis of rock mass indexes and/or classification schemes and hydrogeomechanical classifications for Lagoa slope.

LAGOA SLOPE: CLASSIFICATIONS/INDEXES SUMMARY	HGMZ	Classification/Index					
		Rock mass			Hydrogeomechanical		
		RQD	RMR	SMR	GSI	HP-Value	HC System
1	Section 1	Poor (42)	Poor (25 - IV)	Bad (38 - IVa)	Poor to fair (40 - 50)	Medium inflow to damp/drops (1,3 to 2,8)	3,4-4,9E-02
	Section 2						4,7-6,7E-03
2	Section 1	Fair (60)	Poor (40 - IV)	Fair (53 - IIIa)	Poor to fair (50 - 60)	Medium inflow to damp/drops (2,5 to 3,4)	6,0-7,7E-03
	Section 2						3,7-6,2E-03
3	Slope 1	Fair (50)	Poor to fair (36 to 44 - IV to III)	Fair (46 - IIIb)	Fair to good (55 - 65)	Minor inflow to dry (4,2 to 7,5)	N. D.
	Slope 2	Fair (60)	Poor (40 - IV)	Fair (47 - IIIb)	Fair (45 - 55)	Minor inflow to dry (5,2 to 8,8)	N. D.

N.D. - Not determined

The HGMZ 1 grouped, mainly, poor to fair rock mass quality sections and exhibits the lowest values for RQD, RMR and SMR classifications/indexes. Nevertheless, this slope had higher water seepage and presented the lowest HP-values and higher score of HC-system. The combination of these characteristics, assessed this HGMZ as the lowest rock mass quality zone and more unstable, due to the possibility of higher water seepage. HGMZ 2 is another section with water inflow but presents fewer seepage problems since the overall rock quality improved. HGMZ 3 section is mainly minor inflow to dry, while the rock mass quality is fair. Its overall quality is fair and stands between HGMZ 1 and HGMZ 2. However, for HGMZ 3, slope 1, the RMR and GSI values were higher than HGMZ 2 values.

Amores slope is presented in Table 52, being perceptible a general improvement of the rock mass quality. This slope ranges from fair to good rock mass quality with: i) higher values for the HP-value classification; ii) similar values as Lagoa slope, HC-system results. In this slope, lower values for the HC-system were expected so, these results shall be regarded cautiously and the remark v), previously pointed, has to be taken in consideration.

Table 52 – Synthesis of rock mass indexes and/or classification schemes and hydrogeomechanical classifications for Amores slope.

AMORES SLOPE: CLASSIFICATIONS/ INDEXES SUMMARY	HGMZ	Classification/Index					
		Rock mass			Hydrogeomechanical		
		RQD	RMR	SMR	GSI	HP-Value	HC System
1	Section 1	Fair (60)	Fair (45 - III)	Fair (45 - IIIb)	Fair to good (55 - 65)	Minor inflow to dry (2,8 to 12,5)	2,3-3,0E-02
	Section 2						7,2E-03 to 2,4E-02

Considering Cancela slope (Table 53), this slope served as a dry example for the comparison of rock mass quality and hydraulic behaviour. This slope presented an overall fair rock mass quality beside its weathered fronts and low uniaxial compressive strength values. The clear difference between RMR and SMR values stated that this slope joint set directions have a significant and favourable effect, regarding slope excavation. Its HP-values were considerably above the considered “seepage-limit” (i.e., HP-value < 3), representing also a better rock mass quality. The HC-system classification was not applied to this slope.

Table 53 – Synthesis of rock mass indexes and/or classification schemes and hydrogeomechanical classifications Cancela slope.

CANCELA SLOPE: CLASSIFICATIONS/ INDEXES SUMMARY	HGMZ	Classification/Index					
		Rock mass			Hydrogeomechanical		
		RQD	RMR	SMR	GSI	HP-Value	HC System
1	Slope 1	Fair (60)	Poor (39 - IV)	Fair (52 - IIIa)	Fair (40 - 50)	Dry (30)	N. D.
	Slope 2	Fair (55)	Poor (38 - IV)	Fair (51 - IIIa)	Fair (50 - 60)	Dry to minor inflow (9,8)	N. D.

N. D. - Not determined

3.5.3. Rock mass hydraulic behaviour

Understanding the rock mass hydraulic behaviour of Caldas da Cavaca area is one of the major core aims of this study. Its estimation along with rock mass quality data will be the basis to improve the hydrogeological site model with the hydrogeomechanical focus. In order to, comprehend the following hydrogeomechanical summary tables a few remarks about the HP-value and HC-system parameters assessment are presented:

HP-value

- i) Joint Water Factor (J_w) ratings have a related flow measure, but it cannot have a direct comparison to yield [Q] or to seepage discharge. It is a quantification of water yield for one rock joint, while yield [Q] and specific discharge are parameters that quantify water flow along a specific slope length. Including this factor in the summary tables merely provides an informative general notion of the water presence on the rock mass fractures;
- ii) Yield [Q] and specific capacity [Q/s] values were determined using Gates (2003) approximation. The described intervals consider the lowest and the highest case scenarios for each HGMZ;
- iii) Transmissivity [T] is determined through specific capacity [Q/s] values. The interval values were defined considering the minimum and maximum values obtained from Logan (1964), Huntley et al. (1992) and Batu (1998) formulas (see details in chapter 2);
- iv) Hydraulic conductivity [K] was determined from the previous transmissivity values, considering the potential aquifer thickness, represented, in the present case, by the minor wet slope length;
- v) Seepage discharge represents a relation of the HP-values to the seepage discharge from fractured rock in tunnels and outcropping rock faces;
- vi) Well discharge and seepage discharge represent a relation of the HP-values to the discharge from bedrock wells, as well as, seepage discharge from fractured rocks.

HC-system

- i) Hydraulic conductivity [K] parameter is directly obtained from the HC-system classification. Thus, the presented intervals are attainable through the lowest and highest case scenarios for each HGMZ;
- ii) Transmissivity [T] is achieved considering the potential aquifer thickness, represented, in the present case, by the humid slope length;
- iii) Specific capacity [Q/s] was determined through the transmissivity [T] from the previous remark and, Logan (1964) and Batu (1998) formulas were used for this approximation. Huntley et al. (1992) did not allow an easy approximation.

Since water flow only occurred on Lagoa and Amores slopes, the following hydraulic study will be made individually for each slope.

3.5.3.1. Lagoa slope hydrogeomechanical assessment

Table 54 summarises all the parameters computed from the hydrogeomechanical classifications for Lagoa slope.

Table 54 – Hydrogeomechanical parameters for Lagoa slope.

LAGOA SLOPE: HIDROGEOMECHANICAL PARAMETER COMPARISON	HGMZ	1		2	
		Section 1		Section 2	
		Section 1	Section 2	Section 1	Section 2
	Length (m)	13,9	9,7	28,9	38
HP-Value	Joint water factor J_w^* (L/min)	6,0E-04 to 6,0E-03		6,0E-05 to 6,0E-04	
	Yield Q (L/min)	9,1 to 229,4		2,6 to 19,6	
	Specific capacity [Q/s] (m^2/day)	0,2 to 12,8		0,038 to 0,52	
	Seepage discharge (L/min)	1,9 to 44,6		0,6 to 4,0	
	Well discharge and seepage discharge (L/min)	5,3 to 171,8		4,2 to 10,7	
	Transmissivity T_{HP} (m^2/day)	2,0E-02 to 17,7		2,5E-03 to 7,2E-0,1	
HC System	Hydraulic conductivity K_{HP} (m/day)	1,3E-03 to 1,28	1,8E-03 to 1,83	8,8E-05 to 2,5E-02	6,7E-05 to 1,9E-02
	Hydraulic conductivity K_{HC} (m/day)	1,0-3,3E-03	1,5-2,5E-04	2,2-3,1E-04	1,1-2,3E-04
	Transmissivity T_{HC} (m^2/day)	1,4-4,7E-02	1,5-2,5E-03	6,3-8,9E-03	4,3-8,7E-03
	Specific capacity [Q/s] _{HC} (m^2/day)	1,2-3,8E-02	1,2-2,0E-03	5,2-7,3E-03	3,5-7,1E-03

The HGMZ 1, as previously described, was the zone where water seepage had a higher presence. Thus, when comparing all the zones, this zone recorded higher hydrogeomechanical values. Starting with yield [Q], and according to Gates (2003), this zone had a fairly high yield, from 9 L/min to 229 L/min with a corresponding high specific capacity [Q/s]. The specific capacity [Q/s] values achieved from the HC-system were, approximately, 10 times lower. The “Seepage discharge” and “Well discharge and seepage discharge” are also flow parameters, but their meaning is directly related to the seepage possibilities of the rock mass, one of the most important quantifications of this work. When comparing these measurements to yield [Q], they had a slightly decrease of range, denoting that, although the values decreased, the seepage infiltrations on this HGMZ remained fairly high. Regarding the transmissivity [T] and hydraulic conductivity [K] values, they have also diverged slightly between classifications. The lowest

interval results for the HP-value were coincident with the interval range of the HC-system, achieving the HC-system, for both sections, considerably lower results than the HP-value results. The comparison of values for the highest case scenario, on both classifications, had a difference of 100 times, with the HP-value classification scoring higher, along with a wider range of values. In conclusion, HC-system classifies HGMZ 1 slopes with lower transmissivity and hydraulic conductivity characteristics than those obtained through the HP-value classification.

When comparing HGMZ 2 to HGMZ 1, all the studied parameters scored lower values, as it was expected. The yield [Q] values were lower and ranged 3 L/min to 20 L/min, along with lower specific capacity [Q/s] values. The previous relation stated to the HC system occurs again, being the achieved results for this classification 10 times lower. HGMZ 2 presented lower values for “Seepage discharge” and “Well discharge and seepage discharge” exhibiting less problems regarding seepage infiltrations. Once again, for the transmissivity [T] and hydraulic conductivity [K] values a similar situation to the HGMZ 1 occurred. The values were coincident on the lower interval limit of the HP-value classification, attaining the HC-system the lowest values for these parameters.

3.5.3.2. Amores slope hydrogeomechanical assessment

Regarding Amores slope (Table 55), this slope was mostly dry and the hydrogeomechanical parameters confirmed the almost absence of water seepage and the low hydrogeomechanical characteristics. In the highest case scenario, the yield [Q] value for this HGMZ achieved 9.5 L/min which stands in the middle of HGMZ 2 yield range of Lagoa slope and is close to the lowest values of HGMZ 1 yield of Lagoa slope. Regarding specific capacity [Q/s], the HC-system scored 10 times lower values than the ones achieved through the HP-value classification, which matches the already stated relation regarding the previous described slopes. The higher values for “Seepage discharge” and “Well discharge and seepage discharge” match the lower frontier achieved for the same parameters on both HGMZ of Lagoa slope. Concerning the transmissivity [T] and hydraulic conductivity [K], on both slopes, the obtained HP-values were lower than the Lagoa slope, similar, to the ones achieved through the HC-system. Since, the presence of water seepage on this slope was lower than Lagoa slope, the HC-system results should also have confirmed it through lower values. However, they were identical to the previously determined values of Lagoa slope. Once again, there is an approximation of the lowest scenario, transmissivity and hydraulic conductivity values of the HP-value classification to the interval range obtained through the HC-system. In the Amores slope, slope 2 had a slightly higher transmissivity and hydraulic conductivity than slope 1.

Table 55 – Hydrogeomechanical parameters for Amores slope.

HGMZ		1	
		Section 1	Section 2
Length (m)		32,6	40,4
HP-Value	Joint water factor J_w^* (L/min)	0 to 6,0E-04	
	Yield Q (L/min)	0 to 9,5	
	Specific capacity [Q/s] (m^2/day)	0 to 0,2	
	Seepage discharge (L/min)	0 to 1,9	
	Well discharge and seepage discharge (L/min)	0 to 5,3	
	Transmissivity T_{HP} (m^2/day)	2,0E-2 to 2,9E-01	
Hydraulic conductivity K_{HP} (m/day)		5,8E-04 to 8,9E-03	4,7E-04 to 7,2E-03
HC System	Hydraulic conductivity K_{HC} (m/day)	1,3-2,7E-03	2,8E-04 to 1,5E-03
	Transmissivity T_{HC} (m^2/day)	4,0-8,8E-02	1,0-6,1E-02
	Specific capacity [Q/s] _{HC} (m^2/day)	2,89-7,21E-02	7,2E-03 to 5,0E-02

AMORES SLOPE: HIDROGEOMECHANICAL PARAMETER COMPARISON

3.5.3.3. Boreholes: hydraulic and hydrogeomechanical studies

When considering borehole water abstraction, the available data from borehole core-drills and borehole hydrogeological tests have a different array. Parameters such as the static water level, the hydrodynamic level and the exploration yield are measured, providing different possibilities for achieving the desired hydrogeomechanical parameters. Hsu et al. (2008, 2011) stated that the depth index (DI) parameter is a measure regarding a double packer test. This test is planned and executed for depths where it is expected that the aquifer has higher water flow. In this study, the DI parameter was considered regarding the well screens. Since, their placement is planned for the highest water productivity depth, a common point binds both of these approaches. Table 56 displays the two approaches used for retrieving hydrogeomechanical parameters on boreholes, the HC-system and the *in situ* pumping tests.

Table 56 – Hydrogeomechanical parameters for RA1C and RAM2 boreholes.

		Well Name	RA1C	RAM2
			well screen	well screen
		Length (m)	17,6	33
HC System		Hydraulic conductivity K_{HC} (m/day)	2,0-4,0E-04	3,1-6,4E-04
		Transmissivity T_{HC} (m ² /day)	3,5-7,0E-03	1,0-2,1E-02
		Specific capacity $[Q/s]_{HC}$ (m ² /day)	2,8-5,8E-03	8,5E-03 to 1,7E-02
Pumping test		Static water level (NHE) (m)	21,60	5,56
		Hydrodynamic level (NHD) (m)	68,10	10,90
		Drawdown s (m)	46,50	5,34
		Exploration yield Q (L/min)	66,0	300,0
		Specific capacity $[Q/s]_{PT}$ (m ² /day)	2,0	80,9
		Transmissivity T_{PT} (m ² /day)	0,3 to 2,8	21,4 to 112,0
		Hydraulic conductivity K_{PT} (m/day)	1,7E-02 to 1,6E-01	6,5E-01 to 3,4

Concerning the analysis of the pumping tests, the exploration yield [Q] of these boreholes were 66 L/min for RA1C and 300 L/min for RAM2. These boreholes achieved high values of specific capacity [Q/s], having the RA1C similar values to the previously higher water content slope, Lagoa slope – HGMZ 1. Regarding transmissivity [T] and hydraulic conductivity [K], the results achieved through these boreholes were relative high, with higher values in RAM2 borehole. The HC-system results were, once again, apart from what to be expected. The hydraulic conductivity [K] values were similar to the previous slopes, though they are very different from the results obtained through the pumping tests.

3.5.4. HP-value chart (Gates, 2003) vs HP-value results

In order to compare the obtained HP-value results, they were plotted in the chart proposed by Gates (2003), to confirm their approach accuracy. Figure 27 shows the HP-values regarding Lagoa and Amores slopes for every estimated scenario with their achieved yield and specific capacity.

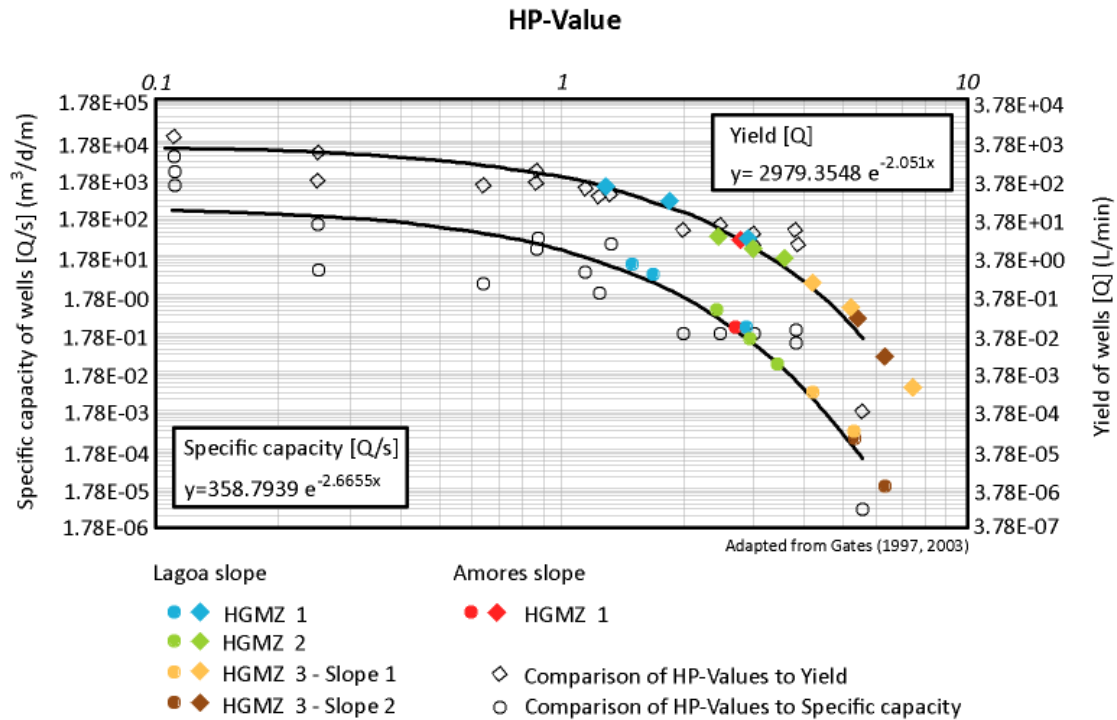


Figure 27 – HP-value chart (Gates, 2003) comparison versus achieved HP-values for studied area.

A few remarks can be done through the analysis of this chart:

- i) The HP-values for HGMZ 1 and HGMZ 2 of Lagoa slope scored higher or similar values to HP-value = 3, which means, in an overall perspective, these zones have higher yields and seepage possibilities;
- ii) Only the highest case scenario was plotted for the Amores slope – HGMZ 1, meaning that, besides lower possibilities of seepage, only when gathering this scenario conditions, seepage would occur;
- iii) It is perceptible that the values of Lagoa slope – HGMZ 1 – are different from the Amores slope values, where, only the lowest values of Lagoa slope – HGMZ 1 – are coincident with Amores slope, highest case scenario;
- iv) The possibilities of seepage increase when, the considered scenarios succeed to be plotted. Lagoa slope – HGMZ 3 –, on both slopes, only plotted two points for each one, meaning that, besides having lower yield values, in one of its scenarios, there was no possible occurrence of water seepage;

The maps presented in Figure 29 and Figure 30 show the RQD and GSI results for Caldas da Cavaca site. It is noticeable a similarity between the zone division on both maps, as the achieved results on both classifications had equivalent rock mass quality quantifications.

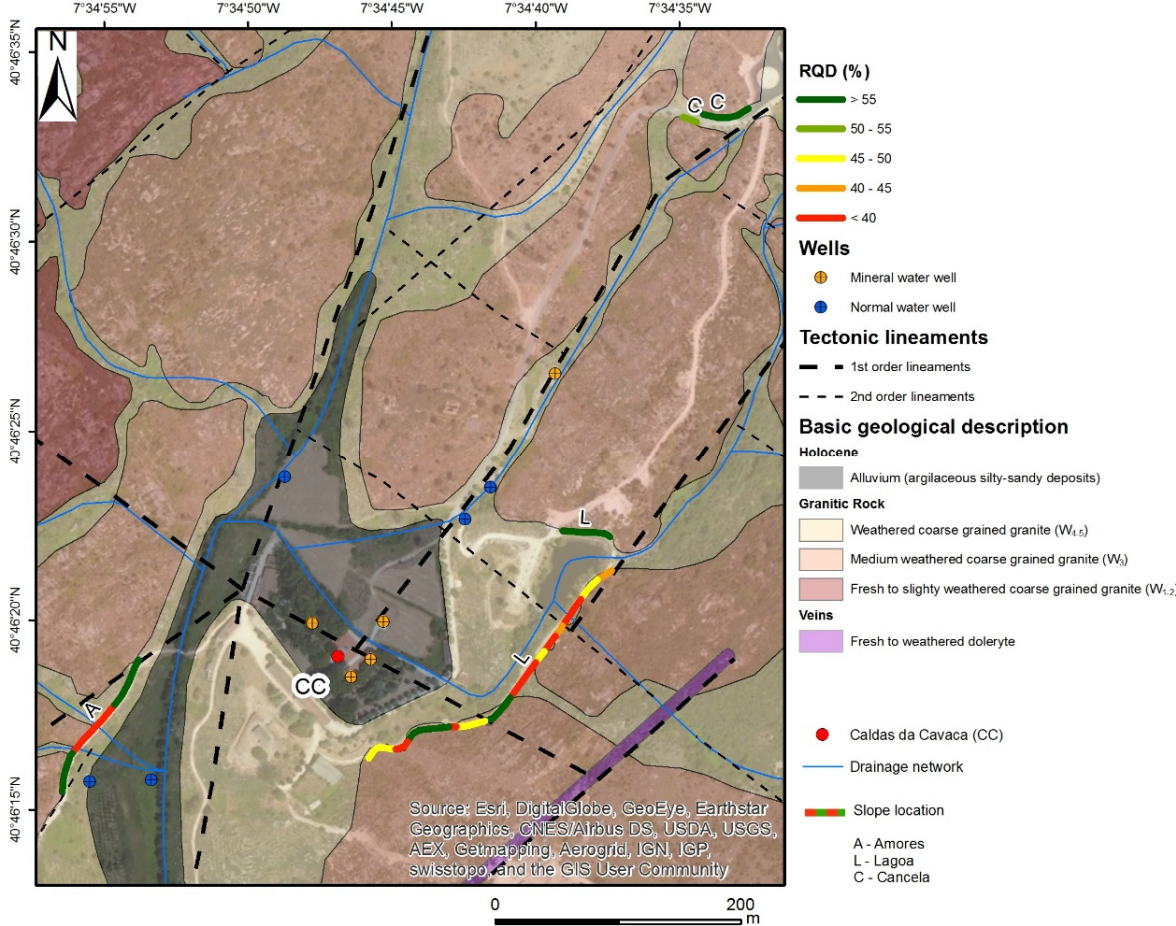


Figure 29 – Hydrogeomechanical map: coupling GIS mapping with RQD index.

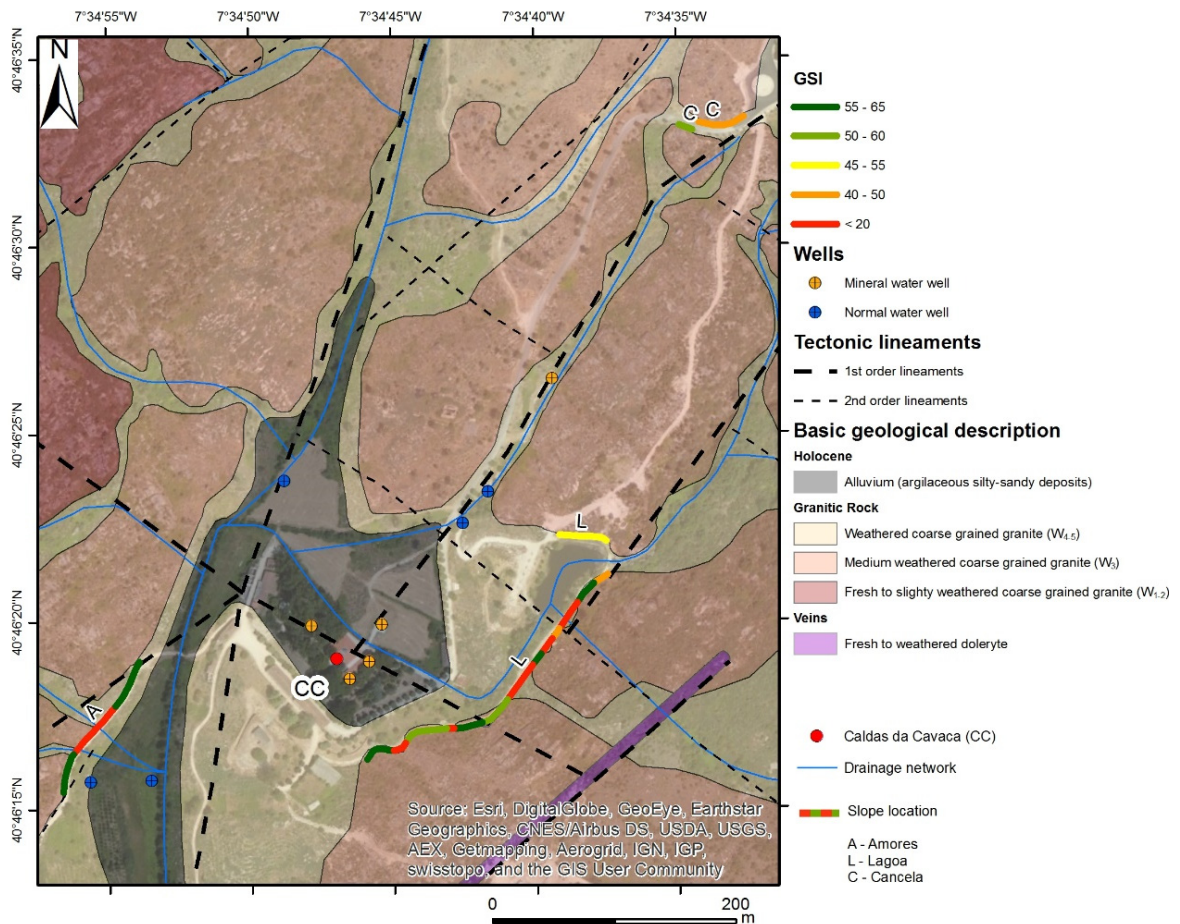


Figure 30 – Hydrogeomechanical map: coupling GIS mapping with GSI index.

Finally, it was plotted the map presented on Figure 31, displaying rock mass quality *versus* its water content along the slopes. This map was based on the HP-value results, having a similar division to the ones described before but with an added description of the rock quality and its corresponding seepage possibilities.

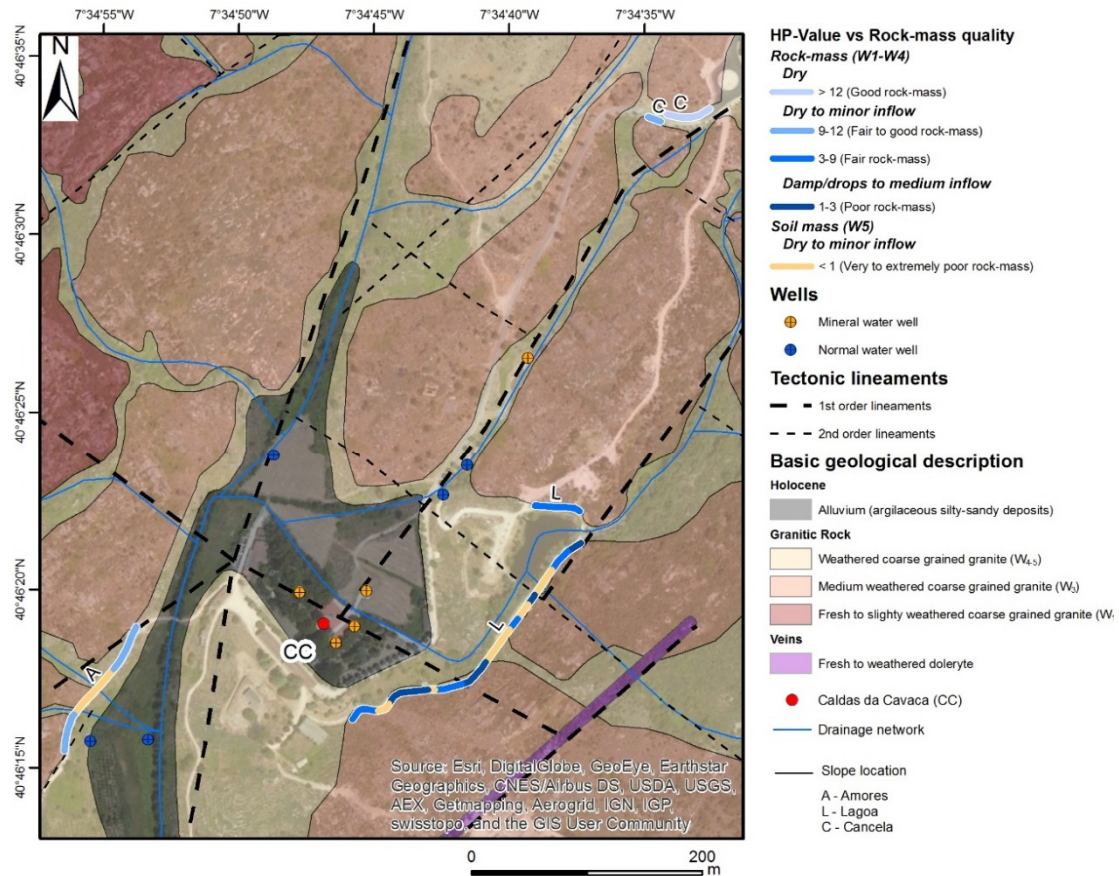


Figure 31 – Hydrogeomechanical map: coupling GIS mapping with a HP-value vs. Rock-mass quality approach.

3.5.6. Hydrogeological conceptual site model: subsurface hydrogeomechanical role

According to Teixeira et al. (2015) the Caldas da Cavaca hydromineral system discharge zone are constituted by three main aquifer types and an outline of the hydrogeological conceptual site model of the area is shown in Figure 32 (details in Teixeira, 2011; Teixeira et al., 2015):

- i) shallow, unconfined aquifer, related to the alluvia cover, and located in the valley bottom, near the Caldas da Cavaca thermal site; the groundwater has a pH 5 - 6.5 and electrical conductivity under 20 $\mu\text{S}/\text{cm}$ (very low mineralisation). Water temperature is strictly dependent of the air temperature;
- ii) An unconfined to semi-confined aquifer, in the weathered rock mass and in fractured granite. These groundwaters have pH of 5 - 6.5 and electrical conductivity varying from 20 - 50 $\mu\text{S}/\text{cm}$ (low mineralisation). The water yields, in the measured springs, are very low (< 0.05 L/s), and the transmissivity is lower than 1 m^2/day ;
- iii) A deep confined hydromineral aquifer controlled by a deep fault zone, in the fresh granite. The hydromineral water has temperatures around 30°C (mesothermal waters), higher electrical conductivities (350 – 400 $\mu\text{S}/\text{cm}$; medium mineralised

waters) and pH around 8.4 – 8.6. These waters have an alkaline reaction, a sodium bicarbonate facies, fluoridated and sulphurous. The transmissivity in the hydromineral aquifer varies from 27 - 136 m²/day. The Ribeira de Coja fault zone, with general NNE–SSW trend, mapped around Caldas da Cavaca area, has a regional cartographic expression, and locally, fault gouge was observed. This may be the main structure controlling the occurrence of hydromineral waters in this site.

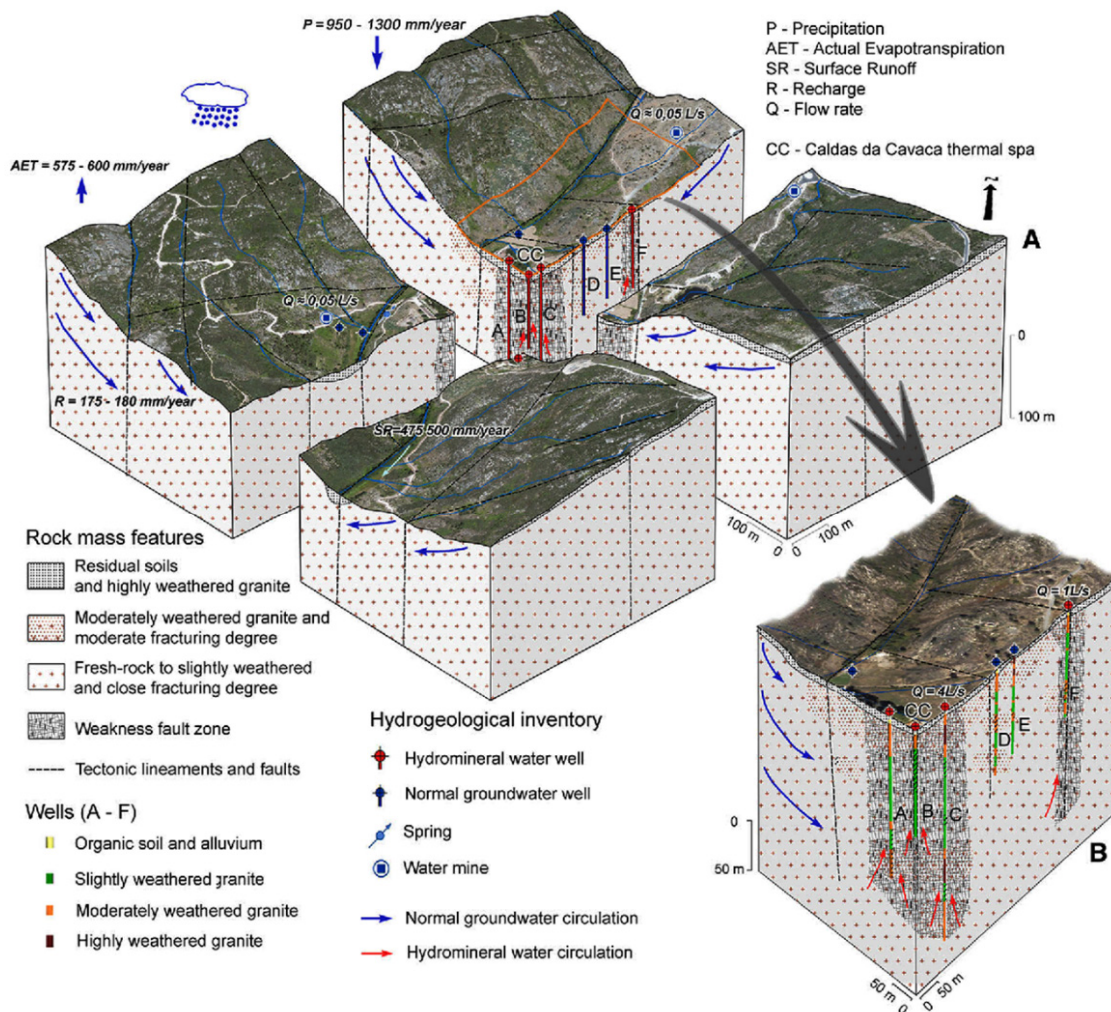


Figure 32 – General (A) and detailed (B) hydrogeological conceptual model from Caldas da Cavaca hydromineral system (after Teixeira et al., 2015).

In this study, when retrieving hydrogeomechanical parameters, the HC-system had a more simplistic approach considering less influential parameters regarding water flow. The lack of consideration for discontinuities characteristics, besides fracture intercept parameter (ISRM,

1981), makes the linkage between classification and rock mass difficult. Mayer et al. (2014) published an interesting article, regarding a statistical study of HP-value and HC-system parameters which, stated that, there is an *“overreliance of RQD as an indication of the fracture state, despite its limitation in closely and widely spaced fracture systems”*. *“(…) Groundwater is conceptualized as fracture-dominated in hard rock settings”* but, the HC-system has a narrow vision since, it considers only the RQD for vaguely determining fracture intercept characteristics, together with the gauge content designation (GCD) parameter to establish the rock mass fracture parameters. Thus, within every zone, the HC-system classification achieved similar values and will not increment the information regarding Caldas da Cavaca hydromineral system. The HP-value index results ranged a much more wider and realistic interval than the ones obtained through the HC-system classification.

As it is possible to observe on the following Figure 33, within each slope and borehole where, hydrogeomechanical parameters were assessed and, using the previously defined hydrogeological conceptual model for Caldas da Cavaca hydromineral system by Teixeira et al. (2015), new information was plotted. The previously determined hydrogeomechanical subsurface parameters, yield [Q], specific capacity [Q/s], transmissivity [T] and hydraulic conductivity [K], established a clearer overview of the hydraulic behaviour on Caldas da Cavaca area.

Once again, Lagoa slope, besides having its higher hydrogeomechanical parameters, is the most interesting zone to look upon. It is located in the contact between medium (W_3) to weathered (W_5) coarse granite; 1st and 2nd order tectonic lineaments intersect several slope sections, one of them where rock mass quality is lower; a drainage network line crosses this slope, possibly increasing its subsurface yield due to, this slope favourable rock mass fracture characteristics; its descendent location adds surface runoff presence on this slope and possibly increases the recharge infiltration on the water transmitting fractures network.

The Amores slope with, fair to good rock mass quality and its rock mass fracture overall features, did not enabled this slope to have a subsurface water circulation potential. Although, some subsurface seepage was found, it was possibly due to the geomorphological features which, cross this slope with two drainage network paths.

Considering the Cancela slope location height, it is in the highest point, being out of any potential drainage network. This slope rock mass characteristics could allow some water seepage and circulation but its location, places it in a non-productive water circulation point-of-view.

3.5.7. Final remarks and outlook

One interesting argument suggested by Mayer et al. (2014), regarding both schemes, was the need of considering each fracture individually when studying the overall hydraulic properties of rock mass. As Mayer et al. (2014) stated: *“Moreover, both systems assume that all fractures contribute equally to the overall hydraulic properties of the rock mass, and fail to explicitly distinguish between the frequencies of permeable and impermeable fractures. Finally, both systems assume average values for fracture properties, i.e. fill, roughness, etc., instead of exploring the influence of individual fractures.”* In the early stages of this work, when defining hydrogeomechanical zoning sections, according to the discontinuities water seepage parameter, several groups of fractures with identical permeability were distinguished. Thus, instead of considering each fracture individually and equally to the overall rock mass hydraulic properties, a number of zones were outlined containing different hydraulic properties along the slopes. When considering rock engineering projects and slope stabilisation, the extrapolation of these fractures hydraulic behaviour to all the rock mass is not precisely accurate but, since these parameters are considered for a specific slope length and not for one fracture, it adds a certain safety coefficient on the measures to be taken.

Mayer et al. (2014) also stated that, *“(…) secondary fracture features such as persistence and aperture undoubtedly play an important role in the overall fluid flow characteristics and need to be taken into consideration in any rock mass permeability scheme.”* It has been proven that characteristics such as, fracture orientation, persistence, aperture, fracture intercept and filling, have a major role when describing fracture interconnectivity and its hydraulic behaviour. While, the HP-value classification take some in consideration along its classification, orientation and persistence are replaced by the number of joint sets while, the HC-system only has in consideration the RQD and gauge content designation (GCD) for fracture characteristics.

Another consideration regarding the HC-system concerns the depth index (DI) parameter. This parameter assumes that when depth increases the rock mass tends to be less fractured and more compact thus, reducing the HC-system final value and, consequently, lowering its hydraulic conductivity values. It contradicts itself since, when planning and positioning, on certain depths, double packer tests, Lugeon tests or well screens, the choosen depth could range from 20 - 200 m and higher water seepage values may be found at higher depths (> 200 m). This means that when depth increases the hydraulic conductivity shall not be reduced but shall be quantified as a seepage water factor, not linearly dependant from its depth but from its yield production.

Regarding borehole parameter collection, Mayer et al. (2014) proposed a core characterisation that *“would represent how well two pieces of core match-up across a given fracture plane”*. This

qualitative approach would be a measure of the aperture since, “*where the core continuity across the [fracture] plane is high, it can be assumed that the in-situ fracture likely has a low aperture and, hence, poor ability to transmit fluid, whereas a poor core continuity would indicate a higher in-situ aperture.*”. This measure would be helpful since, on core sampling techniques, the aperture parameter is of very difficult quantification and, as it was said before, of a major importance among these studies.

Chapter 4.
Conclusions

Synopsis

The GIS-based mapping tools and reasoning has confirmed its importance and contributed to improve the understanding on the subsurface hydrogeomechanical evaluation and hydraulic behaviour on rock masses. The updated conceptual model of the Caldas da Cavaca site focused on hydrogeomechanical issues was very useful to trial the soundness of hydrogeomechanical schemes and/or indexes.

4.1. Concluding remarks

Hydrogeomechanical analysis supported by GIS-based mapping techniques may be a very useful tool in the assessment of groundwater seepage and geohydraulic behaviour of rock masses. All data should be synthesised at adequate scale, and the comparative analysis of the results are improved by GIS integration and visual analysis. The Caldas da Cavaca hydromineral system site corresponds to a hard-rock watershed with granitic bedrock and distinctive morphoclimatic features. Also, the subsurface hydrogeomechanical inputs are significant to build and improve the hydrogeological conceptual model of the study area. Thus, in Caldas da Cavaca site the main factors controlling the water infiltration and recharge are the weathered granite, the close fracturing degree and the planned surfaces in the higher areas. Concerning the discharge, it may be controlled by the fresh granite, in the areas with higher fracturing degree, and especially in the lower areas of the valleys.

The present study attained several remarks concerning the subsurface hydrogeomechanical framework Caldas da Cavaca rock mass site, such as:

- i) By grouping discontinuities in zones, it was possible to characterise and identify the behaviour of this zones, regarding its rock mass quality but also in hydraulic behaviour, accomplishing a hydrogeomechanical section study for each rock mass slopes;
- ii) Among the studied slopes, Lagoa slope presented the highest hydraulic conductivity values and, classified, in terms of water, as the higher productivity zone. However, it presented the lowest values for rock mass quality. Followed by the higher quality slope, Amores slope and the dry Cancela slope;
- iii) Regarding the hydrogeomechanical classifications, the HP-value proved to be efficient and provided a wide range of results when, considering different scenarios. Regarding the HC-system, the approach considered on this work did not proved feasible as, the obtained values were not quite accurate to the slope conditions;
- iv) When utilising the HC-system classification on borehole conditions, its main application, it also did not prove to be accurate thus, it shall be used carefully on future applications;

-
- v) When obtaining the hydraulic conductivity through the HP-value classification, the results were more accurate but, since, for its achievement it was considered a saturated aquifer thickness, the results shall be considered slightly augmented;
 - vi) In conclusion, it was possible to increase the understanding behaviour of water along the Caldas da Cavaca hydromineral system by, achieving results for sub-surface yield, specific capacity, transmissivity and hydraulic conductivity.

The hydrogeomechanical rock mass parameter quantification area is in utmost development with a lot of study possibilities and the need of deepening specific quantification of parameters. The HP-value and the HC-system are good approaches on this type of quantification; however, there are a few possibilities of exploring these schemes, in order to obtain a more suitable in-situ characterisation, such as:

- i) Refining parameters related to fracture interconnectivity should be considered. Parameters such as, persistence should be related to sub-horizontal fractures defining a measure similar to block size but, regarding hydrogeomechanical descriptions;
- ii) Regarding the HP-value classification, an orientation parameter, related to the joints sets or joint spacing could be included to better understand the fracture interconnectivity system obtained from the outcrop rock mass surface;
- iii) New parameter determination solutions on drill cores could also be defined, as it is usually a common procedure in all-types of rock engineering projects. Mayer et al. (2014) described, for example, a simple procedure that could be integrated as an aperture measure from core samples;
- iv) On the HC-system, the depth index parameter shall be redefined making it non-linear with depth but, for example, with productivity lengths along the borehole. It also should include more discontinuity parameters, generating a more specific and applicable classification.

Such vast and heterogeneous study area must have more and more specific analysis, in order to obtain results as close as the inherent reality of the study.

Chapter 5.
References

Abbas S.M., Konietzky H. (2015). Rock mass classification systems. In: Konietzky H. (ed.), Introduction into geomechanics, TU Bergakademie Freiberg, Institut für Geotechnik, University of Freiberg, E-book edition [<https://tu-freiberg.de/fakult3/gt/feme/ebook.php>] (accessed on 28 May 2015).

Acciaiuoli L.M.C. (1952/53). Le Portugal hydromineral, volumes 1 & 2. Direcção Geral dos Serviços Geológicos, Lisbonne.

Aydin A. (2015). ISRM Suggested method for determination of the Schmidt hammer rebound hardness: revised version. In: Ulusay R. (ed.), The ISRM Suggested Methods for Rock Characterization, Testing and Monitoring: 2007–2014. Springer, Cham, Heidelberg, pp. 25-33.

Aydin A., Basu A. (2005). The Schmidt hammer in rock material characterization. *Engineering Geology*, 81:1-14.

Aydan O., Ulusay R., Tokashiki, N. (2014). A new rock mass quality rating system: rock mass quality rating (RMQR) and its application to the estimation of geomechanical characteristics of rock masses. *Rock Mechanics Rock Engineering*, 47(4): 1255-1276.

Barton N. (2000). TBM tunnelling in jointed and faulted rock. Balkema, Rotterdam. 173 pp.

Barton N. (2002). Some new Q-value correlations to assist in site characterisation and tunnel design. *Int. J. Rock. Mech. & Min. Sci.*, 39(2):185-216.

Barton N. (2006). Rock quality, seismic velocity, attenuation and anisotropy. Taylor & Francis, UK. 729 pp.

Barton N. (2007). Rock mass characterization for excavations in mining and civil engineering. In C. Mark, R. Pakalnis, R.J. Tuchman (eds), Proceedings of the International Workshop on Rock Mass Classification in Underground Mining, Pittsburgh: NIOSH, pp. 3–13.

Barton N. (2012). From empiricism, through theory, to problem solving in rock engineering: a shortened version of the 6th Müller Lecture. *ISRM News Journal*, 14: 60–66.

Barton N., Bandis S., Bakhtar K. (1985). Strength, deformation and conductivity coupling of rock joints. *International Journal of Rock Mechanics and Mining Sciences & Geomechanical Abstracts*, 22(2):121-140.

Barton N., Bieniawski Z.T. (2008). RMR and Q-setting records straight. *Tunnels and Tunnelling International*, Feb. 2008, pp. 26-29.

Barton N., Choubey V. (1977). The shear strength of rock joints in theory and practice. *Rock Mechanics*, 1/2: 1-54.

Barton N., Lien R., Lunde J. (1974). Engineering classification of rock masses for the design of tunnel support. *Rock Mechanics*, 6 (4): 189-239.

Barton N., Lien R., Lunde J. (1977). Estimation of support requirements for underground excavations. In: 16th Symposium on Design Methods in Rock Mechanics Rock Mechanics, Minnesota, ASCE, NY, pp. 163-177.

Barton N., Loset F., Lien R., Lunde J. (1980). Application of Q-system in design decisions concerning dimensions and appropriate support for underground installations. In: Bergman M., ed., Proceedings, Subsurface Space, ISRM International Symposium – Rockstore’80, Stockholm. Pergamon Press Ltd., 2: 553-561.

Barton N., Quadros, E.F. (2002). Engineering and hydraulics in jointed rock masses. EUROCK 2002, International Society for Rock Mechanics, Course A, Funchal.

Batu V. (1998) Aquifer hydraulics: a comprehensive guide to hydrogeologic data analysis. Wiley-Interscience. 752 pp.

Bell F.G. (1992). Engineering in rock masses. Butterworth-Heinemann Ltd., London. 580 pp.

Bense V.F., Gleesonb T., Loveless S.E., Bour O., Scibek J. (2013). Fault zone hydrogeology. *Earth-Science Reviews*, 127:171–192.

-
- Bieniawski Z.T. (1973). Engineering classification of jointed rock masses. *Trans. South Afr. Inst. Civ. Engin.* 15: 335–344.
- Bieniawski Z.T. (1975). The point load test in geotechnical practice. *Engineering Geology*, 9(1):1-11.
- Bieniawski Z.T. (1976). Rock mass classification in rock engineering. In: Bieniawski Z.T., ed., *Proceedings of the symposium Exploration for rock engineering*, Cape Town, Balkema, 1: 97-106.
- Bieniawski Z.T. (1979). The geomechanics classification in rock engineering applications. In: *Proceedings of the 4th Congress International Symposium of Rock Mechanics*, Montreux, 2: 41–48.
- Bieniawski Z.T. (1988). The Rock Mass Rating (RMR) system (geomechanics classification) in engineering practice. In: Kirkaldie L., ed., *Rock classification systems for engineering purposes*, ASTM Special Publication, Philadelphia, STP984: 17-34.
- Bieniawski Z.T. (1989). *Engineering rock mass classifications*. Wiley, New York. 251 pp.
- Bieniawski Z.T. (1990). *Tunnel design by Rock Mass Classifications*. Technical Report GL-79-19, US Army Corps of Engineers, Washington, DC. 159 pp. [dtic.mil/dtic/tr/fulltext/u2/a219783.pdf]
- Bieniawski Z.T. (1993). Classification of rock masses for engineering: the RMR system and future trends. Hudson J.A., (ed.), *comprehensive rock engineering: principles, practice, and projects*. Pergamon Press, 33: 553-574.
- Bieniawski, Z.T. (1997). *Quo vadis rock mass classifications?: some thoughts on rating methods for tunnel design*. *Felsbau*, 15(3): 177–178.
- Boorder H. (1965). *Petrological investigations in the Aguiar da Beira granite area, Northern Portugal*. University of Amsterdam, 126 pp. (PhD Thesis).
- Broch E., Franklin J. A. (1972). The point load strength test. *Journal Rock Mech. Min. Sci.* 9: 669-697.
- Cai M., Kaiser P.K., Uno H., Tasaka Y., Minami M. (2004). Estimation of rock mass deformation modulus and strength of jointed hard rock masses using the GSI system. *International Journal of Rock Mechanics and Mining Sciences*, 41: 3-19.
- Caine J.S., Evans J.P., Forster C.B. (1996). Fault zone architecture and permeability structure. *Geology*, 24(2): 1025-1028.
- Cargill J.S., Shakoor A. (1990). Evaluation of empirical methods for measuring the uniaxial compressive strength of rock. *International Journal of Rock Mechanics and Mining Sciences*, 27(6): 495–503.
- Carvalho J.M. (1996). Mineral water exploration and exploitation at the Portuguese Hercynian Massif. *Environmental Geology*, 27:252–258.
- Carvalho J.M., Chaminé H.I., Afonso M.J., Espinha Marques J., Teixeira J., Cerqueira A., Coelho A., Gomes A., Fonseca P.E. (2005b). Prospecção hidrogeológica da área do sistema hidromineral das Caldas da Cavaca (Aguiar da Beira, Portugal Central): implicações na gestão dos recursos hídricos subterrâneos. In: Fernández Rubio R. (ed.), *Actas del I Foro Ibérico sobre Aguas Envasadas y Balnearios*, Madrid, pp. 109–121.
- Carvalho J.M. (2006). *Prospecção e pesquisa de recursos hídricos subterrâneos no Maciço Antigo Português: linhas metodológicas*. Universidade de Aveiro, 292 pp. + anexos (tese de doutoramento / PhD Thesis).
- Celada B., Tardáguila I., Rodríguez A., Varona P., Bieniawski Z.T. (2014a). Innovating tunnel design by an improved experience-based RMR system. In: *Proceedings of the World Tunnel Congress 2014, Tunnels for a better Life*, Foz do Iguaçu, Brazil, pp. 1-9.
- Celada B., Tardáguila I., Rodríguez A., Varona P., Bieniawski Z.T. (2014b). *Actualización y mejora del RMR*. IGP – InGeoPress, 234: 18-22.
- CFCFF – Committee on Fracture Characterization and Fluid Flow (1996). *Rock fractures and fluid flow: contemporary understanding and applications*. National Research Council, National Academy Press, 568 pp.
- Chaminé H.I. (2015). Water resources meet sustainability: new trends in environmental hydrogeology and groundwater engineering. *Environmental Earth Sciences*, 73(6): 2513-2520.

Chaminé H.I., Afonso M.J., Ramos L., Pinheiro R. (2015). Scanline sampling techniques for rock engineering surveys: insights from intrinsic geologic variability and uncertainty (Chapter 61). In: Giordan D., Thuro K., Carranza-Torres C., Wu F., Marinos P., Delgado C. (eds.), *Engineering Geology for Society and Territory – Applied Geology for Major Engineering Projects*, IAEG, Springer, 6: 357-361.

Chaminé H.I., Afonso M.J., Teixeira J., Ramos L., Fonseca L., Pinheiro R., Galiza A.C. (2013b). Using engineering geosciences mapping and GIS-based tools for georesources management: lessons learned from rock quarrying. *European Geologist Magazine, Journal of the European Federation of Geologists*, 36: 27-33.

Chaminé H.I., Carvalho J.M., Afonso M.J., Teixeira J., Freitas L. (2013a). On a dialogue between hard-rock aquifer mapping and hydrogeological conceptual models: insights into groundwater exploration. *European Geologist Magazine, Journal of the European Federation of Geologists*, 35: 26-31.

Chaminé H.I., Gaspar A.F. (1995). Estudo da compartimentação de maciços rochosos pela técnica de amostragem linear: aplicação a uma travessa da Mina de Carvão de Germunde. *Estudos, Notas & Trabalhos Inst. Geol. Min.*, 37: 97-111.

Chen Y.F., Zhou C.B. (2011). Stress/strain-dependent properties of hydraulic conductivity for fractured rocks. In: Dikinya O. (ed.), *Developments in Hydraulic Conductivity Research*, InTech, Rijeka, Croatia, pp. 3-48.

Choi Y., Yoon S.-Y., Park H.-D. (2009). Tunnelling analyst: a 3D GIS extension for rock mass classification and fault zone analysis in tunnelling. *Computers & Geosciences*, 35(6): 1322-1333.

Cunha A.P., Muralha J. (1990). Scale effects in the mechanical behaviour of joints and rock masses. *Memória 763, LNEC, Lisboa*. 44 pp.

de Freitas M.H. (2009). *Geology: its principles, practice and potential for geotechnics*. *Quarterly Journal of Engineering Geology and Hydrogeology*, 42: 397-441.

Deere D.U. (1963). Technical description of rock cores for engineering purposes. *Rock mechanics and engineering geology/ Felsmechanik und Ingenieurgeologie*, 1(1): 1-18.

Deere D.U. (1989). *Rock quality designation (RQD) after twenty years*. U.S. Army Corps of Engineers Contract Report GL-89-1. Waterways Experiment Station, Vicksburg, MS 67.

Deere D.U., Deere D.W. (1988). The rock quality designation (RQD) index in practice. In: Kirkaldie L., ed., *Rock classification systems for engineering purposes*, ASTM Special Publication, Philadelphia, STP984: 91-101.

Deere D.U., Hendron A.J., Patton F.D., Cording E.J. (1967). Design of surface and near surface construction in rock. In: C. Fairhurst, (ed.), *Failure and breakage of rock, proceeding 8th U. S. symposium rock mechanics*. Soc. Min. Engrs, Am. Inst. Min. Metall. Petrol. Engrs., pp. 237-302.

Deere D.U., Miller R.P. (1966). Engineering classification and index properties for intact rock. Air Force Weapons Laboratory, Contract AF 29(601)-6319, Technical report No. AFWL-TR-65-116, New Mexico, 327 pp. [www.dtic.mil/dtic/tr/fulltext/u2/646610.pdf]

Delormanli A.H., Onargan T. (2003). Rock mass classification using a computer program: ClassMass. In: *Proceedings 18th International Mining Congress and Exhibition of Turkey*, pp. 113–118.

Dinis da Gama C. (1995). Aspectos geotécnicos y de fracturación en la explotación de canteras. In: López Jimeno, C. (Ed.). *Cap. 10 del Manual de Rocas Ornamentales. Entorno Gráfico*. S.L., Madrid, pp. 231-246.

Evans J.P., Forster C.B., Goddard J.V. (1997). Permeability of fault-related rocks and implications for hydraulic structure of fault zones. *Journal of Structural Geology*, 19(11): 1393-1404.

Faulkner D.R., Jackson C.A.L., Lunn R.J., Schlische R.W., Shipton Z.K., Wibberley C.A.J., Withjack M.O. (2010). A review of recent developments concerning the structure, mechanics and fluid flow properties of fault zones. *Journal of Structural Geology*, 32: 1557-1575.

Fetter C.W. (2014). *Applied hydrogeology*. 4th ed., Pearson new international ed., 612 pp.

Fitts C.R. (2013). *Groundwater science*. 2nd ed., Academic Press, Waltham, MA, 692 pp.

Fonseca L., Ramos L., Galiza A.C., Chaminé H.I. (2010). Avaliação geomecânica de maciços rochosos fracturados e as tecnologias de perfuração: consequências técnico-económicas. In: Actas do 12º Congresso Nacional de geotecnia, SPG/UM, Guimarães, 10 pp. (CD-ROM).

Foulger G. (2010). Plates vs Plumes: a geological controversy. Wiley-Blackwell, Oxford, 364 pp.

Franklin J.A. (1985). Suggested method for determining point load strength. *International Journal of Rock Mechanics and Mining Sciences & Geomechanics Abstracts*, 22(2):51-60.

Freeze R.A., Cherry J.A. (1979). *Groundwater*. Prentice-Hall, New Jersey, 604 pp.

Freire de Andrade C. (1935). Projecto de modificação de captagem das águas das Caldas da Cavaca. Lisboa, 11 pp. (unpublished report)

Freire de Andrade C. (1937). Os vales submarinos portugueses e o diastrofismo das Berlengas e da Estremadura. *Serviços Geológicos de Portugal*, Lisboa 236 p.

Freire de Andrade C. (1938). Nota acerca dos trabalhos realizados para a modificação da captagem das aguas medicinaes das Caldas da Cavaca. Lisboa , 7 pp. (unpublished report).

Gates W.C.B., 1995. The hydro-potential (HP) value: a proposed rock classification technique for evaluation of the groundwater potential in fractured bedrock. In: *Abstracts from the 1st symposium on the hydrogeology of Washington State*, Washington Department of Ecology, pp. 142.

Gates W.C.B., 1997. The hydro-potential value: a rock classification technique for examination of groundwater potential in fractured bedrock. *Environmental Engineering and Geoscience*, 3: 231-267.

Gates W.C.B., 2003. The Hydro-Potential (HP) Value: a rock classification technique for estimating seepage into excavations. In: Culligan P.J., Einstein H.H., Whittle A.J., eds, *Proceedings, 12th Panamerican Conference on Soil Mechanics and Geotechnical Engineering*, pp. 1283-1290.

Grimstad E., Barton N. (1993). Updating of the Q-System for NMT. In: *Kompen, Opsahl, Berg, eds., Proceedings of the International Symposium on Sprayed Concrete: Modern Use of Wet Mix Sprayed Concrete for Underground Support*, Norwegian Concrete Association, Oslo.

González de Vallejo L.I. (1983). A new classification system for underground assessment using surface data. *Proceedings of the International Congress of Engineering Geology and Underground Construction*, Lisbon, 1 (II): 85-94.

González de Vallejo L.I. (2003). SRC Rock Mass Classification of tunnels under high tectonic stress excavated in weak rocks. *Engineering Geology*, 69: 273-285.

González de Vallejo L.I., Ferrer M. (2011). *Geological engineering*. CRC Press, Taylor-Francis group, 725 pp.

Goodman R.E., Smith H.R. (1980). RQD and fracture spacing. *J. Geotechnical Engineering Division, ASCE*, 106: 191-193.

Grotzinger J., Jordan T.H., Press, F., Siever, R. (2010). *Understanding Earth*. 6th ed., W. H. Freeman and Company, 672 pp.

GSE [Geological Society Engineering Group Working Party Report] (1995). The description and classification of weathered rocks for engineering purposes. *Quarterly Journal of Engineering Geology, Geological Society*, 28(3):207-242.

Gunsallus K.L., Kullhawy F.N. (1984). A comparative evaluation of rock strength measures. *Int. J. Rock Mech. Min. Sci. & Geomech. Abstr*, 21: 233-248

Gustafson G. (2012). *Hydrogeology for rock engineers*. BeFo and ISRM Edition, Stockholm. 170 p.

Gutierrez M., Bowman D., Dove J., Mauldon M., Westman E. (2006). An IT-based system for planning, designing and constructing tunnels in rocks. *Tunnelling and Underground Space Technology*, 21 (3-4): 221.

Hack R., Huisman M. (2002). Estimating the intact rock strength of a rock mass by simple means. In: *van Rooy L., Jermy C.A., eds., Engineering Geology for Developing Countries, Proceedings of 9th Congress of the International Association for Engineering Geology and the Environment*, Durban, South Africa, pp. 1971-1977.

-
- Hamblin W.K., Christiannsen E.H. (2003). *Earth's dynamic systems*. 10th ed. Prentice Hall, 816 pp.
- Hamm S., Kim, M., Cheong J., Kim J., Son M., Kim T. (2007). Relationship between hydraulic conductivity and fracture properties estimated from packer tests and borehole data in a fractured granite. *Engineering Geology*, 92: 73-87.
- Harp E. L., Noble M.A. (1993). An engineering rock classification to evaluate seismic rock-fall susceptibility and its application to the Wasatch Front. *Bulletin of the Association of Engineering Geologists*, 30(3):293-319.
- Heirtzler J.R., Le Pichon X., Baron J. (1966). Magnetic anomalies over the Reykjanes Ridge. *Deep Sea Research*, 13(3): 427-432,
- Hess H.H. (1962). History of ocean basins. In: Engel A.E.J., James H.L., and Leonard B.F., eds, *Petrologic studies: a volume to honor of A.F. Buddington*. Geological Society of America, Boulder, CO. pp. 599-620.
- Hoek E. (1994). Strength of rock and rock masses. *News Journal of ISRM*, 2(2): 4-16.
- Hoek E. (1998). Reliability of Hoek-Brown estimates of rock mass properties and their impact on design. *International Journal of Rock Mechanics & Mining Sciences*, 35(1): 63-68.
- Hoek E. (2007). *Practical rock engineering*. RocScience: Hoek's Corner, 342 pp.
- Hoek E., Kaiser R.K., Bawden W.E. (1998). Support of underground excavations in hard rock. A.A. Balkema, Rotterdam, 215 pp.
- Hoek E., Brown E.T. (1980a). *Underground excavations in rock*. Institution of Mining and Metallurgy, London, 627 pp
- Hoek E., Brown E.T. (1980b). Empirical strength criterion for rock masses. *J. Geotech. Eng., ASCE* 106 (GT9): 1013-1035.
- Hoek E., Brown E.T. (1997). Practical estimates of rock mass strength. *Int. J. Rock Mech. Min. Sci. Geomech. Abstr.*, 34: 1165-1186.
- Hoek E., Marinos P. (2007). A brief history of the development of the Hoek-Brown failure criterion. *Soils and Rocks: Int. J. Geotech. Geoenv. Eng.*, 30(2): 85-92.
- Hoek E., Carranza-Torres C., Corkum B. (2002). Hoek-Brown failure criterion: 2002 edition. *Proceedings of the NARMS-TAC Conference, Toronto*, 1: 267-273.
- Hoek E., Carter T.G., Diederichs M.S. (2013). Quantification of the geological strength index chart. In: *Proceedings geomechanics symposium 47th US rock mechanics, San Francisco, CA, ARMA* 13-672, pp 1-8.
- Hoek E., Diederichs, M.S. (2006). Empirical estimation of rock mass modulus. *International Journal of Rock Mechanics & Mining Sciences*, 43(2): 203-215.
- Hoek E., Marinos P. (2000). Predicting tunnel squeezing problems in weak heterogeneous rock masses: Part 1 (estimating rock mass strength); Part 2 (potential squeezing problems in deep tunnels). *Tunnels and Tunnelling International*, 132(12):1-21.
- Hoek E., Marinos P., Benissi M. (1998). Applicability of the Geological Strength Index (GSI) classification for very weak and sheared rock masses: the case of the Athens Schist Formation. *Bull. Eng. Geol. Env.*, 57(2): 151-160.
- Hoek E., Wood D., Shah S. (1992). A modified Hoek-Brown criterion for jointed rock masses. In: Hudson J.A., ed., *Proceedings of the Rock Characterization, Symp. Int. Soc. Rock Mech., Eurock '92*, pp. 209-214.
- Holmes A. (1929). A review of the continental drift hypothesis. *Mining Magazine*, 40: 205-209.
- Hsu S.-M., Chung M.C., Ku C.-Y., Tan C.H., Chi S.-Y. (2008). A rock mass classification scheme for estimating hydraulic conductivity of fractured rocks. In: Alshawabkeh A.N., Reddy K.R., Khire M.V., (eds.), *Proceedings of the selected sessions of GeoCongress 2008, New Orleans, Louisiana, ASCE Geotechnical Special Publication*, 179: 452-459.
- Hsu S.-M., Lo H.-C., Chi S.-Y., Ku C.-Y. (2011). Rock mass hydraulic conductivity estimated by two empirical models. In: Dikinya O. (ed.), *Developments in Hydraulic Conductivity Research, InTech, Rijeka, Croatia*, pp. 133-158.
-

-
- Hudson J.A. (1992). *Rock engineering systems: theory and practice*. Ellis Horwood, New York. 185 pp.
- Hudson J.A., Cosgrove J.W. (1997). Integrated structural geology and engineering rock mechanics approach to site characterization. *Int. J. Rock. Mech. Min. Sci. Geomech. Abs.*, 34(3/4):136.1–136.15
- Hudson J.A., Harrison J.P. (2000). *Engineering rock mechanics: an introduction to the principles*. 2nd edition, Pergamon, Press. 444 pp.
- Hudson J.A., Priest S.D. (1983). Discontinuity frequency in rock masses. *Int. J. Rock. Mech. Min. Sci. Geomech. Abs.*, 20:73–89.
- Huntley D., Nommensen R., Steffey D. (1992). The use of specific capacity to assess transmissivity in fractured-rock aquifers. *Ground Water*, 30(3): 396-402.
- Ingebritsen S.E., Manning C.E. (1999). Geological implications of a permeability-depth curve for the continental crust. *Geology*, 27(12):1107–10.
- Ingebritsen S.E., Sanford W.E., Neuzil C.E. (2006). *Groundwater in geologic processes*. 2nd ed., Cambridge University Press, Cambridge, 564 pp.
- ISRM – International Society for Rock Mechanics (1978). Suggested methods for the quantitative description of discontinuities in rock masses. *Int. J. Rock Mech. Min. Sci. & Geom. Abstr.*, 15, 6: 319-368.
- ISRM – International Society for Rock Mechanics (1981). Basic geotechnical description of rock masses. *Int. J. Rock Mech. Min. Sci. & Geom. Abstr.*, 18: 85-110.
- ISRM – International Society for Rock Mechanics (1985). Suggested method for determining point load strength. *Int. J. Rock Mech. Min. Sci. & Geom. Abstr.*, 22: 51-60.
- ISRM – International Society for Rock Mechanics (2007). The complete ISRM suggested methods for characterization, testing and monitoring: 1974-2006. In: Ulusay R. & Hudson J.A., eds., suggested methods prepared by the commission on testing methods, ISRM. Ankara, Turkey. 628 pp.
- ISRM – International Society for Rock Mechanics (2015). The ISRM Suggested Methods for Rock Characterization, Testing and Monitoring: 2007–2014. In: Ulusay R., ed., suggested methods prepared by the commission on testing methods, ISRM. Springer, Cham, Heidelberg. 293 pp.
- Jakubec J., Laubscher D.H. (2000). The MRMR rock mass rating classification system in mining practice, *MassMin 2000*, Brisbane, Queensland, AusIMM, pp. 413-421.
- Kahraman S. (2001). Evaluation of simple methods for assessing the uniaxial compressive strength of rock. *Int. J. Rock Mech Min. Sci.*, 38: 981–94.
- Kahraman S., Fener M., Gunaydin O. (2002). Predicting the Schmidt hammer values of in-situ intact rock from core sample values. *Int. J. Rock Mech. Min. Sci.*, 39: 395-399.
- Katza O., Rechesa Z., Roegiersc J.C. (2000). Evaluation of mechanical rock properties using a Schmidt Hammer. *Int. J. Rock Mech. Min. Sci.*, 37: 723-728
- Keaton J. (2013). Engineering geology: fundamental input or random variable?. In Withiam J.L., Phoon K.-K., Hussein M. (ed.), *Foundation Engineering in the Face of Uncertainty: Honoring Fred H. Kulhawy*. ASCE. GSP 229. pp. 232-253.
- Kirkaldie L. (1988). *Rock classification systems for engineering purposes*. ASTM Special Publication, Philadelphia, STP984, 133 pp.
- Kovári K. (1993). Erroneous concepts behind NATM. Lecture of the Rabcewicz-Geomechanical Colloquium in Salzburg, pp. 1-19. [<http://geotechpedia.com/Publication/Category/30/Tunnel-Design>]
- Kresik N., Mikszewski, A. (2013). *Hydrogeological conceptual site models: data analysis and visualization*. CRC Press, Boca Raton, FL, USA.
- Laubscher D.H. (1977). Geomechanics classification of jointed rock masses: mining applications. *Transactions of the Institution of Mining and Metallurgy, Section A, Mining industry (London)*, 86: A1-A8.
- Laubscher D.H. (1990). A geomechanics classification system for rating of rock mass in mine design. *Journal of the South African Institute of Mining and Metallurgy* 90 (10): 257–273.
-

-
- Laubscher D.H., Jakubec J. (2000). The IRMR/MRMR rock mass classification for jointed rock masses. *SME journal (Society for Mining, Metallurgy, and Exploration)*, pp. 475-481.
- Le Pichon X. (1968). Sea-floor spreading and continental drift. *Journal of Geophysical Research*, 73(12): 3661–3697.
- Lloyd J.W. (1999). Water resources of hard rock aquifers in arid and semi-arid zones. *Studies and Reports in Hydrology*, 58, UNESCO, Paris, 284 pp.
- Louis C. (1969). A study of groundwater flow in jointed rock and its influence on the stability of rock masses. *Imperial College Rock Mechanics Research Report 10*, Imperial College of London, UK. 90.
- Mahé S. Gasc-Barbier M., Soliva R. (2015). Joint set intensity estimation: comparison between investigation modes. *Bulletin of Engineering Geology and the Environment*, 74(1): 171-180.
- Marinos V. (2012). Assessing rock mass behaviour for tunnelling. *Environmental and Engineering Geoscience* 18(4):327–341.
- Marinos V., Proutzopoulos G., Fortsakis P., Koumoutsou D., Korkaris K., Papouli, D. (2013). Tunnel Information and Analysis System: a geotechnical database for tunnels. *Geotechnical and Geological Engineering*, 31(3):891–910.
- Marinos V., Korkaris K., Fortsakis P., Proutzopoulos G., Mirmiris K., Papouli D., Marinos P. (2010). TIAS database: a tunnel information and analysis system. In: A.L. Williams, G.M. Pinches, C.Y. Chin, T.J. McMorran & C.I. Massey (eds), *Geologically Active*, Auckland, New Zealand. CRC Press: Taylor & Francis Group.
- Marinos P., Hoek E. (2000). GSI: a geologically friendly tool for rock mass strength estimation. In: *Proceedings GeoEng2000 on Geotechnical and Geological Engineering (Melbourne, Victoria, Australia)*. Technomic Publishers, Lancaster, PA, pp. 1422-1442.
- Marinos P., Hoek E. (2001). Estimating the geotechnical properties of heterogeneous rock masses such as flysch. *Bull. Eng. Geol. Env.*, 60: 85-92.
- Marinos P., Hoek E., Marinos V. (2006). Variability of the engineering properties of rock masses quantified by the geological strength index: the case of ophiolites with special emphasis on tunnelling. *Bull. Eng. Geol. Env.*, 65(2): 129-142.
- Marinos P., Marinos V., Hoek E. (2007). The geological strength index (GSI): a characterization tool for assessing engineering properties for rock masses. In: Mark C., Pakalnis R. & Tuchman R.J., eds., *Proceedings of the International Workshop on Rock Mass Classification in Underground Mining*. pp. 87-94.
- Marinos V., Marinos P., Hoek, E. (2005). The geological strength index: applications and limitations. *Bull. Eng. Geol. Environ*, 64: 55-65.
- Mazzoccola D.F., Millar D.L., Hudson J.A. (1997). Information, uncertainty and decision making in site investigation for rock engineering. *Geotechnical and Geological Engineering*, 15: 145-180.
- McKnight T.L., Hess D. (2000). Climate zones and types: the Köppen system. In: McKnight T.L., Hess D. (eds), *Physical geography: a landscape appreciation*. Prentice Hall, New Jersey.
- Miller R.P. (1965). Engineering classification and index properties for intact rock. University of Illinois, 282 pp. (PhD Thesis)
- Miranda T., Gomes Correia A., Ribeiro e Sousa L. (2006). Determinação de parâmetros geomecânicos em formações rochosas e maciços heterogêneos. *Revista Engenharia Civil, UM*, 25: 17-40.
- Missteart B., Banks D., Clark L. (2006). *Water wells and boreholes*. John Wiley & Sons. 498 pp.
- NGI [Norwegian Geotechnical Institute] (2013). Using the Q-system: Rock mass classification and support design. *NGI handbook*, Oslo, 56 pp.
- Palassi M., Franklin J.A. (1998). Tunnex: an expert system for tunnelling through rock. In: *Proceedings Fourth International Conference on Case Histories in Geotechnical Engineering*, St. Louis, Missouri. pp. 782–788.

Palmström A. (1975). Characterization of degree of jointing and rock mass quality. Intern. Report Ing. AB. Berdel, A.S. Oslo.

Palmström A. (1995). RMI: a rock mass characterization system for rock engineering purposes. University of Oslo, 400 p. (PhD Thesis).

Palmström A. (1996a). Characterization of rock masses by the RMI for use in practical rock engineering. *Tunnel Underground Space Technol.*, 11(2): 175-186 (part 1); 11(3):287-303 (part 2).

Palmström A. (1996b) RMI: a system for characterizing rock mass strength for use in rock engineering. *J. Rock Mech. Tunn. Technol.*, 1(2):69–108.

Palmström A. (2009). Combining the RMR, Q, and RMI classification systems. *Tunnelling and Underground Space Technology*, 24(4): 491-492.

Palmström A., Stille H. (2010). *Rock engineering*. Thomas Telford Ltd., 408 pp.

Peacock D.C.P. (2006). Predicting variability in joint frequencies from boreholes. *J. Struct. Geol.*, 28(2): 353-361.

Peacock D.C.P., Harris S.D., Mauldon M. (2003). Use of curved scanlines and boreholes to predict fracture frequencies. *J. Struct. Geol.*, 25(1): 109-119.

Peel M.C., Finlayson B.L., McMahon T.A. (2007). Updated world map of the Köppen-Geiger climate classification. *Hydrol. Earth Syst. Sci.*, 11:1633–1644.

Pinheiro R., Ramos L., Teixeira J., Afonso M.J., Chaminé H.I. (2014). MGC–RocDesign|CALC: a geomechanical calculator tool for rock design. In: L.R. Alejano, A. Peruchó, C. Olalla & R. Jiménez (Eds.), *Proceedings of Eurock2014, Rock Engineering and Rock Mechanics: Structures in and on Rock Masses (ISRM European Regional Symposium, Vigo, Spain, 26-28 May 2014)*, CRC Press/Balkema Taylor & Francis Group, London, p. 655-660. (on pen-drive insert, ISRM Paper CH100).

Priest S.D. (1993). *Discontinuity analysis for rock engineering*. Kluwer Academic Publishers. 473 pp.

Priest S.D., Hudson J.A. (1976). Discontinuity spacing in rock. *Int. Journ. Rock Mech. Min. Sci. & Geom. Abstr.*, 13: 135-148.

Priest S.D., Hudson J.A. (1981). Estimation of discontinuity spacing and trace length using scanline surveys *Int. Journ. Rock Mech. Min. Sci. & Geom. Abstr.*, 18: 183-197.

Ribeiro A. (2002). *Soft plate and impact tectonics*. Springer, 324 pp.

Ribeiro A., Munhá J., Dias R., Mateus A., Pereira E., Ribeiro L., Fonseca P.E., Araújo A., Oliveira J.T., Romão J., Chaminé H.I., Coke C., Pedro J., 2007. Geodynamic evolution of the SW Europe Variscides. *Tectonics*, 26, TC6009, 24 pp. [doi: 10.1029/2006TC002058].

Ribeiro O. (1949). Le Portugal Central. In: *Livret-guide de l'excursion C, Union Géographique Internationale. XVI Congrès International de Géographie, Lisbonne*, p 180.

Ritter W. (1879). *Die Statik der Tunnelgewölbe*. Springer, Berlin, 66 pp.

Romana M. (1985). New adjustment rating for application of the Bieniawski classification to slopes. In: *Proceedings Int. Symp. Rock Mechanics Mining Civ. Works. ISRM, Zacatecas, Mexico*, pp. 59-63.

Romana M. (1993). A geomechanical classification for slopes: Slope Mass Rating. In: Hudson J., Ed., *Comprehensive Rock Engineering*, Pergamon, 3: 575-600.

Romana M. (2003). DMR, a new geomechanics classification for use in dams foundations, adapted from RMR. In: *Proceedings of the 4th International Symposium on Roller Compacted Concrete (RCC) Dams, Madrid*. 9 pp.

Romana M. 2004). DMR (an adaptation of RMR), a new geomechanics classification for use in dams foundations. In: *Actas do 9º Congresso Nacional de Geotecnia, Aveiro*. 12 pp.

Romana M., Serón J.B., Montalar E. (2003). SMR Geomechanics classification: application, experience and validation. In: *Proceeding ISRM 2003, Technology roadmap for rock mechanics, South African Institute of Mining and Metallurgy*, 4 pp.

-
- Rose D. (1982). Revising Terzaghi's tunnel rock load coefficients. *Proceedings 23rd U.S. Symposium Rock Mechanics*. AIME, New York, pp. 953-960.
- Scesi L., Gattinoni P. (2009). *Water circulation in rocks*. Springer, Dordrecht, 165 pp.
- Schmidt E. (1951). A non-destructive concrete tester. *Concrete*, 59(8): 34-35.
- Sem Z. (1984). RQD models and fracture spacing. *Journal of Geotechnical Engineering, ASCE*, 110:203-216.
- Sem Z. (1990). Cumulative core index for rock quality evaluations. *International Journal of Rock Mechanics and Mining Sciences & Geomechanics Abstracts*, 27(2):87-94.
- Serafim J.L., Pereira J.P. (1983). Consideration of the geomechanics classification of Bieniawski. In: *Proceedings of the International Symposium on Engineering Geology and Underground Constructions*, p. 1133-1144.
- Sibson R.H. (1977). Fault rocks and fault mechanisms. *Journal of Geological Society of London*, 133: 191-231.
- Singh B., Goel R.K. (2011). *Engineering rock mass classification: tunneling, foundations, and landslides*. Butterworth-Heinemann, Elsevier Inc., 365 pp.
- Singhal B.B.S., Gupta R.P. (2010). *Applied hydrogeology of fractured rocks*. 2nd ed., Springer, Dordrecht, 408 pp.
- Skinner E.H. (1988). A ground support prediction concept: the rock structure rating (RSR) model. In L. Kirkaldie (ed), *Rock Classification Systems for Engineering Purposes*. ASTM International, STP984:43-64.
- Smith J.V. (2004). Determining the size and shape of blocks from linear sampling for geotechnical rock mass classification and assessment. *Journal of Structural Geology*, 26(6-7):1317-1339.
- Snow D.T. (1969). Anisotropic permeability of fractured media. *Water Resources Research*, 5(6):1273-1289.
- Sterrett R.J. (2007). *Ground Water and Wells*. Johnson Screens. 812 pp.
- Tapia M.A., Valverde M.A., Amadei B., Madrigal H. (1998). The REX expert system: a new alternative for rock excavation design. *International Journal of Rock Mechanics and Mining Sciences* 35(4-5): 675-676.
- Teixeira J., Chaminé H.I., Espinha Marques J., Gomes A., Carvalho J.M., Pérez-Alberti A., Rocha F. (2010). Integrated approach of hydrogeomorphology and GIS mapping to the evaluation of ground water resources: an example from the hydromineral system of Caldas da Cavaca, NW Portugal. In: Paliwal B.S. (ed.) *Global Groundwater Resources and Management, Selected Papers from the 33rd International Geological Congress, General Symposium: Hydrogeology, Oslo (Norway) Aug. 6-14, 2008*, Scientific Publishers (India), Jodhpur, pp. 227-249.
- Teixeira J., Chaminé H.I., Carvalho J.M., Pérez-Alberti A., Rocha F. (2013). Hydrogeomorphological mapping as a tool in groundwater exploration. *Journal of Maps*, 9(2): 263-273.
- Teixeira J., Chaminé H.I., Espinha Marques J., Carvalho J.M., Pereira A.J., Carvalho M.R., Fonseca P.E., Pérez-Alberti A., Rocha F. (2015). A comprehensive analysis of groundwater resources using GIS and multicriteria tools (Caldas da Cavaca, Central Portugal): environmental issues. *Environmental Earth Sciences*, 73(6):2699-2715.
- Terzaghi K. (1946). Rock defects and locals on tunnel supports. In: Proctor R.V. & White T.L., eds, *Rock tunnelling with steel supports*, The Commercial Shearing & Stamping Co. Youngstown, Ohio, 1: 17-99.
- Terzaghi R.D. (1965). Sources of errors in joint surveys. *Géotechnique*, 15:287-304.
- Thorntwaite C.W., Mather J.R. (1955). *The water balance*. Publications in Climatology, New Jersey.
- Tóth J. (1999). Groundwater as a geologic agent: an overview of the causes, processes, and manifestations. *Hydrogeology Journal*, 7(1):1-14.
- Underwood J.R. (2001). Anthropogenic rocks as a fourth basic class. *Environmental and Engineering Geoscience*, 7: 104-110.

Vardakos S. (2004). A rock mass classification tool for personal digital assistants. The Charles E. Via Jr. Department of Civil and Environmental Engineering, Geotechnical Engineering Group. Blacksburg, Virginia. 61 pp.

Vardakos S., Gutierrez M. (2005). A PDA field book for rock mass characterization and classification. Proceedings 40th U.S. Symposium on Rock Mechanics, Anchorage, Alaska, American Rock Mechanics Association, ARMA-05-753, 11 pp.

Vine F.J. (1966). Spreading of the ocean floor: new evidence. *Science*, 154(3755): 1405–1415.

Vine F.J., Matthews D.H. (1963). Magnetic anomalies over oceanic ridges. *Nature*, 199(4897): 947–949.

Vine F.J., Wilson J.T (1965). Magnetic anomalies over a young oceanic ridge off Vancouver Island. *Science*, 150(3695): 485–489.

Wang H.F. (2000). Theory of linear poroelasticity with applications to geomechanics and hydrogeology. Princeton University Press, 276 pp.

Watkins H., Bond C.E., Healy D., Robert, Butler R.W.H. (2015). Appraisal of fracture sampling methods and a new workflow to characterise heterogeneous fracture networks at outcrop. *Journal Structural Geology*, 72:67-82.

Wegener A. (1924). The origin of continents and oceans. 3rd ed., Dutton, 212 pp.

Wei Z.Q., Egger P., Descoedres F. (1995). Permeability predictions for jointed rock masses. *International Journal of Rock Mechanics, Mineral Science and Geomechanics*, 32:251-261.

Wickham G.E., Tiedemann H.R., Skinner E.H. (1972). Support determination based on geologic predictions. In: K.S. Lane & L.A. Garfield, (eds), Proceedings of the 1st North American Rapid Excavation Tunneling Conference (RETC), Chicago. AIME, NewYork, pp. 43–64.

Wickham G.E., Tiedemann H.R., Skinner E.H. (1974). Ground support prediction model: RSR concept. In: Proceedings 2nd North American Rapid Excavation & Tunnelling Conference (RETC), San Francisco. AIME, New York, pp. 691–707.

William G. (1975). Continental drift and plate tectonics. Merrill Pub Co., 188 pp.

Wilson J.T. (1963). Hypothesis on the Earth's behaviour. *Nature*, 198(4884): 849–865.

Wilson J.T. (1966). Did the Atlantic close and then re-open?. *Nature*, 211(5050): 676–681.

Younger P.L. (2007). Groundwater in the environment: an introduction. Blackwell Publishing, Oxford, 336 pp.

Zhou C.B., Sharma R.S., Chen Y.F., Guan Rong G. (2008). Flow-stress coupled permeability tensor for fractured rock masses. *International Journal for Numerical and Analytical Methods in Geomechanics*, 32(11):1289–1309.